Heterologous expression and functional analysis of extremophilic enzymes by koji molds

仙波, 弘雅

(Degree)
博士（農学）

(Date of Degree)
2024-03-25

(Date of Publication)
2025-03-01

(Resource Type)
doctoral thesis

(Report Number)
甲第8953号

(URL)
https://hdl.handle.net/20.500.14094/0100490178

Doctoral Dissertation

Heterologous expression and functional analysis of extremophilic enzymes by koji molds

極限環境微生物由来酵素の麹菌による異種発現と機能解析

January, 2024

Hironori SEMBA

Graduate School of Agricultural Science

Kobe University

Contents

General Introduction **1–2**

Chapter 1 **3–44**

Improvement in salt-tolerance of *Aspergillus oryzae* γ-glutamyl transpeptidase via protein chimerization with *Aspergillus sydowii* homolog

Introduction 3–5
Materials and Methods 5–11
Results and Discussion 11–19
Figures and tables 20–44

Chapter 2 **45–72**

Heterologous expression and characterization of salt-tolerant β-glucosidase from xerophilic *Aspergillus chevalieri* for hydrolysis of marine biomass

Introduction 45–46
Materials and Methods 46–53
Results and Discussion 53–58
Figures and tables 59–72

Chapter 3 **73–97**

Effects of heterologous expression and N-glycosylation on the hyperthermostable endoglucanase of *Pyrococcus furiosus*

Introduction 73–74
Materials and Methods 74–80
Results and Discussion 80–85
Figures and tables 86–97

Concluding Discussion **98–99**

Acknowledgements **100**

References **101–127**

General Introduction

Extremophiles are microorganisms that survive in hostile environments where humans are unable to survive. These microorganisms are adapted to various extreme environments such as thermophilic, acidophilic, alkaliphilic, halophilic, and xerophilic environments, and these enzymes are known to be highly active and tolerant of each extreme environment (1). Therefore, extremophiles are expected to be a source of industrially useful enzymes (2),(3). However, the low production of these extremozymes or the difficulty of cultivating the microorganisms themselves have been obstacles to their characterization and industrial application (4),(5). As a solution to this problem, it is effective to isolate enzyme genes derived from extremophiles and heterologously express them for characterization, improvement, and overexpression of extremozymes (4),(5).

The hosts for expression of heterologous proteins include *Escherichia coli*, *Pichia pastoris*, and filamentous fungi of the genus *Aspergillus*. Among these, koji molds such as *Aspergillus oryzae* and *Aspergillus niger* are widely used in the fermentation industry and are generally recognized as safe (GRAS). In addition, koji molds have excellent ability to secrete and produce proteins, and many studies have been conducted on koji molds as a host for heterologous expression of industrially important enzymes (6),(7). In this study, we investigated the heterologous expression and functional analysis of enzymes derived from extremophiles using filamentous fungi of the genus *Aspergillus* as a host.

In chapter 1 and chapter 2, heterologous expression and functional analysis of enzymes from koji mold isolated from katsuobushi were conducted. Katsuobushi can be classified into two types: arabushi, which are the form before fermentation and karebushi, which are fermented with molds such as *Aspergillus* spp.. Karebushi, in particular, has a

moisture content reduced to <13% [≈0.62 aw] during the fermentation process (8). Enzymes produced by molds growing in this extremely dry environment have been reported to have excellent desiccation/salt tolerance properties and are expected to be an attractive source of isolation of industrially important enzyme genes (9),(10).

In chapter 1, to investigate the mechanism of salt tolerance of γ-glutamyl transpeptidase from *Aspergillus sydowii*, a chimeric enzyme with γ-glutamyl transpeptidase from *A. oryzae* was designed and characterized. In Chapter 2, heterologous expression and characterization of a salt-tolerant β-glucosidase from *Aspergillus chevalieri* were carried out, and its application to marine biomass degradation was investigated. In Chapter 3, heterologous expression of endoglucanase from hyperthermophilic archaeon *Pyrococcus furiosus* was conducted using *A. niger* as an expression host. Here, the construction of overexpression system using *A. niger* and the improvement of enzyme activity and thermostability by addition of glycosylation were reported.

Chapter 1

Improvement in salt-tolerance of *Aspergillus oryzae* γ-glutamyl transpeptidase via protein chimerization with *Aspergillus sydowii* homolog

Introduction

γ-Glutamyl transpeptidase (GGT; EC 2.3.2.2) is an enzyme that is widely distributed in nature and is known to catalyze the hydrolysis of γ-glutamyl bonds in glutamine, as well as the transfer of the released γ-glutamyl group to amino acids or short peptides (11). Because of its diverse applications in various biotechnology fields, the biochemical, genetic, and molecular biological properties of microbial GGTs have been extensively studied (11),(12). After the formation of a γ-glutamyl-GGT intermediate, it then reacts with water to produce glutamate by hydrolysis or with amino acids or peptides to produce the corresponding γ-glutamyl peptides by transpeptidation. Among microbial GGTs, protein engineering of *Bacillus* GGTs has been performed to enhance post-translational auto-processing (11),(13),(14), overproduction (15),(16), and enzyme activity and stability (11),(14),(17)–(19), for the biocatalytic synthesis of valuable γ-glutamyl peptides. However, there is limited information on enhancing the hydrolysis ability of GGTs for producing glutamate from glutamine (17),(20).

In traditional Japanese soy sauce and soybean fermentation under high salt conditions (c. 17%single bond18% NaCl), glutaminases produced by koji molds such as *A. oryzae* and *A. sojae* are key hydrolytic enzymes for flavor enhancement, as they convert L-glutamine to L-glutamic acid (21),(22). However, fungal glutaminases, including GGTs, are non-salt-tolerant enzymes, and their hydrolytic activity markedly decreases under high salt conditions (21),(22). Salt-tolerant (halotolerant) enzymes are

defined as those that retain their activity and stability under a broad range of salt concentrations (23). Therefore, various salt-tolerant glutaminases, including GGT, have been isolated and characterized from bacteria and yeasts (24) for application in wheat and soybean fermentation instead of *A. oryzae* GGTs. While several *Bacillus* GGTs are categorized as a salt-tolerant type (20),(25)–(27), *Bacillus* spp. proliferates very rapidly during koji fermentation, which is the process of culturing *A. oryzae* on cooked soybean, rice, and barley (28). Moreover, *Bacillus* spp. not only antagonistically prevent the growth of *A. oryzae*, but also produce an off-flavor (28). Thus, the salt-tolerant GGT-producing *Bacillus* spp. and their crude GGT preparations cannot be utilized for koji fermentation with *A. oryzae*. Furthermore, *B. subtilis* GGT shows low sequence identity (c. 30%) with *A. oryzae* extracellular GGTs (29), which makes it difficult to improve the salt-tolerance of *A. oryzae* GGTs by protein engineering based on reported sequence and structural data analysis of bacterial GGTs.

Recently, a salt-tolerant GGT, termed ASggtA, has been isolated and characterized from a xerophilic mold, *A. sydowii* MA0196 (29). ASggtA has high salt-tolerance compared with previously reported *Aspergillus* GGTs (29). The deduced amino acid sequence of ASggtA showed high identity (73% [435 / 593 amino acids]) with that of AOggtA (29), making ASggtA a potential salt-tolerant counterpart for enhancing salt-tolerance in AOggtA. Halophilic and salt-tolerant enzymes generally contain a relatively high proportion of acidic amino acids (Asp and Glu) compared with homologous non-halophilic/salt-tolerant proteins (23),(30)–(32). Thus, protein surface engineering by multiple substitution with Asp and/or Glu residues has been applied for improvement of the salt-tolerance of highly desirable enzymes, such as glucose dehydrogenase, carbonic anhydrase, and xylanase (33)–(35). However, no clear differences in protein surface

properties were detected between AOggtA and ASggtA mature proteins (29). There is considerable different in the terms of N-terminal region for revealing salt-tolerant mechanism and/or for protein engineering in non-salt-tolerant AOggtA, described below (Fig. 1-1(a)).

In this chapter, we designed a chimeric enzyme, in which the N-terminus of salt-tolerant ASggtA was connected by protein fusion to the C-terminus of non-salt-tolerant AOggtA. The chimera and its parental GGTs were heterologously expressed, to elucidate the role of the N-terminal region for enzymatic stability and tolerance under high salt conditions. In addition, differences in thermo- and pH-stabilities and catalytic properties were characterized and compared between the chimera and its parental enzymes.

Materials and Methods

Microorganisms, plasmid, and culture conditions

A. sydowii MA0196 and *A. oryzae* NBRC 100959 (other culture collection no. RIB 40) were used as the source of γ-glutamyl transpeptidase genes encoding ASggtA (accession no. LC752792) and AOggtA (XP_023088840.1), respectively. These strains were cultivated on katsuobushi solid medium and wheat bran solid medium, respectively, as described previously (29). *A. oryzae* niaD^{-} (a nitrate reductase gene (niaD)-deficient mutant), derivative strain NBRC 100959 was used as the recipient strain for a heterologous expression host (36). The expression vector pUNA, containing the *amyB* promoter and terminator, was newly constructed from pUC118, based on a previously reported expression vector (37). *A. oryzae* transformants were cultivated on DPY medium (2% (w/v) dextrin, 1% (w/v) polypeptone, 1.0% (w/v) yeast extract, 0.5% (w/v) KH_2PO_4, and 0.05% (w/v) $MgSO_4 \cdot 7H2O$ (38)) with shaking at 130 rpm for 3–4 d.

Construction of GGT expression vectors and transformation of A. oryzae

Gene cloning of ASggtA and AOggtA and preparation of their chimeric gene, ASAOggtA. The extraction of total RNA and synthesis of first-strand cDNA were carried out as described previously (39). DNA fragments encoding ASggtA and AOggtA were amplified using the synthesized cDNA solution, PrimeSTAR MAX DNA polymerase (Takara Bio Inc., Shiga, Japan), and primers AS_ggtA_infF (P1) and AS_ggtA_infR (P2), and AO_ggtA_infF (P3) and AO_ggtA_infR (P4), respectively (Fig. 1-1(b), Table 1-1). The chimeric enzyme, ASAOggtA, consisted of ^{1}Met to ^{148}Gly of ASggtA and ^{142}Leu to ^{584}Val of AOggtA (Fig. 1-1(a)-(c)). Primers AS_ggtA_infF (P1) and AS_ggtA_486nt_R (P5) were used to amplify the N-terminal region of the ASggtA gene (Fig. 1-1(b), Table 1-1). Primers AOggtA_1305nt_infF (P6) and AO_ggtA_infR (P4) were used to amplify the corresponding modular regions of the AOggtA gene (Fig. 1-1(b), Table 1-1). According to the In-fusion HD Cloning kit User manual, the purified PCR products were ligated into the plasmid, pUNA, linearized using restriction enzymes ApaI and XbaI (Fig. 1-1(d)). The constructed recombinant plasmids were then transformed into *E. coli* HST08, according to the manufacturer's instructions.

Transformation experiments. Transformation of *A. oryzae* was carried out according to the previously reported procedures (40) with the following modification. The plasmids were linearized by restriction enzyme *Xho*I or *Hpa*I and introduced into *A. oryzae* niaD^{-} by means of niaD-based homologous recombination, according to the previously described method (40). Protoplasts were prepared from 1-day old mycelial cultures by treatment with Yatalase (Takara Bio Inc.) for 3 h at 30 °C. Transformants that possessed the niaD marker gene were selected on Czapek–Dox minimal agar medium

plates containing $NaNO_3$ as sole N source (40). GGT-producing transformants were cultured in DPY medium (Table 1-2), as described above. Measurement of GGT gene copy number in chromosomal DNA was carried out according to the previously reported procedures (41), Table 1-1].

Enzyme assays

Enzyme assays were conducted based on previous methods (29) with modification. For hydrolysis activity, a reaction mixture (1.1 mL) containing 100 mM Tris–HCl buffer (pH 8.0), 0.5 mM L-γ-glutamyl-*p*-nitroanilide monohydrate (γ-GpNA), and 100 μL enzyme solution was incubated at 40 °C for 20 min. Absorbance at 405 nm was measured. For transpeptidation activity, a reaction mixture (1.1 mL) containing 100 mM Tris–HCl buffer (pH 8.0), 0.5 mM γ-GpNA, 33 mM glycylglycine, and 100 μL enzyme solution was incubated at 40 °C for 20 min. Absorbance at 405 nm was measured. One unit of activity was defined as the amount of enzyme that released 1 μmol *p*-nitroanilide per minute under these conditions.

Purification of recombinant GGTs and chimeric GGT

All operations were conducted at around 4 °C. Unless otherwise stated, a 20 mM Tris–HCl buffer (pH 7.5) (buffer A) was used for the purification procedure, as previously described (29). Sartorius Vivaspin Turbo 15 ultrafiltration centrifugal concentrators (Sartorius AG, Göttingen, Germany) were used for concentration of active fractions. During column chromatography, the most active fraction, and fractions before and after with > 70% relative activity, were pooled for the next chromatography step. The ion-exchange and hydrophobic chromatography were carried out based on previous methods

(29) with modification (see foot note in Table 1-3). After Butyl-Toyopearl chromatography, the active fraction contained Taka-amylase A, produced by the *A. oryzae* transformants because of the amylase promoter in the expression vector (Fig. 1-1(d)). Recombinant GGTs and amylase were separated by soluble starch gel affinity chromatography, following previously reported procedures (42). The affinity matrix of soluble starch gel was prepared by cross-linking by reaction with epichlorohydrin, as described previously (42). The recombinant GGTs were collected as washed fractions since the amylase had an affinity for the matrix gel in buffer A containing 1 M ammonium sulfate.

Characterization of recombinant GGTs and chimeric GGT

Hydrolysis and transpeptidation activities were assayed as described above. Purified GGTs were used for characterization. Unless otherwise stated, the protein amount corresponded to 20–70 mU/mL (ASggtA), 20–120 mU/mL (AOggtA), and 35–200 mU/mL (ASAOggtA) hydrolysis activities and 65–200 mU/mL (ASggtA), 65–110 mU/mL (AOggtA), and 90–200 mU/mL (ASAOggtA) transpeptidase activities.

Effect of NaCl concentration on enzyme activity and stability. Hydrolysis and transpeptidation assays were carried out using the purified GGTs in a reaction mixture containing NaCl (0%–20% (w/v) final concentration). The purified GGT solution (5 mL) was dialyzed against 20 mM Tris–HCl buffer (pH 8.0) without and with 10% NaCl and 20% NaCl at 4 °C. The solution was taken weekly and further dialyzed against 20 mM Tris–HCl buffer (pH 8.0) at 4 °C for one day. Residual activities were calculated based on the specific activities measured using the enzyme solution incubated without NaCl for one week.

Effect of pH on enzyme activity and stability. The pH (3.5–11.0) of a 100 mM 3,3-dimethylglutaric acid (G), 100 mM Tris (T), and 100 mM 2-amino-2-methyl-1,3-propanediol (A) mixture (denoted "GTA") was adjusted by adding 1.0 M HCl and 1.0 M NaOH, according to the previously described procedure for preparing GTA buffer (43). In addition, 100 mM Na_2HPO_4–citric acid buffer (pH 2.0–3.0) and 100 mM Na_2HPO_4–NaOH (pH 11.0–12.0) were also prepared. Enzyme activities were measured using the purified GGTs in 50 mM GTA buffer (pH 3.5–11.0). The pH stability of MA0196 GGT was determined by mixing concentrated purified GGT with various 100 mM buffer (pH 2.0–12.0) at 4 °C for 15 h. The enzyme solution was concentrated 10-fold using Sartorius Vivaspin Turbo 15 ultrafiltration centrifugal concentrators. The concentrated enzyme solution and each buffer solution were mixed at a ratio of 1:9 (v/v), and the residual activity was measured.

Effect of temperature on enzyme activity and stability. The effect of temperature on the hydrolysis and transpeptidation activities of the purified GGT was determined over the range 20–70 °C. The purified GGT was pre-incubated at various temperatures (10–65 °C) for 10 min, and residual activities were measured.

Substrate specificity toward γ-glutamyl acceptors. Substrate specificity toward γ-glutamyl acceptors was measured by the transpeptidation activity assay using the acceptors instead of glycylglycine.

Determination of kinetic parameters. Kinetic parameters of the purified GGTs were determined by performing steady-state kinetic studies with various concentrations of γ-GpNA with and without 33 mM glycylglycine. The parameters were also determined in a buffer containing 20% (w/v) NaCl.

Hydrolysis of glutamine by GGTs. Enzymatic hydrolysis of glutamine by

GGTs was examined in a reaction mixture (1.1 mL) containing 50 mM Tris–HCl buffer (pH 8.5), 100 mM L-glutamine, and 0.1 mL purified GGTs (40 mU/mL) that was incubated at 30 °C for 12 h. A Hitachi L-7100 HPLC system equipped with a 5 C18-PAQ column (4.6 mm I.D. × 150 mm, Nacalai Tesque Inc., Kyoto, Japan) was used for measuring substrate and reaction products. The flow rate at room temperature was 1.0 min/mL. Samples were eluted with 5 mM sodium pentanesulfonate–20 mM phosphoric acid with monitoring at 210 nm. The retention times of L-glutamine, L-glutamate, and γ-glutamyl-glutamine (Toronto Research Chemicals Inc., Toronto, ON, Canada) were 9.9, 12.8, and 15.8 min, respectively.

In silico analysis of GGTs

The sequence data of GGTs were compared with appropriate reference data using the ClustalW algorithm and GENETYX-win software (Version 14.0; GENETYX, Tokyo, Japan). Signal peptide searches and predictions, N-glycosylation sites, and structural modeling of ASggtA and AOggtA were performed and predicted using the Signal P-6.0 server, NetNGly 1.0 server, and NetSurfP-2.0 (44),(45). Structural modeling of ASggtA and AOggtA was performed using the SWISS-MODEL web server (Fig. 1-1(c)). The crystallographic structure of GGT (Ecggt) from *E. coli* K-12 (PDB ID, 2E0W) was used as the template for homology modeling. The global model quality estimate (GMQE) values of ASggtA and AOggtA with Ecggt were 0.64 and 0.66, respectively.

Statistical analysis

All experiments were performed in duplicate and replicated at least three times. All data were calculated as the mean ± standard deviation. Analysis of variance (ANOVA)

was selected to test value differences ($p < 0.05$). For comparison of different groups, the data were analyzed using one-way ANOVA and Tukey's multiple comparison. All calculations were conducted using GraphPad Prism software (ver. 6.02 for Windows, La Jolla, CA, USA).

Results and Discussion

Comparison of sequence and structure between salt-tolerant and non-salt-tolerant GGTs from Aspergillus spp. for design of chimeric enzyme

Sequence alignment between AOggtA and ASggtA revealed significant differences in the N-terminal regions downstream of the signal peptide. Specifically, the sequence of mature ASggtA (^{28}Ser to ^{56}Pro) was found to be quite different from that of AOggtA (^{28}Ser to ^{49}Glu) (Fig. 1-1(a)). The differences cannot be explained solely by the fact that ASggtA is salt-tolerant while AOggtA is not, as mentioned in the Introduction (30). Thus, neutral and/or basic amino acid residues in the N-terminal region of AOggtA were not always substituted with acidic amino acid residues in that of ASggtA. Furthermore, the predicted models of AOggtA and ASggtA did not provide information on the secondary structures of the N-terminal regions (Fig. 1-1(c)). These findings suggested that other factors might be involved in the salt-tolerance of these GGTs. Studies of N-terminal truncated GGTs from *B. pumilus* KS 12 indicated that the N-terminal region up to 95 amino acids did not affect the autoprocessing of GGT, but rather the proper folding of the enzyme and its activity (13). To investigate the impact of N-terminal region of *Aspergillus* GGTs on salt-tolerance, a chimeric enzyme, named ASAOggtA, was constructed by fusing the N-terminus of salt-tolerant ASggtA (^{1}Met to ^{148}Gly) to the corresponding downstream region, the C-terminus of non-salt-tolerant AOggtA (^{142}Leu

to ^{584}Val) (Fig. 1-1(b)).

Expression and purification of recombinant AOggtA and ASggtA and chimera ASAOggtA

The recombinant parental enzymes and their chimera were heterologously expressed in *A. oryzae*. Hydrolysis and transpeptidase activities in culture filtrates were compared among the host, *A. oryzae* niaD^{-}, AOggtA-, ASggtA-, and ASAOggtA-producing transformants (Table 1-2). The production of ASAOggtA (transpeptidation activity, 0.18 U/mL, Table 1-2) was much higher than that of GGT in the parent, *A. sydowii* MA0196 (0.02 U/mL, (29)), although still low compared with the production in *B. licheniformis* ER15 (5.2 U/mL) (46) and *B. subtilis* SK11.004 (22.4 U/mL) (47). There was no correlation between GGT production and copy number (Table 1-2). For over-expression of ASAOggtA, it might be necessary to optimize cultural conditions and/or to enhance target gene transcriptional expression (48), rather than obtaining multi-copy type mutants.

AOggtA, ASggtA, and ASAOggtA were purified by sequential column chromatography procedures and the hydrolysis and transpeptidation activities of the collected fractions were measured (Table 1-3). The GGTs were purified to homogeneity (Fig. 1-2). All three GGTs are composed of a large subunit of 56 kDa and a small subunit of 33 kDa, and both polypeptides are glycosylated (Fig. 1-2). After Butyl-Toyopearl hydrophobic chromatography, the active fractions of ASggtA and ASAOggtA contained amylase derived from the host strain, *A. oryzae*, because the *amyB* expression cassette was used for heterologous expression (Fig. 1-1(d)). Thus, soluble starch affinity chromatography was used to separate GGTs and amylase. The ratios of the transpeptidase

and hydrolysis activities (T/H ratio) of the final preparation of AOggtA, ASggtA, and ASAOggtA were 1.5, 3.2, and 2.0, respectively (Table 1-3). After this, we focused on the hydrolytic properties of the three GGTs; part of the detailed data on the transpeptidase activities are summarized in Fig. 1-6–1-8.

Effect of NaCl concentrations on enzyme activity and stability

GGT from *B. amyloliquefaciens* ZS5 retains the enzyme activity and is stable over a broad salt concentration range (1–5 M NaCl); it has been proposed that the salt-tolerance is attributable to the large amount of negative charges in the ZS5 GGT protein (27). The chimera, ASAOggtA, produced by swapping N-terminal regions, rather than substitution with acidic amino acid residues, was significantly improved over the parental AOggtA for salt-tolerance. ASggtA and ASAOggtA retained hydrolysis and transpeptidase activities under high NaCl concentrations, compared with AOggtA (Fig. 1-3), while the relative activity of AOggtA decreased significantly to less than 18% under high salt (Fig. 1-3). The specific activities (as hydrolysis activity) of AOggtA, ASggtA, and ASAOggtA under 18% NaCl were 0.81 U/mg, 2.0 U/mg, and 1.8 U/mg, respectively (Fig. 1-3). The three GGTs reported here were stable in the absence and presence of 10% and 20% (w/v) NaCl after incubating for more than one month, maintaining almost 100% activity (Table 1-4 and Fig. 1-6).

Fluorescence spectroscopy studies of AOggtA, ASggtA, and ASAOggtA were carried out in the absence and presence of different salt concentrations (10% and 20%) (Fig. 1-4). The fluorescence emission intensity peaked at 330–335 nm for the native state in buffer without NaCl, and showed a typical decrease of signal intensity with increasing NaCl concentration (Fig. 1-4). AOggtA showed more markedly decreased fluorescence

intensity with increasing salt concentration than did ASggtA and ASAOggtA (Fig. 1-4). In the salt-tolerant bacterial GGTs, the protein structures gradually changed with increasing salt concentration (26),(46). A red shift of the emission peak (to λmax = c. 340 nm), indicating an unfolding transition, was not observed in the three GGTs (Fig. 1-4), including the previously reported salt-tolerant enzymes (26),(46),(49),(50). Such red shifts, which have been observed for many proteins during the unfolding process, are caused by increased solvent accessibility of tryptophan residues (51). Enzymes that tolerate extremely high and moderately high NaCl concentrations are referred to as halophilic and salt-tolerant, respectively. Halophilic enzymes retain their structure and physiological activities under high salt concentration, but not necessarily at low concentrations (52). They can irreversibly denature under the latter conditions (52). Here, effect of NaCl concentration on GGT activity (Fig. 1-3), stability (Fig. 1-6) and structure (Fig. 1-4) indicated that the enzyme activity gradually decreased with increasing NaCl concentration, but the enzyme activity returned to the original level under low NaCl concentration, indicating that the GGT protein structure did not change irreversibly (46). Analysis by far-ultraviolet circular dichroism spectroscopy might provide additional information on changes in α-helix conformation of the three GGTs in the absence and presence of NaCl, as previously investigated (53).

In the absence of glycylglycine (hydrolysis in Table 1-5), AOggtA showed an increase in K_m value for γ-GpNA and decrease in V_{max} value with 20% NaCl; together, these factors resulted in an extreme decrease in catalytic efficiency (k_{cat}/K_m). This also indicated that AOggtA is a non-salt-tolerant type. In contrast, the decrease in catalytic efficiency in ASAOggtA was less than that in AOggtA, and was the result of the decrease in the V_{max} value with 20% NaCl. After formation of the enzyme–substrate complex,

cleavage of the γ-glutamyl bond (hydrolysis step) of γ-GpNA in ASggtA was probably not affected by the presence of NaCl. Under high salt conditions, AOggtA and ASAOggtA were probably affected in both substrate binding and the hydrolysis step. In the presence of glycylglycine (transpeptidation in Table 1-5), the K_m values for γ-GpNA for the three enzymes were lower in the presence of NaCl; however, k_{cat} values were also lower for AOggtA and ASAOggtA. The steps after the formation of the enzyme–substrate complex, such as cleavage of the γ-glutamyl bond and transfer of the γ-glutamyl moiety to glycylglycine, might be affected by NaCl in AOggtA and ASAOggtA. Among the enzymes tested, the k_{cat}/K_m value for ASggtA was still higher than that of AOggtA and ASAOggtA, because the V_{max} and k_{cat} values of ASggtA were not significantly reduced.

Effects of pH and temperature on enzyme activity and stability

ASggtA was notably unstable below pH 5.0 and above pH 10.5, whereas ASAOggtA was as stable as AOggtA over a wide pH range (pH 3.0–10.5), with maximum activity at pH 8.5–9.5 (Table 1-4, Fig. 1-5 and 1-7). In the second stage of soy sauce fermentation (brine fermentation), the pH of the fermenting mixture, consisting of koji and 20% salt brine (called moromi mash), decreases from pH 6.5 to pH 4–5, because of lactic acid fermentation by halophilic lactic acid bacteria (22),(54). Thus, hydrolytic enzymes including GGT that work in the brine fermentation stage is required to have not only salt-tolerance but also pH stability under weak acidic conditions (55). ASAOggtA is considered to be more suitable for the second fermentation step than ASggtA. Bacterial GGTs optimally function under alkaline conditions ranging from pH 8 to pH 11, typically with different pH optima for hydrolysis and transpeptidation reactions (11). *Bacillus* GGTs show good stability in the range pH 6–10 (17),(27), and GGT from *B. subtilis*

reached maximum activities for hydrolysis and transpeptidation at pH 9 and pH 10, respectively (56). The hydrolysis and transpeptidation activities in ASAOggtA reached a maximum at pH 8.0 (Table 1-4 and Fig. 1-7), but the optimal pH for hydrolysis activity was slightly lower than that for transpeptidation activity in AOggtA and ASAOggtA. The T/H ratio of AOggtA, ASggtA, and ASAOggtA at pH 9.0 were 1.7, 2.5, and 2.4, respectively. In contrast, at pH 6.0, the T/H ratio of ASggtA (4.4) was higher than those of AOggtA (2.2) and ASAOggtA (3.0). The optimal temperature for hydrolysis and transpeptidase activities in ASggtA were lowest among three GGTs, because its thermostability and T1/2 value were also low (Table 1-4; Fig. 1-5 and Fig. 1-8). ASAOggtA inherited some features of AOggtA, such as thermostability. Most GGTs from *Bacillus* sp. have been reported to be most active at alkaline pH ranging from pH 8 to pH 10, with varying temperature optima in the range of 37–62 °C (46). To further enhance the thermostability of ASAOggtA, it may be beneficial to consider amino acid substitution. Additionally, immobilization of the chimeric enzyme could be necessary for creating a robust enzyme preparation that exhibits recyclability and storage stability (46). GGT from *B. licheniformis* ER15, immobilized with chitosan, shows promise for potential use in soy sauce brewing (46).

Substrate specificity for γ-glutamyl acceptors

The transfer of the γ-glutamyl group from γ-GpNA to various amino acids, amines, and peptides by AOggtA, ASggtA, and ASAOggtA was examined (Table 1-4). The transfer activity with glycylglycine as the substrate was taken as 100% for each enzyme. From the previously reported substrate specificity of GGT from *A. sydowii* (29), we selected six preferred and four non-preferred amino acids. AOggtA showed higher

activity for the six preferred amino acids than ASggtA. ASAOggtA showed slightly higher activity than ASggtA, with some exceptions (e.g., L-Val). ASAOggtA showed the highest activity toward Gly. AOggtA showed the highest activity towards eight amines. The substrate specificity toward various amino acid acceptors in the R109K mutant of *Bacillus* GGT remained unaltered from the parental GGT (17). In *Aspergillus* GGTs studied here, an Arg residue was conserved at the position 125 in ASggtA and 118 in AOggtA (Fig. 1-1(a)), and so it is probable that there was no change in substrate specificity in ASAOggtA. In a representative soy sauce (Koikuchi soy sauce), the major amino acids are L-Glu (22.5% of total composition) and L-Asp (10.5%) (54). In addition, L-Leu (7.3%), L-Pro (6.5%), L-Lys (6.5%), L-Val (5.5%), and L-Ile (4.8%) are present in substantial quantities (54). To make ASAOggtA suitable for brine fermentation, it is necessary not only to characterize glutamine hydrolysis in the presence of amino acids (such as L-Ile, L-Val, L-Lys from Table 1-4), but also to enhance its hydrolytic activity while decreasing its transpeptidation activity.

Hydrolysis of glutamine by AOggtA, ASggtA, and ASAOggtA

The enzymatic reaction products in the reaction mixture containing 100 mM L-glutamine as substrate were analyzed using HPLC. The products were identified as L-glutamic acid, produced via hydrolysis, and γ-glutamyl-glutamine, produced via auto-transpeptidation. The conversion ratios of γ-glutamyl-glutamine to L-glutamic acid were calculated (Table 1-6). AOggtA and ASAOggtA showed higher hydrolysis activity toward L-glutamine compared with ASggtA. Consequently, the ratios of γ-glutamyl-glutamine to L-glutamic acid were lower for these two enzymes than for ASggtA. For biotechnological applications, it would be desirable to examine the effect of NaCl concentration on the

hydrolysis of L-glutamine, but test samples containing high NaCl concentrations cannot be used for reversed-phase liquid chromatography with the ion-pairing regent, sodium octane sulfonate.

The use of flavor enhancers including glutamate can help to reduce excessive salt intake, which contributes to cardiovascular disease (57). To effectively use ASAOggtA for glutamine hydrolysis and increase glutamate production in brine fermentation, it is desirable to eliminate its transpeptidation activity while enhancing its hydrolytic activity by substituting key amino acid residues. For example, in GGT from *B. licheniformis* ER-15 (EU293873.1), the R109M and R109L mutants retained only hydrolytic activity (17). GGTs from *Thermus thermophilus* HB27 (WP_011172851.1) (58) and *Picrophilus torridus* DSM 9790 (WP_011177986.1) (59) showed only hydrolysis activity. Multiple alignment analysis revealed that ^{109}Arg in ER-15 GGT was conserved at position 125 of ASggtA and position 118 of AOggtA, and the residue was replaced with serine at position 84 of HB27 GGT and position 68 of DSM 9790 GGT (Fig. 1-1(a) and Fig. 1-9). Furthermore, ^{125}Arg in ASggtA and ^{109}Arg in ER-15 GGT were located in the same position in the structure models of ASggtA and ER-15 GGT, which were predicted from the template model (PDB ID, 4OTT). Substituting the ^{125}Arg residue in ASAOggtA might achieve functional modification to improve hydrolytic activity and salt-tolerance simultaneously (17).

Functional modification through protein chimerization

Construction of chimeric enzymes has proven to be a useful strategy for investigating structure–function relationships in the parental enzymes of chimeras and for modifying catalytic properties, thermo- and/or pH-stability (60),(61). Previous studies

have shown that thermostability can be improved by swapping the N-terminal or C-terminal region between homologous enzymes, because the literature on TIM barrel enzymes (62) suggests that the amino acid residues contributing to thermostability are most likely to be located in the N-terminal region. Moreover, chimeric enzymes can inherit some characteristics from each parental enzyme (63),(64). For instance, a chimeric enzyme consisting of 26% of the N-terminal region of polyhydroxyalkanoate synthase from *Aeromonas caviae* (PhaCAc) and 74% of the C-terminal of PhaCRe inherits broad substrate specificity and produces short and medium-chain-length polyhydroxyalkanoates (64).

In the case of the chimeric ASAOggtA, the mature protein (564 amino acids) consists of 21.8% from the N-terminal region of ASggtA and 78.2% from the C-terminal region of AOggtA (Fig. 1-1(a)). Our results suggest that a relatively limited region might contribute to improving salt-tolerance. However, there was no substantial difference in the number of polar amino acid residues in the focused N-terminal region (Fig. 1-1(a)), as described earlier. It is also worth noting that the improvement in salt-tolerance obtained by protein chimerization cannot be explained solely by changes in the number of polar amino acid residues located on the protein surface.

The location and structure of the mature N-terminal regions of AOggtA (^{28}Ser to ^{45}Glu) and ASggtA (^{28}Ser to ^{52}Ala) cannot be predicted from the crystallographic structure of GGT from *E. coli* K-12 (2E0W). Thus, crystal structure analyses of parental and/or chimeric enzymes will be necessary to clarify the mechanism of salt-tolerance in *Aspergillus* GGTs. Furthermore, it is expected that these analyses will lead to further improvements in salt-tolerance and hydrolysis activity under saline conditions.

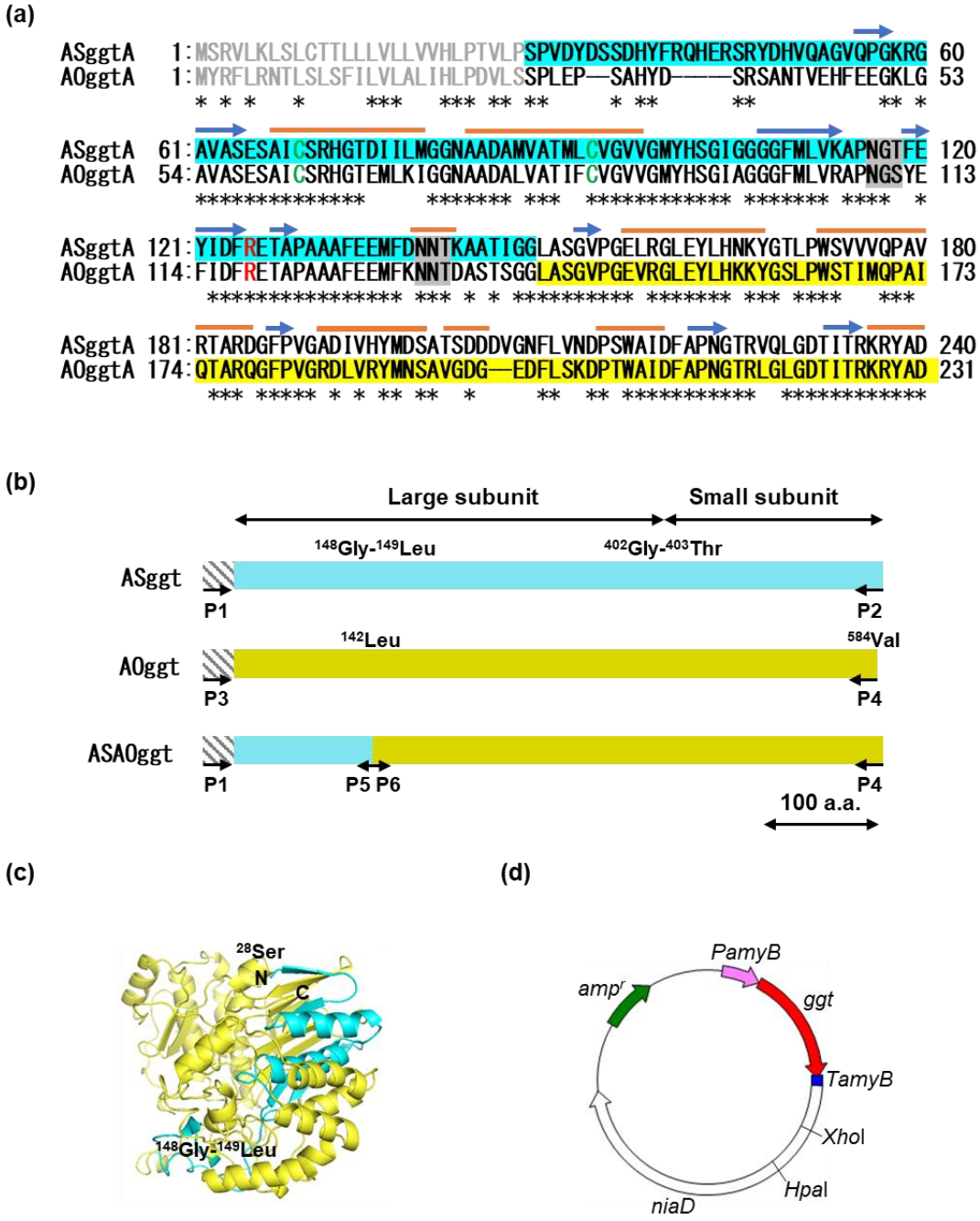

Fig. 1-1. Construction and expression of chimeric γ-glutamyl transpeptidase. (a) Multiple sequence alignment of N-terminal regions of salt-tolerant ASggtA and non-salt-tolerant AOggtA. Identical residues are indicated by an asterisk; similar residues are indicated by a period or colon. Disulfide-forming Cys residue and substrate-binding

residue are shown in green and red, respectively. The secondary structure α-helices (orange bar) and β-strands (blue arrow) inferred from the *E. coli* enzyme structure (2E0W) are shown above the alignment. **(b)** Construction strategy for chimeric enzyme (ASAOggtA) between ASggtA (cyan) from *A. sydowii* MA0196 and AOggtA (yellow) from *A. oryzae* NBRC 100959. In γ-glutamyl transpeptidase, after cleavage of the signal peptide (shown as diagonal lines), the resulting unique precursor pro-GGT is modified through a self-proteolytic cleavage event (termed auto-processing) to yield an active mature heterodimer of large and small subunits (11). The positions for focused fusion and self-proteolytic cleavage in ASggtA are shown as ^{148}Gly–^{149}Leu and ^{402}Gly–^{403}Thr, respectively. PCR primers, P1 to P6 (Table 1-1) for amplification of each gene fragment are shown by arrows. **(c)** Predicted ASggtA structure. Structural modeling of ASggtA was performed using the SWISS-MODEL web server. γ-Glutamyl transpeptidase from *E. coli* K-12 (2E0W) was used as a modeling template. N- and C- terminal positions are shown. **(d)** Structure of the vector used for gene expression. The recombinant enzymes reported here were expressed in *A. oryzae* niaD^{-} (40).

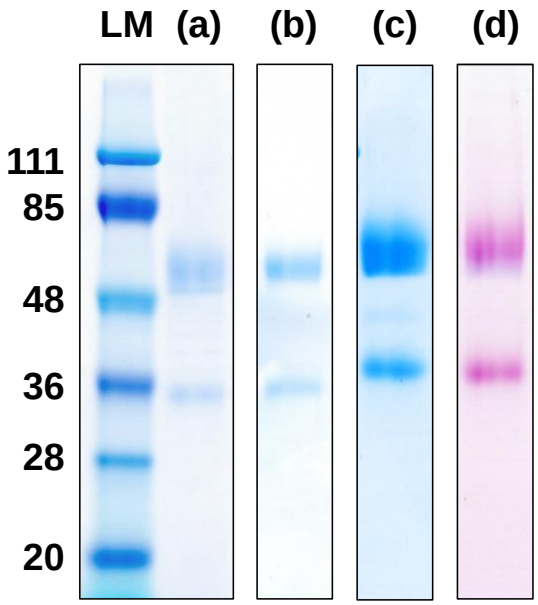

Fig. 1-2. SDS-PAGE analysis of the purified γ-glutamyl transpeptidases, AOggtA, ASggtA, and ASAOggtA. The purified samples (1–3 μg protein) were electrophoresed on a 12.5% precast-gel (ePAGEL, catalog number E-T12.5L (ATTO Corp., Tokyo, Japan) using an ATTO AE6530 gel electrophoresis system, following the manufacturer's instructions. Protein molecular mass markers (broad range type: 9–200 kDa) were from Nacalai Tesque Inc. The protein bands were detected by EzStain AQua AE-1340, according to the manufacturer's instructions. Lanes: LM, protein molecular mass markers (broad-range type: 9–200 kDa, Nacalai Tesque, Inc.); **(a),** AOggtA; **(b)**, ASggtA; **(c)**, ASAOggtA (approximately 3 μg of protein, Coomassie blue staining with EzStain Aqua (ATTO Co.); and **(d)**, Purified ASAOggtA (approximately 3 μg of MA0196 GGT, Periodic acid Schiff staining (65)).

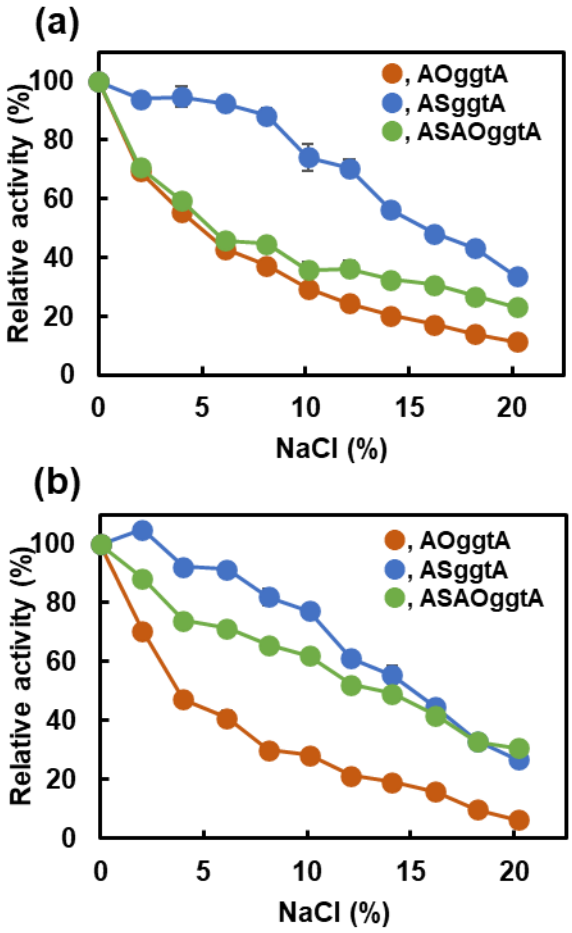

Fig. 1-3. Effect of NaCl concentration on enzyme activity. The reaction mixture containing 50 mM Tris–HCl (pH 7.5), 0.5 mM L-γ-glutamyl-p-nitroanilide, and the purified γ-glutamyl transpeptidase in the presence ((a) for hydrolysis assay) and absence ((b) for transpeptidase assay) of 33 mM glycylglycine was incubated at 30 °C. The reaction mixture consisted of various concentrations of NaCl (0–20% (w/v) final concentration). The relative activities were calculated based on hydrolysis and transpeptidase activities in the absence of NaCl. In AOggtA, ASggtA, and ASAOggtA, the specific activities for hydrolysis and transpeptidation without NaCl were 6.2 and 9.1 U/mg, 4.7 and 15 U/mg, and 7.1 and 14 U/mg, respectively.

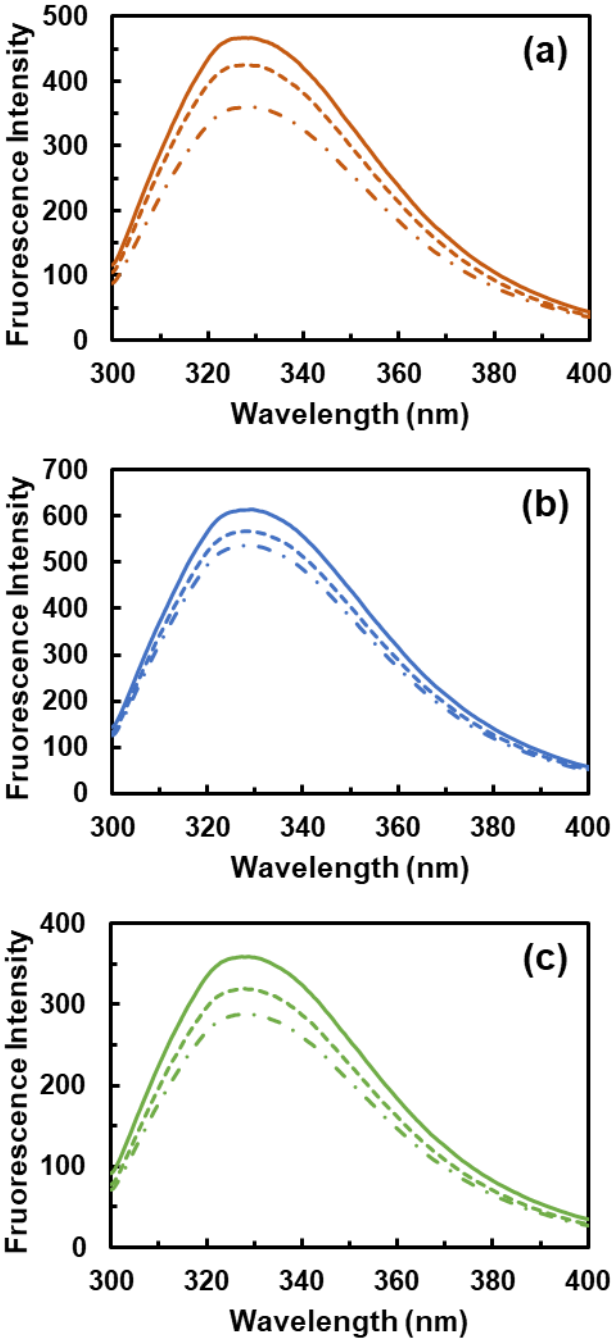

Fig. 1-4. Emission fluorescence spectra of (a) AOggtA, (b) ASggtA, and (c) ASAOggtA. The spectra were obtained using γ-glutamyl transpeptidase (0.07–0.1 mg protein/mL in 20 mM Tris–HCl buffer (pH 7.5)) in the absence (solid line) and presence of 10% NaCl (dashed line) and 20% NaCl (dashed-dotted line). The excitation

wavelength was 280 nm and emission spectra were recorded in the range 300–400 nm using a Hitachi F-270 fluorescence spectrophotometer (Tokyo, Japan).

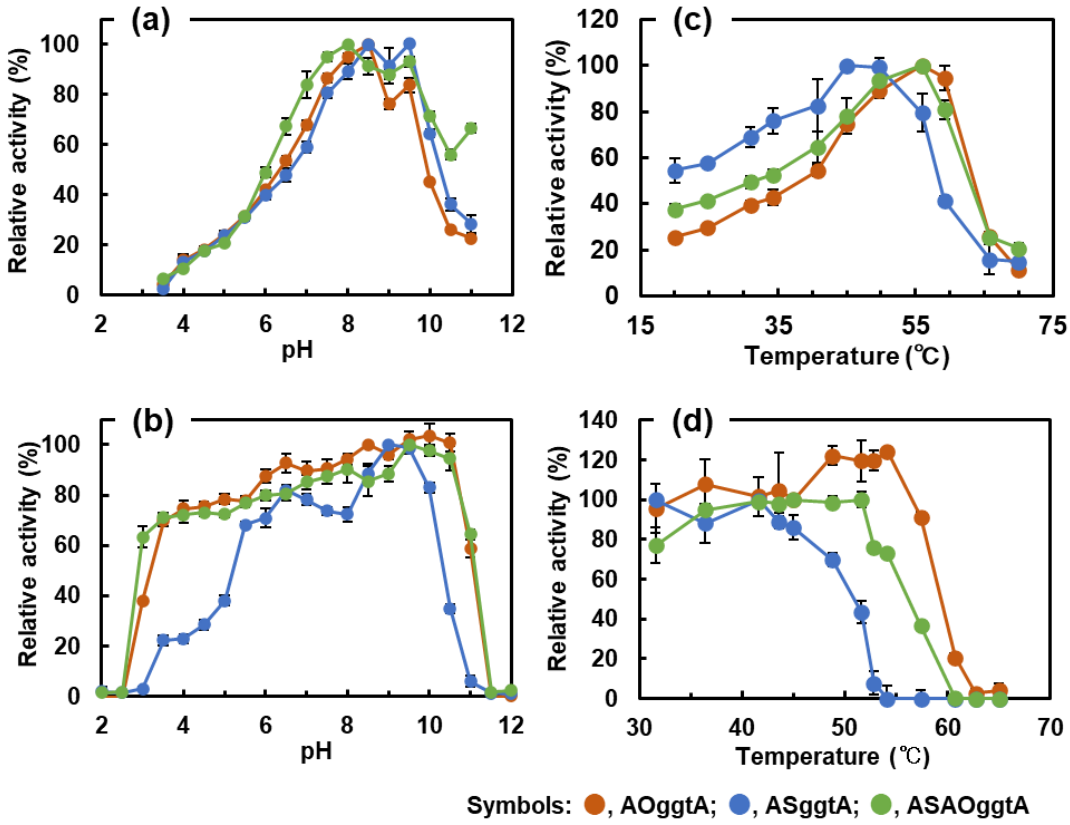

Fig. 1-5. Effect of pH and temperature on enzyme activity and stability. The effect of pH was tested using different buffers: 100 mM Na_2HPO_4–100 mM citric acid buffer (pH 2.0–3.0); GTA buffer (pH 3.5–10.5); and 100 mM Na_2HPO_4–100 mM NaOH buffer (pH 11.0–12.0). **(a)** Effect of pH on enzyme activity. Hydrolysis activities were measured using the purified γ-glutamyl transpeptidases over the range pH 2.0–12.0. The relative activities were calculated based on hydrolysis activity under maximal condition. For AOggtA, ASggtA, and ASAOggtA, the specific activities of hydrolysis were 7.2 U/mg (pH 8.5), 5.8 U/mg (pH 8.5), and 7.1 U/mg (pH 8.0), respectively. **(b)** pH stability. The pH stability of the γ-glutamyl transpeptidases was determined by mixing the concentrated purified enzyme with buffer (pH 3.5–11.0) at 4 °C for 15 h. For AOggtA, ASggtA, and ASAOggtA, the specific activities of hydrolysis were 6.8 U/mg (pH 8.5), 6.3 U/mg (pH 9.0), and 8.1 U/mg (pH 9.5), respectively. **(c)** Effect of

temperature on enzyme activity. The effect of temperature on the hydrolysis activities of the purified enzyme was determined over a temperature range 20–70 °C. For AOggtA, ASggtA, and ASAOggtA, the specific activities of hydrolysis were 13.4 U/mg (56 °C), 6.2 U/mg (45 °C), and 10.1 U/mg (50 °C), respectively. **(d)** Thermostability. The purified enzymes were pre-incubated at various temperatures (10–70 °C) for 10 min, then residual activities were measured. For AOggtA, ASggtA, and ASAOggtA, the specific activities of hydrolysis at 40 °C were 6.2 U/mg, 4.7 U/mg, and 7.1 U/mg, respectively.

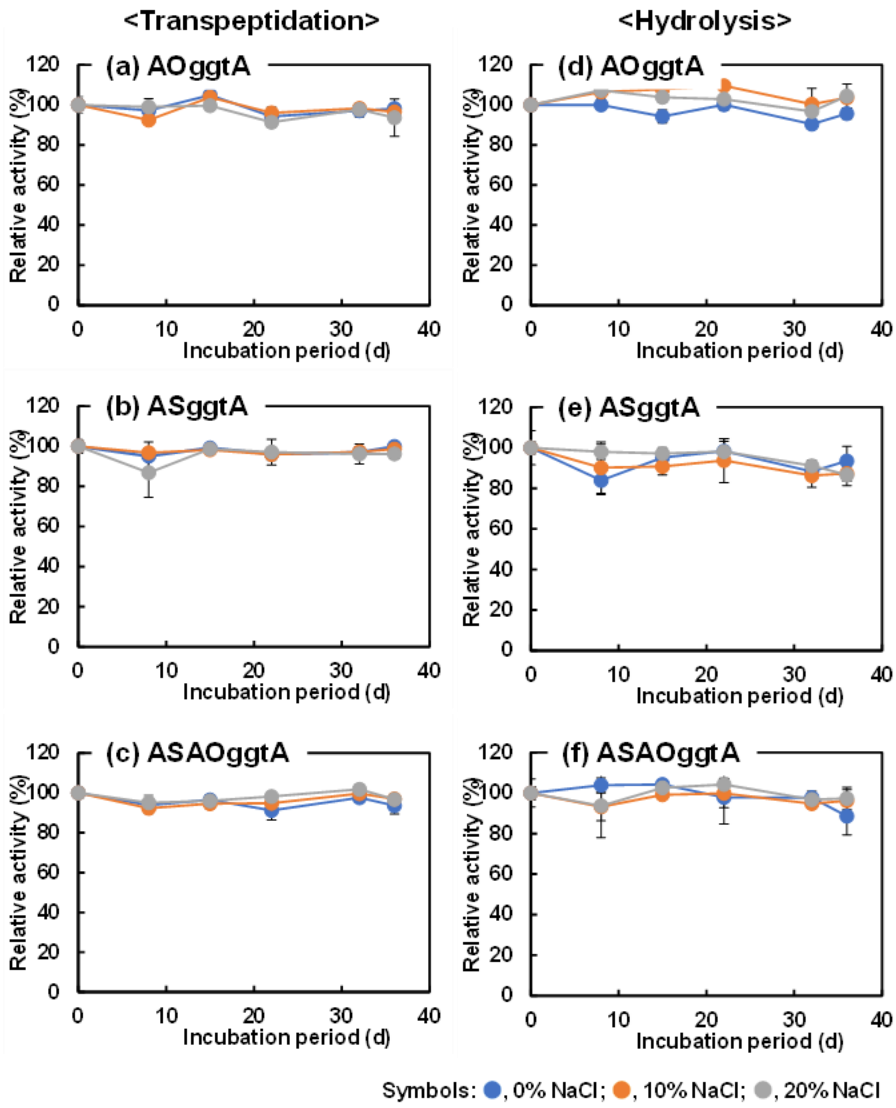

Fig. 1-6. Effect of NaCl concentration on stability. The reaction mixture containing 50 mM Tris-HCl (pH 7.5), 0.5 mM L-γ-glutamyl-*p*-nitroanilide, and the purified γ-glutamyl transpeptidase in the presence [(a) AOggtA, (b) ASggtA, and (c) ASAOggtA] and absence [(d) AOggtA, (e) ASggtA, and (f) ASAOggtA] of 33 mM glycylglycine was incubated at 40 °C. The purified enzymes were incubated in 20 mM Tris-HCl buffer (pH 7.5) without and with 10% (w/v) NaCl and 20% (w/v) NaCl at 4 °C for 3 months. In AOggtA, ASggtA, and ASAOggtA, the specific activities for transpeptidation and hydrolysis at the initial

day were 9.1 and 6.2 U/mg, 15 and 4.7 U/mg, and 14 and 7.1 U/mg, respectively. The relative activity was calculated based on these specific activities.

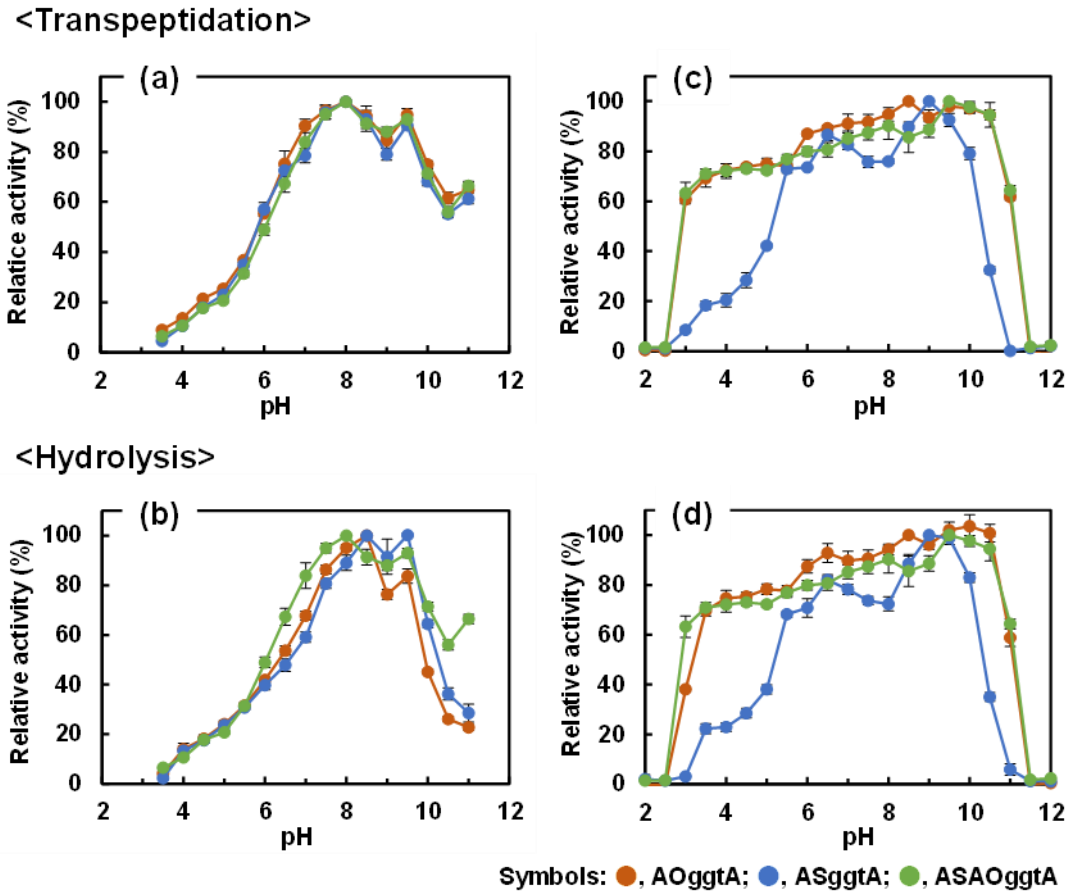

Fig. 1-7. Effect of pH on enzyme activity and stability of γ-glutamyl transpeptidases, AOggtA, ASggtA, and ASAOggtA. (a) and (b) Effect of pH on enzyme activities. The pH (3.5 to 11) of 100 mM 3,3-dimethylglutaric acid (G), 100 mM tris(hydroxymethyl)aminomethane (T), and 100 mM 2-amino-2-methyl-1,3-propanediol (A) was adjusted by the addition of 1.0 N HCl and 1.0 N NaOH, according to the previously described procedure for GTA buffer preparation (43). Transpeptidation (a) and hydrolysis (b) activities were measured using purified AOggtA, ASggtA, and ASAOggtA in 100 mM GTA buffer (pH 3.5–11) at 40 °C. The reaction mixture contained 0.5 mM L-γ-glutamyl-p-nitroanilide in the presence (for transpeptidase assay) and absence (for hydrolysis assay) of 33 mM glycylglycine. In AOggtA, ASggtA, and ASAOggtA, the specific activities for transpeptidation and hydrolysis were 9.1 (pH 8.0)

and 7.2 (pH 8.5) U/mg, 15 (pH 8.0) and 5.8 (pH 8.5) U/mg, and 14 (pH 8.0) and 7.1 (pH 8.0) U/mg, respectively. The relative activity was calculated based on these specific activities.

(c) and (d) pH stability. The pH stability of purified enzyme was determined by mixing the concentrated purified enzyme with 100 mM KCl-HCl buffer (2.0-3.0), 100 mM GTA buffer (pH 3.5–11.0), and 100 mM Na2HPO4-NaOH buffer (pH 11.5-12) at 4 °C for 15 h. The enzyme solution was concentrated 10-fold using an Amicon Ultra-15 filter (Merck KGaA). The concentrated enzyme solution and each buffer solution were mixed at a ratio of 1:9 (v/v), and the remaining transpeptidation and hydrolysis activities were measured at 40 °C. In AOggtA, ASggtA, and ASAOggtA, the specific activities for transpeptidation and hydrolysis were 9.9 (at pH 8.5) and 6.8 (at pH 8.5) U/mg, 19.8 (at pH 9.0) and 6.3 (at pH 9.0) U/mg, and 16 (at pH 9.5) and 8.1 (at pH 9.5) U/mg, respectively. The relative activity was calculated based on these specific activities.

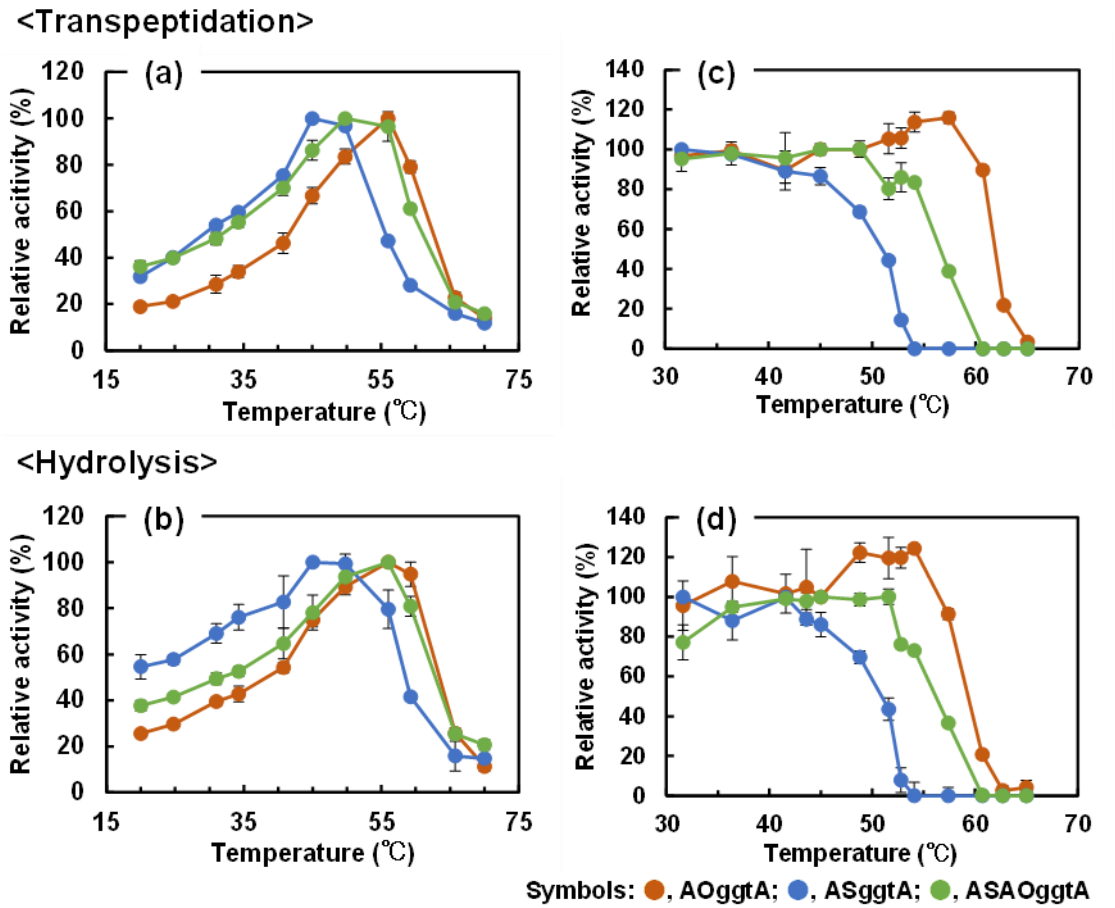

Fig. 1-8. Effect of temperature on enzyme activity and stability of γ-glutamyl transpeptidases, AOggtA, ASggtA, and ASAOggtA. (a) and (b) Effect of temperature on enzyme activities. Transpeptidation (a) and hydrolysis (b) activities of the purified enzyme at pH 8.0 were determined over a temperature range 20–70 °C. The reaction mixture containing 100 mM Tris-HCl (pH 8.0), 0.5 mM L-γ-glutamyl-*p*-nitroanilide, and the purified enzyme in the presence (for transpeptidase assay) and absence (for hydrolysis assay) of 33 mM glycylglycine was incubated at various temperature for 20 min. The maximal activities of transpeptidation and hydrolysis of AOggtA, ASggtA, and ASAOggtA were 19.7 (56 °C) and 13.4 (56 °C) U/mg, 19.9 (45 °C) and 6.2 (45 °C) U/mg, and 20 (50 °C) and 10 (50 °C) U/mg, respectively. The relative activities were calculated based on these specific activities.

(c) and (d) Thermostability. The purified enzyme was pre-incubated at various temperatures (32–65 °C) for 10 min, and the remaining transpeptidation (c) and hydrolysis (d) activities were then measured at 30 °C, as described above. The specific activities of transpeptidation and hydrolysis of AOggtA, ASggtA, and ASAOggtA preincubated at 30 °C for 10 min were 9.1 and 6.2 U/mg, 15 and 4.7 U/mg, and 14 and 7.1 U/mg, respectively. The remaining activities was calculated based on these specific activities.

```
ASggtA    1:MSRVLKLSLCTTLLLVLLVVHLPTVLPSPVDYDSSDHYFRQHERSRYDHVQAGVQPGKRG 60
BLggt     1:---------MRR-----LAFLVVAFCLAVGCFFSPVSKAEGVMSGG---DGDKVAVGKDG 43
BSggt     1:---------MKRTWNVCLTALLSVLLVAGSVPFHAEAKKP-PKSYD---EYKQVDVGKDG 47
ECggt     1:----------MIKLTFLRRVAIAALLSGSCFSAAAAPPAPPVSYGVEEDVFHPVRAKQG 49
PNggt     1:----------------MRVFHFSKLPLGVAILAASSS-----------VFATLDG--G 29
GTggt     1:-----------------MDYLYHPYPS---------------------QRMTVFAKNG 20
PTggt     1:-------------------------------------------------MYMNY 5
                              .       .                        . .

ASggtA   61:AVASESAICSRHGTDIILMGGNAADAMVATMLCVGVVGMYHSGIGGGGFMLVKAPN-GTF 119
BLggt    44:MVATAHPLASKIGAEVLKKGGNAIDAAIAIQYALNVTEPMMSGIGGGGFMMVYDGETKET 103
BSggt    48:MVATAHPLASEIGADVLKKGGNAIDAAVAIQFALNVTEPMMSGIGGGGFMMVYDGKTKDT 107
ECggt    50:MVASVDATATQVGVDILKEGGNAVDAAVAVGYALAVTHPQAGNLGGGGFMLIRSKN-GNT 108
PNggt    30:AVAAPDQYGAKVAAEILKKGGNAVDAAVATAFTLAVTYPEAGNIGGGGFMTLYVD--GKP 87
GTggt    21:IVATSQPLAAQAGLEVLKKGGNAIDAAIATAACLTVVEPTSNGIGGDAFALVWTNG--KL 78
PTggt     6:AVASSHPLSTFVGNEILKDGGNAYDAAIATSAALVVVQPHLNGLGGDFFSTIIDN---DI 62
             **   ...   . .....**** **..*.  .. *. .   ..**..*. .

ASggtA  120:EYIDFRETAPAAAFEEMFDNN------TKAATIGGLASGVPGELRGLEYLHNKYGTLPWS 173
BLggt   104:SIINSRERAPEGAKPDMFLDEDGKVIPFSERSRHGNAVGVPGTLKGLEAAHKKWGTKKME 163
BSggt   108:TIIDSRERAPAGATPDMFLDENGKAIPFSERVTKGTAVGVPGTLKGLEEALDKWGTRSMK 167
ECggt   109:TAIDFREMAPAKATRDMFLDDQGNPDSKKS-LTSHLASGTPGTVAGFSLALDKYGTMPLN 167
PNggt    88:YFLDYREIAPKAATKTMYLNEKGEVIENLS-LVGAKAAGVPGTVMGLWEAHQRFGKLKWS 146
GTggt    79:YGLNASGYAPAAISLDVLKERGYTEMPKYG----FAPVTVPGAPAAWAALSKRFGRLSLA 134
PTggt    63:YSINGSGNAPELATIEFFHRNGYNKIPEQG---PLSSFSIPGLVSSWEILYKN-ATMKLE 118
               .. .. **. .. ....   .  ..          . ..**.  ... .  . ..

ASggtA  174:VVVQPAVRTARDGFPVGADIVHYMDSATSDDDVGNFLVNDPSWAIDFAPNGTRVQLGDTI 233
BLggt   164:DLISPSIKLTEEGFPIDSVLADAIKDH------QDKLSKT-AAKDIFLPDGEPLKEGDIL 216
BSggt   168:QLITPSIKLAEKGFPIDSVLAEAISDY------QEKLSRT-AAKDVFLPNGEPLKEGDTL 220
ECggt   168:KVVQPAFKLARDGFIVNDALADDLKTYG-----SEVLPNHENSKAIFWKEGEPLKKGDTL 222
PNggt   147:ELLTPAIGYAQTGFKV----ADQQYQYR-----QDAIALF-NGKTNFGDYFGTMKPGEVF 196
GTggt   135:ETLAPAIAYAENGYPVSPVLGKYWANAYRVYKEALHGPEFGSWFETFAPAGRAPNIGEVW 194
PTggt   119:KLFSRAISFAMDGFIPSNSILKAIKNFK---------------YGDVDFNNIYYNNERLL 163
             .  ...  .  *...   ..                .      .  . . . .  . .. .

ASggtA  234:TRKRYADTLETIGSEGPGAFYEGPIAETTIRALQKANGTMTLEDLRGYKAVVRNISQIDY 293
BLggt   217:VQKDMAKTFKLIRKEGSKAFYDGEIGRAIADVVQDFGGSMTPDDLSRYEVTTDKPIWGEY 276
BSggt   221:IQKDLAKTFKLIRSKGTDAFYKGKFAKTLSDTVQDFGGSMTEKDLENYDITIDEPIWGDY 280
ECggt   223:VQANLAKSLEMIAENGPDEFYKGTIAEQIAQEMQKNGGLITKEDLAAYKAVERTPISGDY 282
PNggt   197:KQPELAKTLERIADKGPDDFYKGETAKLLIAQMKQDGGLITSDDLVDYQAKWREPMRIDW 256
GTggt   195:ASPDHAATLRSIAETEAESFYRGELAEKIVAFSKQYNGFLTLEDLAEYEPEWVEPISVSY 254
PTggt   164:VQRALGKTLKLLAEKGLESFYHGDIARAIEDDMIKKHGLIRFNDLDSYSASVVKPLEIRY 223
             .  .....  ..  .   ** * ..  .    .  .* .  **  * .   ..  ..

ASggtA  294:RGYRVTSTTTPSSG-TVALNMLKVLDTYGPLFGPDNVN--LSTHRMDEAMRFGYGLR-TV 349
BLggt   277:HGYDIASMPPPSSGGVFMLQMLKLIDD--FHLSQYDPKSFEKYHLLAETMHLSYADRAAY 334
BSggt   281:QGYQIATTPPPSSGGIFLLQMLKILDH--FNLSQYDVRSWEKYQLLAETMHLSYADRASY 338
ECggt   283:RGYQVYSMPPPSSGGIHIVQILNILEN--FDMKKYGFGSADAMQIMAEAEKYAYADRSEY 340
PNggt   257:QGNTLYTAPLPSSGGIALAQLIGIKEQRAADFKGVELNSAKYIHLLSEIEKRVFADRADY 316
GTggt   255:HGYDVWEIP-PNGQGLVALMALNIMNG----FDVPNVPDVETYHRQIEAMKLAFADGKAY 309
PTggt   224:RNYSVYTNP-PVSQGATALYWLNRLNK----YDLYTMPDDLYYSSLINEMYPSYEFRKSM 278
             .. .   . *....   .. . ..          .   .   .. . . .   .... .
```

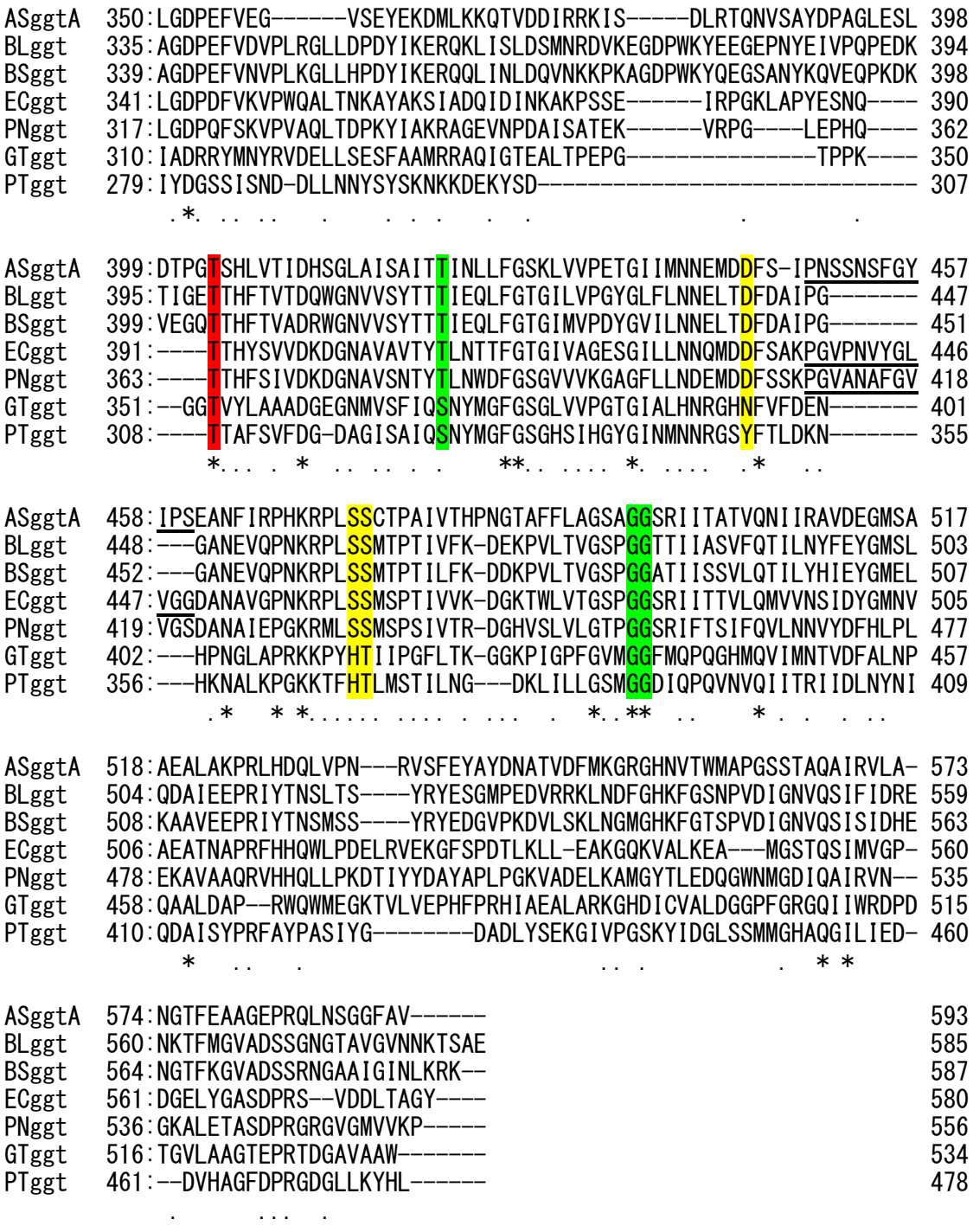

Fig. 1-9. Multiple sequence alignment of γ-glutamyltranspeptidase (ASggtA) from *A. sydowii* MA0196 with other bacterial and eukaryotic homologues. The amino acid sequence of ASggtA was aligned with those of *E. coli* (WP_160532025), *B. licheniformis* ER-15 (EU293873), *B. subtilis* 168 (NP_389723), *Pseudomonas*

nitroreducens NBRC 12694 (AB548627), *Geobacillus thermodenitrificans* NG80-2 (ABO68619), *Picrophilus torridus* (WP_011177986), according to the previously reported multiple sequence aliment analysis (58). The conserved Thr residues (^{403}Thr in ASggtA) responsible for autoprocessing of the enzyme are highlighted in red. Residues conserved or semi-conserved in all γ-GTs and involved in binding of the γ-glutamyl moiety (^{409}Thr, ^{483}Gly, and ^{484}Gly in ECggt) are highlighted in green. The other residue responsible for substrate binding and catalytic activity of GGTs, but not conserved in GTggt and PTggt are highlighted in yellow (^{114}Arg, ^{433}Asp, ^{444}Tyr, ^{462}Ser, and ^{463}Ser in ECggt). The lid loop extending towards the active site (spanning from ^{438}Phe to ^{449}Gly of EcGT) in ASggtA, ECggt, and PNggt is underlined.

Table 1-1. Primer list in this study

No.	Primer	Sequence (5' to 3')
P1	AS_ggtB_infF	AAACCCCACAGAAGGCATTTATGTCGCGTGTTTTGAAACTC
P2	AS_ggtB_infR	TCTCCACCCTTCTAGACTAGACAGCAAACCCCCCAG
P3	AO_ggtA_infF	AAACCCCACAGAAGGCATTTATGTATCGTTTTTTAAGGAA
P4	AO_ggtA_infR	TCTCCACCCTTCTAGATCAGACCGCGAAACCACCAG
P5	AS_ggtB_468nt_R	TTCGCCGGGGACGCCACTTGCTAGC
P6	AO_ggtA_1305nt_infF	GGCGTCCCCGGCGAAGTGCGAGGCCTGGAATACCT
P7	Amp-F [#]	GCTAGAGTAAGTAGTTCGCCAGTTA
P8	Amp-R [#]	TCGCCTTGATCGTTGGGAAC
P9	NucS1-F [#]	TGCCCTGAAATTCGTGGTTCA
P10	NucS1-R [#]	CGTCACATCAATACCGTTACCAC

[#] The copy number for each GGT gene and the reference gene, *nuc*S (D45902.1), was quantified by real-time PCR using fluorescent probes (P7 to P10) according to the previously reported procedures (41). Quantitative PCR was performed using a Thermal Cycler Dice Real Time System III (Takara Bio Inc.) and a Probe qPCR Mix (Takara Bio Inc.). Normalized copy numbers were calculated using the *ΔΔ*Ct method with *nuc*S as the house-keeping gene.

Table 1-2. Heterologous expression of γ-glutamyl transpeptidases in *A. oryzae* transformants

Strain	Enzyme activity (mU/mL)		Copy number of GGT gene
	Hydrolysis	Transpeptidation	
A. sydowii MA0196 [a]	6.42±0.72	33.3±0.55	–
A. oryzae niaD^{-}	0.98±0.13	1.2±0.3	–
AOggtA-transformant	70.6±2.4	87.2±4.7	1
ASggtA-transformant	58.2±1.7	150±3.2	6
ASAOggtA-transformant	110±3.3	176±6.5	5

[a] (29). [b] Auxotrophic host strain as control.

Table 1-3. Summary of the purification of γ-glutamyl transpeptidases

(a) AOggtA from *A. oryzae*

Fraction	Total activity (mU)		Total protein (mg)	Specific activity (mU/mg)		Recovery (%)	
	T	H		T	H	T	H
CEP	4,400	3,500	74	60	50	100	100
DEAE-Toyopearl	3,700	2,800	19	200	150	84	80
Butyl-Toyopearl	1,500	900	0.19	7,900	4,700	34	26
Soluble starch affinity	410	280	0.045	9,100	6,200	9	8

(b) ASggtA from *A. sydowii*

Fraction	Total activity (mU)		Total protein (mg)	Specific activity (mU/mg)		Recovery (%)	
	T	H		T	H	T	H
CEP	8,000	3,000	90	90	30	100	100
DEAE-Toyopearl	7,400	2,800	0.52	14, 000	5,400	93	93
Butyl-Toyopearl	5,300	1,700	0.36	15,000	4,700	66	57

(c) Chmeric ASAOggtA

Fraction	Total activity (mU)		Total protein (mg)	Specific activity (mU/mg)		Recovery (%)	
	T	H		T	H	T	H
CEP	8,800	5,500	115	77	48	100	100
DEAE-Toyopearl	7,300	4,100	19	380	220	83	75
Butyl-Toyopearl	4,600	2,200	6.3	730	350	52	40
Soluble starch affinity	2,300	1,200	0.17	14,000	7,100	26	22

Abbreviations: CEP, crude enzyme preparation; T, transpeptidation activity; H, hydrolysis activity.

DEAE-Toyopearl chromatography: Cultural supernatant (45 mL) was dialyzed twice against 1 L of 20 mM Tris–HCl buffer (pH 7.5) (buffer A), then 50 mL of the dialyzed enzyme solution was loaded onto a DEAE-Toyopearl column (1.5 × 28 cm, Tosoh

Corp., Tokyo, Japan) equilibrated with buffer A. After loading, the column was washed with three column volumes (150 mL) of buffer A. Proteins were eluted with a linear gradient (0–0.3 M) of NaCl in 750 mL buffer A. The flow rate was 1.0 mL/min and 7 mL fractions were collected.

Butyl-Toyopearl chromatography: The pooled fraction was adjusted to a final concentration of 2 M ammonium sulfate and loaded onto a Butyl-Toyopearl column (1.5 × 18 cm, Tosoh Corp.) equilibrated with buffer A containing 2 M ammonium sulfate. After loading, the column was washed with three column volumes (90 mL) of buffer A containing 2 M ammonium sulfate. Proteins were eluted with a linear gradient (2.0–0 M) of ammonium sulfate in 450 mL of buffer A. The flow rate was 1.0 mL/min, and 6 mL fractions were collected.

Protein contents were measured using BCA protein assay kit (Nacalai Tesque, Kyoto, Japan) and bovine serum albumin as a standard, according to the manufacturer's instructions.

Table 1-4. Catalytic properties of γ-glutamyl transpeptidases, AOggtA, ASggtA, and ASAOggtA.

Effects of various factors on the enzyme activity			
	AOggtA	ASggtA	ASAOggtA
Optimum temperature [a, d]	56 °C 56 °C	45 °C 45 °C	56 °C 50 °C
Optimum pH [a, d]	7.5−9.5 (> 80%) 7.0−9.5 (> 80%)	7.5−9.5 (> 80%) 7.0−9.5 (> 80%)	7.0−9.5 (> 80%) 7.0−9.5 (> 80%)
Substrate specificity toward α-amino acid, amine, and peptide [b]			
L-Met	71.6 ± 3.8%	45.0 ± 1.2 %	53.5 ± 1.2%
L-Ile	69.5 ± 2.3%	37.1 ± 1.2%	43.6 ± 1.5%
L-Val	51.4 ± 1.7%	35.1 ± 1.6%^{A}	34.8 ± 0.39%^{A}
L-Leu	67.4 ± 2.5%	34.5 ± 0.83%	43.0 ± 0.68%
L-Lys	61.3 ± 1.4%	35.2 ± 0.86%	38.1 ± 0.87%
L-Typ	64.1 ± 1.2%	31.7 ± 0.22%	44.3 ± 0.90%
L-Ala	8.73 ± 0.55%^{B}	5.43 ± 1.0%	9.60 ± 0.55%^{B}
Gly	14.0 ± 0.59%	3.74 ± 0.60%	20.2 ± 0.58%
L-Cys	2.18 ± 0.83%^{C}	0.53 ± 0.86%^{C}	< 0.5%^{C}
L-Asp	3.00 ± 1.2%^{D}	< 0.5%	1.11 ± 0.54%^{D}
Beta-Alanine	55.7 ± 1.3%	29.6 ± 0.42%	41.9 ± 0.42%
Ethylamine	69.4 ± 1.4%	37.4 ± 0.47%	42.4 ± 0.90%
Taurine	77.0 ± 1.3%	46.8 ± 0.36%^{E}	51.1 ± 1.49%^{E}
Creatine	70.1 ± 1.6%	35.9 ± 0.36%	45.1 ± 1.3%
Creatinine	71.0 ± 0.87%	35.2 ± 1.1%	45.5 ± 1.3%
Gly-Gly	100%	100%	100%
Anserine	56.6 ± 1.1%	29.1 ± 0.32%	35.3 ± 1.2%
Carnosine	68.9 ± 1.1%	36.3 ± 0.43%	45.4 ± 1.3%
Gly-Glu	24.0 ± 1.3%	15.6 ± 1.1%^{F}	16.4 ± 0.59%^{F}
Stability			
Temperature [c, d]	~57 °C (> 80%) ~57 °C (> 80%)	~45 °C (> 80%) ~45 °C (> 80%)	~52 °C (> 80%) ~54 °C (> 80%)
$T_{1/2}$	22.5 min (57.5°C) 32.5 min (57.5°C)	10 min (50°C) 12.5 min (50°C)	16 min (55°C) 20.5 min (55°C)
pH [c, d]	3.0−10.5 (> 60%) 3.5−11.0 (> 60%)	5.5−10.0 (> 60%) 5.5−10.0 (> 60%)	3.0−11.0 (> 60%) 3.0−11.0 (> 60%)

[a] Effects of pH and temperature on hydrolysis and transpeptidase activities are shown in Fig. 1-5, 1-7, and 1-8.

[b] Relative activities sharing a superscript capital letter were not significantly different at the 5% level.

[c] pH- and thermo- stabilities of AOggtA, ASggtA, and ASAOggtA are shown in Fig. 1-

5, 1-7, and 1-8.

[d] Hydrolysis and transpeptidase activities were shown in the upper and lower rows, respectively.

Table 1-5. Effect of NaCl concentration on kinetic parameters for hydrolysis and transpeptidase activities of γ-glutamyl transpeptidases, AOggtA, ASggtA, and ASAOggtA.

	K_m (mM)	V_{max} (μmol/min/mg protein)	k_{cat} (s^{-1})	k_{cat}/K_m (M^{-1} s^{-1})
Hydrolysis				
AOggtA				
0	0.35 ± 0.036	9.57 ± 1.06	9.55 ± 1.06	27.6 ± 1.48
20% (w/v) NaCl	1.40 ± 0.51	4.26 ± 1.71	4.25 ± 1.70	3.00 ± 0.23
ASggtA				
0	0.17±0.016	8.45±0.43	8.57±0.44	50.3±4.35
20% (w/v) NaCl	0.17±0.029	7.43±0.45	7.54±0.46	44.1±5.33
ASAOggtA				
0	0.27 ± 0.038	10.3 ± 1.27	10.47 ± 1.29	39.2 ± 2.31
20% (v/v) NaCl	0.18 ± 0.037	1.97 ± 0.23	2.00 ± 0.23	11.6 ± 1.15
Transpeptidation				
AOggtA				
0	1.13 ± 0.16	27.1 ± 5.15	27.1 ± 5.14	23.9 ± 1.07
20% (w/v) NaCl	0.34 ± 0.057	1.82 ± 0.18	1.82 ± 0.18	5.36 ± 0.73
ASggtA				
0	1.08±0.14	44.6±2.47	45.3±2.51	42.2±3.54
20% (w/v) NaCl	0.56±0.063	19.2±2.40	19.4±2.44	34.8±0.70
ASAOggtA				
0	0.82 ± 0.069	25.5 ± 1.37	25.9 ± 1.39	31.8 ± 2.08
20% (w/v) NaCl	0.32 ± 0.063	3.89 ± 0.47	3.95 ± 0.48	12.4 ± 1.70

[#] Kinetic parameters of the purified enzymes were determined by performing steady-state kinetic studies with various concentrations of L-γ-glutamyl-*p*-nitroanilide (0.03–1 mM) in 100 mM Tris-HCl buffer (pH 8.0) at 40 °C for 20 min. Hydrolysis and transpeptidation assays were performed with and without 33 mM glycylglycine. The parameters were also determined in a buffer containing 20% (w/v) NaCl.

Table 1-6. Hydrolysis of L-glutamine by γ-glutamyl transpeptidases, AOggtA, ASggtA, and ASAOggtA.

GGT	Concentration (mM)			Ratio (γ-GGln / L-Glu) [a]
	L-Gln	L-Glu	γ-GGln [a]	
AOggtA	45.4±1.1	29.4±1.1	15.3±0.3	0.52±0.01
ASggtA	66.0±1.2	10.2±0.7	13.8±0.3	1.36±0.09
ASAOggtA	45.0±1.5	24.7±1.4	20.3±0.7	0.82±0.03

[a] Abbreviations: γ-GGln, γ-glutamyl-glutamine.

Chapter 2

Heterologous expression and characterization of salt-tolerant β-glucosidase from xerophilic *Aspergillus chevalieri* for hydrolysis of marine biomass

Introduction

β-Glucosidase (β-D-glucopyranoside glucohydrolase, EC 3.2.1.21) is a versatile enzyme found in a variety of microorganisms (1),(66). It plays a crucial role in hydrolyzing β-glucosidic linkages between carbohydrate residues in alkyl-β-D-glucosides, short chain oligosaccharides and disaccharides in various physiological conditions (1),(66). Because of its versatility, β-glucosidase has gained significant attention in multiple biotechnological processes. For instance, the enzyme is employed in the saccharification of lignocellulosic biomass (66),(67) and marine biomass (68). In addition, it is used for the biotransformation of pharmaceuticals (69), fine chemicals (70), and food ingredients (71).

Extremophilic enzymes have become increasingly sought after in biotechnological fields because of their stability and activity in extreme conditions (1). Microorganisms adapted to extreme conditions, such as thermophilic, acidophilic, alkaliphilic, halophilic, and psychrophilic environments, represent a major source for isolating and purifying extremophilic enzymes (2),(3), including β-glucosidase. These microorganisms have developed diverse mechanisms and strategies to thrive in their extreme habitats (1). For example, xerophilic molds, such as *Aspergillus glaucus* and related species, have shown salt-adaptive properties and are expected to be used in biomass degradation (9),(10). Xerophilic molds and their extracellular enzymes possess potential molecular adaptation mechanisms for high salt and/or low water activity

conditions and are therefore attractive genetic resources for isolating salt- and/or osmo-adaptive enzymes (29),(72)–(74).

This study reports on the biochemical and molecular characterization of a salt-tolerant β-glucosidase (BGL_MK86) from the xerophilic mold *A. chevalieri* MK86. BGL_MK86 exhibited high salt tolerance, and its hydrolytic activity toward laminarin from marine biomass was examined in the presence and absence of NaCl.

Materials and Methods

Organism and culture conditions

A. chevalieri MK86 was isolated from the surface of katsuobushi filet fermented in low water activity conditions (39). A salt-tolerant β-1,3-glucosidase (BGL_MK86) was purified and its gene was cloned from strain MK86. Strain MK86 was cultivated on katsuobushi solid medium, according to previously described methods (39). A niaD^{-} derivative strain of *A. oryzae* NBRC 100959 [a nitrate reductase gene (niaD)-deficient mutant] was used as the recipient strain for heterologous expression (75). The expression vector pUNA, containing the *amyB* promoter and terminator, was newly constructed from pUC118, based on a previously reported expression vector (75). *A. oryzae* transformants were cultivated on DPY medium [2% (w/v) dextrin, 1% (w/v) polypeptone, 1.0% (w/v) yeast extract, 0.5% (w/v) KH_2PO_4, and 0.05% (w/v) $MgSO_4 \cdot 7H2O$] (75) with shaking at 130 rpm for 3–4 d.

Purification of β-1,3-glucosidase from A. chevalieri MK86

Wild-type β-glucosidases including BGL_MK86 were purified from *A. chevalieri* MK86 for selection of a salt-tolerant β-glucosidase and protein identification

by liquid chromatography-tandem mass spectrometry (LC-MSMS) with Mascot analysis.

Weak ion-exchange chromatography on DEAE-Toyopearl The crude preparations (135 mL) were dialyzed against 20 mM Tris-HCl buffer (pH 7.5; buffer A) with two exchanges of the same buffer. The dialyzed enzyme solution (150 mL) was divided into four parts, and each part was subjected to chromatography. The crude enzyme preparation (30 mL), including parental enzyme, BGL_MK86, was loaded onto a DEAE-Toyopearl column (1.5×20 cm, Tosoh Corp.) equilibrated with buffer A. After washing with 90 mL of buffer A, the β-glucosidases were eluted with a linear gradient of 0-0.3 M NaCl in buffer A at a flow rate of 1.0 mL/min. The column chromatography operation was repeated five times. The BGL_MK86 fraction and another fraction were separately collected and dialyzed against buffer A for the next step chromatography. The high active fractions were collected and used for gel filtration chromatography.

Gel filtration chromatography on Toyopearl HW-55 The active fraction was concentrated to 1.5 mL using an Amicon Ultra-15 10 K (Merck KGaA, Darmstadt, Germany). The concentrated enzyme solution was loaded onto a column (2.5×50 cm) of Toyopearl HW-55 (Tosoh Corp.) equilibrated with buffer A containing 0.2 M NaCl and eluted with the same solution at a flow rate of 0.35 mL/min.

Hydrophobic chromatography on Butyl-Toyopearl The pooled active fraction was supplemented with $(NH_4)_2SO_4$ to a final concentration of 2 M. The fraction was loaded onto a Butyl-Toyopearl column (1.5×20 cm, Tosoh Corp.) equilibrated with buffer A containing 2 M $(NH_4)_2SO_4$. After washing with 90 mL of the same buffer, proteins were eluted with a linear gradient of 2.0-0 M $(NH_4)_2SO_4$ in buffer A at a flow rate of 1.0 mL/min. A summary of a typical purification is shown in Table 2-1.

Genomic DNA and RNA isolation for cloning of BGL_MK86-encoding gene

Genomic DNA was extracted from strain MK86 using a DNeasy Blood & Tissue Kit according to the manufacturer's instructions (Qiagen, Hilden, Germany). The DNA fragment encoding β-glucosidase BGL_MK86 was amplified using the purified genomic DNA, PrimeSTAR MAX DNA polymerase, and primers BGL_MK86F (ATGTTTGCCAAACTCTGCGTAA) and BGL_MK86R (TTAGCCGCACTGACCGGGGA), according to the manufacturer's instructions (Takara Bio Inc., Shiga, Japan). Total RNA was extracted from strain MK86 using RNAiso Plus according to the manufacturer's instructions (Takara Bio Inc.). First-strand cDNA was synthesized using a PrimeScrip 1st Strand cDNA Synthesis Kit (Takara Bio Inc.). DNA encoding BGL_MK86 was amplified using the cDNA mixture as the template, PrimeSTAR MAX DNA polymerase, and primers BGL_MK86F and BGL_MK86R. The ligation of PCR products and pMD20 (Takara Bio Inc.) was carried out using a Mighty TA-cloning kit (Takara Bio Inc.). The primers were designed based on our in-house database for strain MK86.

Construction of BGL_MK86 expression vector and transformation of A. oryzae

A DNA fragment encoding BGL_MK86 was amplified using the synthesized cDNA solution (see above), PrimeSTAR MAX DNA polymerase, and primers BGL_MK86F_AO (AAACCCCACAGAAGGCATTTATGTTTGCCAAACTCTCGCGTA) and BGL_MK86R_AO (TCTCCACCCTTCTAGATTAGCCGCACTGACCGGG). According to the user manual of the In-fusion HD Cloning kit (Takara Bio Inc.), the purified PCR product was ligated into plasmid pUNA linearized using restriction

enzymes *Apa*I and *Xba*I. The constructed recombinant plasmid was then transformed into *Escherichia coli* HST08 (Takara Bio Inc.), according to the manufacturer's instructions. Transformation of *A. oryzae* was carried out according to previously reported procedures (75). The plasmid was linearized by using restriction enzyme *Xho*I or *Hpa*I and introduced into *A. oryzae* niaD^{-} by means of niaD-based homologous recombination. Protoplasts were prepared from 1-day old mycelial cultures by treatment with Yatalase (Takara Bio Inc.) for 3 h at 30 °C. Transformants that reintroduced the niaD gene as well as the BGL_MK86 gene were selected on Czapek–Dox minimal agar medium plates containing $NaNO_3$ as the sole N source (75). Recombinant BGL_MK86 (rBGL_MK86)-producing transformants were cultured in DPY medium, as described above.

Purification of recombinant BGL_MK86 heterologously expressed by A. oryzae

To collect rBGL_MK86 extracellularly produced by *A. oryzae* transformants, the liquid culture (20 mL/100 mL flask) was vacuum filtered and the filtered solution was dialyzed against 20 mM Tris–HCl buffer (pH 7.5). The dialyzed solution (the crude enzyme preparation) was used for enzyme assay and purification. The crude enzyme preparation (20 mL) including rBGL_MK86 was loaded onto a DEAE-Toyopearl column (1.5 × 20 cm; Tosoh Corp., Tokyo, Japan) equilibrated with 20 mM Tris–HCl buffer (pH 7.5) (buffer A). After washing with 90 mL of buffer A, the β-glucosidase was eluted with a linear gradient of 0–0.3 M NaCl in buffer A at a flow-rate of 1.0 mL/min. Tris–glycine-SDS–PAGE was performed to check enzyme purity using a 12.5% precast polyacrylamide gel (e-PAGEL precast gel E-T12.5L) with electrophoresis buffer containing 25 mM Tris, 192 mM glycine, and 0.1% (w/v) SDS and an ATTO AE6530 gel electrophoresis system (ATTO Corp., Tokyo, Japan), used according to the

manufacturer's instructions (Fig. 2-1).

Enzyme assays

β-Glucosidase activity was assayed using the method developed by Riou et al. (76) with slight modifications. The activity was measured at 40 °C with 1 mM *p*-nitrophenyl-β-D-glucopyranoside (pNPBG; Sigma Aldrich, St. Louis, MI, USA) as the substrate in 0.1 mL of 100 mM acetate buffer (pH 6.0) and with appropriately diluted enzyme preparation (10 μL). After incubation for 30 min, the reaction was stopped by adding 0.2 mL of 1 M Na_2CO_3, and the release of *p*-nitrophenol was measured by determining the absorbance at 400 nm. The results were calculated using the equation obtained from a standard curve. One unit of β-glucosidase activity was defined as the amount of enzyme that yielded 1 μmol of *p*-nitrophenol per minute in the assay conditions. Hydrolytic activity toward natural substrates such as soluble starch, sodium carboxymethyl cellulose, and laminarin [from *Laminaria digitata* (Sigma Aldrich) and *Eisenia bicyclis* (Tokyo Chemical Industry Co., Ltd., Tokyo, Japan)] was determined using previously described methods (77) (Table 2-2). Briefly, a reaction mixture (100 μL) consisting of appropriately diluted enzyme preparation, 50 mM sodium–citrate buffer (pH 6.0), and 0.5% (w/v) substrate was incubated at 40 °C for 30 min, and the produced reducing sugar was measured using the 3,5-dinitrosalicylic acid method (78). D-Glucose (0 to 6.0 mM) was used as the standard reducing sugar. One unit of hydrolytic activity was defined as the amount of enzyme that produced 1 μmol of reducing sugar per minute. Protein concentration was measured by the Lowry method using bovine serum albumin as a standard.

Characterization of recombinant BGL_MK86

The enzyme activity toward pNPBG was assayed using rBGL_MK86 purified as described above, unless otherwise stated.

Effect of NaCl concentration on enzyme activity

Enzyme assay with pNPBG or laminarin from the seaweed (kelp) *E. bicyclis* as substrate was carried out in a reaction mixture containing NaCl [0%–18.2% (w/v) final concentration].

Effect of glucose concentration on enzyme activity

Enzyme assay was carried out in a reaction mixture containing D-glucose [0–18.2% (w/v) final concentration].

Effect of pH on enzyme activity and stability

Enzyme assay was carried out at pH 4.0–10.0 in the following 100 mM buffers: sodium acetate (pH 4.0–6.0), MES (2-morpholinoethanesulfonic acid, monohydrate)–NaOH (pH 5.5–7.0), sodium potassium phosphate (pH 5.0–8.0), Tris–HCl (pH 7.5–9.0), and glycine–NaOH (pH 9.0–10.0). The pH stability of the enzyme was determined by dialyzing rBGL_MK86 against the buffers listed above at 4 °C for 15 h and then measuring the residual enzyme activity at pH 6.0 and 40 °C.

Effect of temperature on enzyme activity and stability

The effect of temperature on enzyme activity was determined in the range 20–65 °C. To determine thermal stability, purified enzyme was preincubated at various

temperatures (20–95 °C) for 1 h, and residual activities were measured at pH 6.0 and 40 °C.

Determination of kinetic parameters

Kinetic parameters were determined by performing steady-state kinetic studies without and with 3.6%, 7.3%, 10.9%, 14.5%, and 18.2% (w/v) NaCl (Table 2-3).

Detection of enzymatic reaction product by thin-layer chromatography (TLC)

A reaction mixture (100 μL) consisting of the enzyme preparation, 50 mM sodium–citrate buffer (pH 6.0), and 10 mg/mL laminaribiose or gentiobiose was incubated at 40 °C. The reaction mixture was mixed with an equal volume of ethanol. TLC was performed on Merck silica gel 60F254 plates (Merck KGaA, Darmstadt, Germany). The substrate and its reaction products were chromatographed with mobile solvent (n-butanol/acetic acid/water = 2:1:1, v/v/v). The TLC plate was sprayed with detection reagent (sulfuric acid/ethanol = 1:9, v/v) and incubated on a hotplate at 130 °C.

Hydrolysis of crude and partially purified laminarin from E. bicyclis

Extraction and partial purification of laminarin from *E. bicyclis* was carried out using a modified version of previously reported procedures (79). Briefly, desiccated seaweed samples (2.5 g) were stirred in 25 mL of 0.09 M HCl at 0 °C for 2 h. The resulting solution was centrifuged at 3000 × g for 5 min, and the resulting precipitate was washed twice with 5 mL of 0.05 M HCl. The supernatant and washing solutions were combined to obtain the combined laminarin solution, which was then neutralized with 0.05 M NaOH. This solution was mixed with an equal volume of water to obtain crude laminarin solution

1 (Table 2-4). The combined solution was also neutralized with 0.05 M NaOH and then mixed with an equal volume of 100 mM sodium citrate buffer (pH 6.0) to obtain crude laminarin solution 2 (Table 2-4). In addition, the combined solution was adjusted to an 85% (v/v) ethanol concentration, and the resulting precipitate was recovered by centrifugation at 3,000 × g for 5 min. The precipitate was washed twice with 5 mL of methanol and five times with 40 mL of ether. Finally, the precipitate was dissolved in 50 mM sodium citrate buffer (pH 6.0) to obtain partially purified laminarin solution (solution 3; see Table 2-4). The hydrolysis of crude and partially purified laminarin from *E. bicyclis* was evaluated using the enzyme assay described above.

Statistical analysis

All experiments were performed in duplicate and replicated at least three times. All data were calculated as the mean ± standard deviation. Analysis of variance (ANOVA) was selected to test value differences ($p < 0.05$). For comparison of different groups, the data were analyzed using one-way ANOVA and Tukey's multiple comparison. All calculations were conducted using GraphPad Prism software (ver. 6.02 for Windows, La Jolla, CA, USA).

Results and Discussion

Isolation of salt-tolerant β-glucosidase from A. chevalieri MK86

LC-MSMS Mascot analysis identified lipolytic enzymes involved in katsuobushi fermentation and ripening, as well as putative β-glucosidases, based on our in-house sequence database of *A. chevalieri* MK86 (39). To further investigate these extracellularly produced β-glucosidases, crude enzyme preparations were obtained from solid-state

culture of *A. chevalieri* strain MK86 and active fractions were purified (Fig. 2-1). From the purified enzymes, a salt-tolerant type of β-glucosidase, designated BGL_MK86, was selected (Fig. 2-1, Table 2-1). BGL_MK86 had approximately 110% activity toward pNPBG in the presence of 18.2% (w/v) NaCl compared with the absence of NaCl.

A 1359-bp fragment was amplified from genomic DNA of strain MK86 with primers BGL_MK86F and BGL_MK86R, with two introns interrupting the coding sequence. The full-length cDNA of BGL_MK86 was obtained by reverse transcription-PCR using the same primers and contains an open reading frame of 1248 bp (LC767509). SignalP analysis (http://www.cbs.dtu.dk/services/SignalP/) indicated the presence of an N-terminal signal peptide (amino acid residues 1-22). The mature BGL_MK86 protein contains 393 amino acid residues with a calculated molecular mass of 43.4 kDa, which is consistent with the purified enzyme on SDS-PAGE (Fig. 2-1). Based on analysis using the ExPASy server (http://web.expasy.org/protparam/), the theoretical isoelectronic point (pI), instability index, aliphatic index, and grand average hydropathy of the mature enzyme were 4.51, 24.20, 80.61, and -0.348, respectively. Protein–protein BLAST search against the UniProtKB/SwissProt database, along with the glucose tolerance described below, indicated that BGL_MK86 probably belongs to the aryl-phospho-β-D-glucosidases (also called BglC).

The SWISS-MODEL web server was used to perform structural modeling of BGL_MK86 using BglC from *Candida albicans* [PDB ID, 2PB1; Global Model Quality Estimate, 0.82; identity, 43% (170/393 amino acids (a.a.))] (Fig. 2-2), which belongs to glycosyl hydrolase family (GH) 5, as the template. The two catalytic glutamate residues [the nucleophile (^{209}Glu) and proton donor (^{307}Glu)] and other amino acid residues, ^{113}Arg, ^{156}His, ^{208}Asn, ^{267}His, ^{269}Tyr, and ^{371}Trp in BGL_MK86 were conserved in *C. albicans*

BglC (80) (Fig. 2-2). The $(\beta/\alpha)_8$-barrel structure, commonly observed in structurally characterized clan GH-A β-glucosidases (families GH 1, 5, and 30), was present in the structural model of BGL_MK86. Docking structure analysis of BGL_MK86 with BglC from *C. albicans* was carried out (Fig. 2-2). It revealed no significant interaction of the enzymatic reaction product glucose with active site residues, as suggested by Zada et al. (81) (Fig. 2-2). This observation could explain the glucose tolerance observed for BGL_MK86.

Phylogenetic analysis revealed that BGL_MK86 is closely related to the putative BglCs from *A. ruber* CBS135680 (XP_040638068) and *A. terreus* NIH2624 (Q0CR35) that belong to family GH5 (Fig. 2-3). *A. ruber* and *A. terreus* were categorized as xerophilic (82),(83) and/or salt-tolerant fungi (84). Therefore, these putative BglCs may also be stable and exhibit activity in moderately-high-salt conditions.

Characterization of rBGL_MK86

Recombinant BGL_MK86 (rBGL_MK86) was secreted following heterologous expression in *A. oryzae* and purified through a single-column chromatography step, resulting in a 100-fold purification with an overall yield of 32.5% (Table 2-5). Notably, rBGL_MK86 production was significantly higher (4.4 mg from 20 mL of filtered culture) than that of the native BGL_MK86 from *A. chevalieri* strain MK86 (0.11 mg from 150 mL of crude enzyme preparation). rBGL_MK86 showed increasing activity toward pNPBG and laminarin from *L. digitata* with increasing NaCl concentration, indicating salt-tolerance (Fig. 2-4a); this salt-tolerance was clear via an increase in both substrate affinity (K_m) and the turnover number of rBGL_MK86 (k_{cat}) (Table 2-3). While salt-tolerant GH1 β-glucosidases have been characterized from *Thermobifida halotolerans*

YIM 90462 (85), *Alteromonas* sp. L82 (86), and *Bacteroides cellulosilyticus* DSM 2522 (87), the effect of NaCl on the kinetic parameters of these enzymes is not well understood. The salt-tolerant GH1 β-glucosidase from *Bacillus* sp. SJ-10 exhibited high activity toward pNPBG in the presence of 15% (w/v) NaCl and a kinetic profile similar to that of rBGL_MK86 (88), but the underlying mechanism remains unclear (88).

rBGL_MK86 was categorized as a glucose-tolerant β-glucosidase based on its response to glucose, and as a GH1 family β-glucosidase in clan GH-A (89) (Fig. 2-4b). Its pH stability was broader than that of the GH1 family β-glucosidases from *T. halotolerans* YIM 90462, *Alteromonas* sp. L82, *Bacteroides cellulosilyticus* DSM 2522, and *Bacillus* sp. SJ-10 (Fig. 2-4c and d). However, there were no significant differences in thermostability and optimum reaction temperature among the five enzymes including rBGL_MK86 (Fig. 2-4e and f). In addition to hydrolyzing pNPBG, rBGL_MK86 showed activity toward *p*-nitrophenyl-β-D-xylopyranoside and laminaribiose (β-1,3-linked glucose dimer) (Fig. 2-5), but not cellobiose (β-1,4 linked glucose dimer) or gentiobiose (β-1,6 linked glucose dimer) (Table 2-2). rBGL_MK86 showed higher activity toward laminarin (a linear polymer of β-1,3 glucan) from the seaweed *L. digitata* than laminarin (β-1,3/β-1,6 glucan) from *E. bicyclis*, likely due to its inability to act on gentiobiose. TLC analysis indicated that rBGL_MK86 had transglycosylation activity and produced glucose from laminaribiose, consistent with the properties of exoglucanases (90)–(92).

Proposed molecular mechanism of salt adaptation in salt-tolerant BGL

Enzymes that are halophilic or salt-tolerant typically have a higher proportion of acidic amino acids (Asp and Glu) located on the protein surface than non-halophilic/salt-tolerant enzymes (30),(31),(48). This results in a reduction in the theoretical pI and an

increase in the hydration of the protein surface (30),(31),(48). As noted above, the molecular mechanism responsible for the salt tolerance of β-glucosidases is not yet fully understood. However, Cai et al. proposed that ^{492}Glu, which is located close to the acid/base active site residue ^{493}Glu, may contribute to the halophilic properties of β-glucosidase 2 (MH744150) from *A. niger* ZJUBE-1 (93). Although there is no non-salt-tolerant β-glucosidase that shows high similarity to BGL_MK86, *C. albicans* BglC was chosen for comparison. The number of acidic amino acid residues in BGL_MK86 and *C. albicans* BglC was 59 and 45, respectively, and the theoretical pI of BGL_MK86 (4.51) was lower than that of *C. albicans* BglC (5.35). The pIs of the BglCs from *A. ruber* CBS135680 and *A. terreus* NIH2624, which belong to the same group as BGL_MK86 (Fig. 2-3) were 4.31 and 4.41, respectively. Further experimental studies are needed to test the salt tolerance of *C. albicans* BglC, but it is possible that acidic amino acid residues contribute to the salt tolerance of BGL_MK86 and other salt tolerant β-glucosidases.

Effect of NaCl on hydrolysis of laminarin from E. bicyclis by rBGL_MK86

The halophilic β-glucosidase from *Trichoderma harzianum* HTASA has shown potential for saccharification of cellulosic raw materials in the presence of NaCl in practical conditions (94). To investigate the salt-tolerance characteristics of rBGL_MK86, its hydrolytic activity profiles were examined using various grades of laminarin from *E. bicyclis* as substrate (Tables 2-4 and 2-6). Partially purified laminarin (0.32 g) was obtained from 2.5 g of dried *E. bicyclis* as described in Materials and methods. Crude laminarin solutions 1 and 2 (Table 2-4) were prepared by subjecting the partially purified laminarin to HCl treatment and NaOH neutralization. After neutralization, these solutions contained approximately 0.079 M NaCl [equivalent to 0.46% (w/v) NaCl] and 0.91%

(w/v) laminarin. Enzymatic hydrolysis by rBGL_MK86 was performed using this crude laminarin solution diluted twofold with water (to form solution 1) or citrate buffer (solution 2, Table 2-4). rBGL_MK86 exhibited its highest activity toward partially purified *E. bicyclis* laminarin (solution 3, Table 2-4). The hydrolysis of the crude laminarin samples showed no significant difference compared with hydrolysis of commercially obtained *E. bicyclis* laminarin (solution 4, Table 2-4). The hydrolysis capability of rBGL_MK86 for the crude laminarin was investigated (Fig. 2-6). The total sugar content in the crude laminarin solution (solution 2, refer to Table 2-4), measured using the phenol–sulfuric acid method, was determined to be 8.33 ± 0.55 mg/ml (as D-glucose equivalent). During the 5 h-reaction period, continuous production of reducing sugars, predominantly consisting of D-glucose, was observed through hydrolysis of the crude laminarin by rBGL_MK86 (Fig. 2-6). However, the increase reached a plateau after that. It was estimated that 37.5% of the crude laminarin in the reaction mixture was released as reducing sugar, mainly D-glucose (Fig. 2-6). Further investigation of the hydrolysis profiles of the crude laminarin in combination with other endo-acting enzymes is required for efficient saccharification.

Additionally, the effect of NaCl concentration on laminarin hydrolysis was investigated (Table 2-6). rBGL_MK86 showed approximately 80% relative activity at the same salt concentration as seawater [around 3.5% (w/v) NaCl]. These findings indicate that rBGL_MK86 exhibits salt-tolerant characteristics and can effectively hydrolyze laminarin from *E. bicyclis*. The ability of the enzyme to tolerate high salt concentrations might provide potential advantages for the production of oligosaccharides from crude and/or pretreated laminarin.

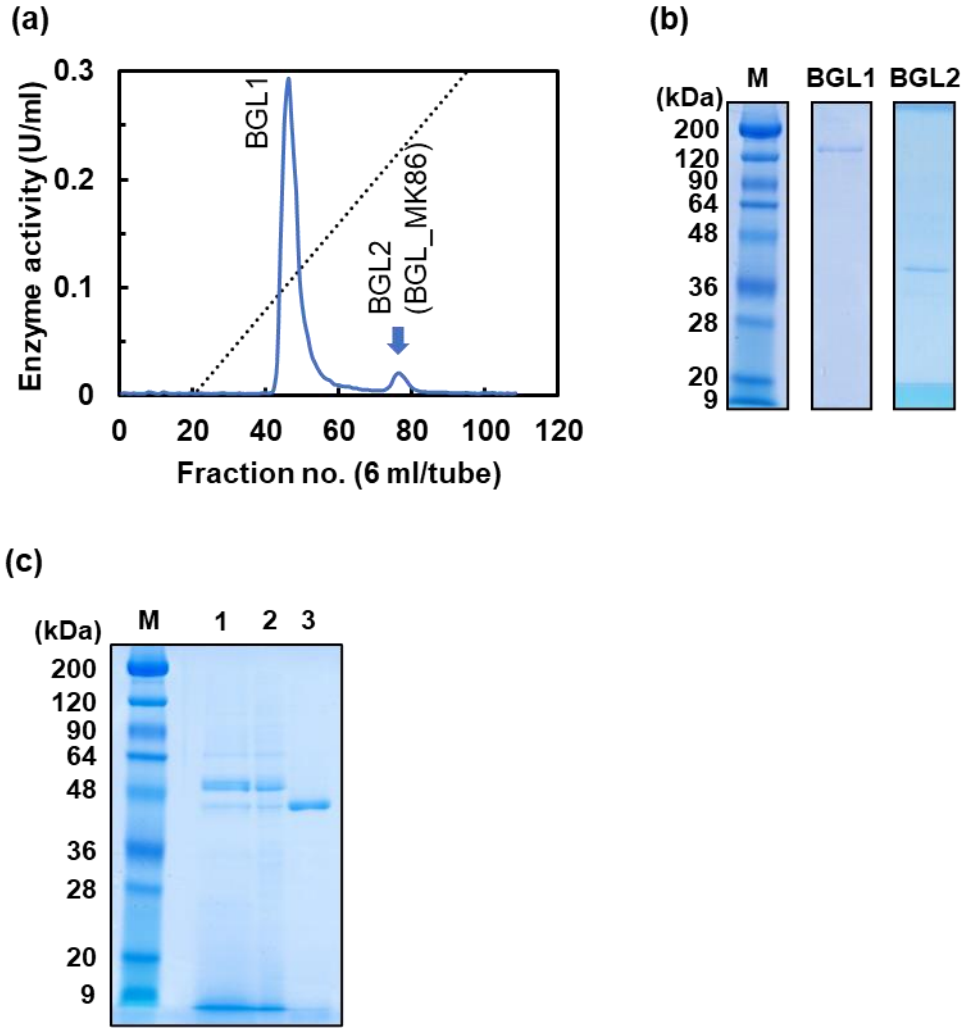

Fig. 2-1. Purification of β-1,3-glucosidase from *A. chevalieri* MK86 and reconbinant BGL_MK86. (a) DEAE-Toyopearl chromatography of crude enzyme preparations from *A. chevalieri.* **(b)** SDS-PAGE of purified final preparations of BGL1 and BGL2 (BGL_MK86). **(c)** SDS-PAGE of purified final preparations of recombinant BGL_MK86 heterologous expressed in *A. oryzae* transformant. Lanes: M, Protein marker; 1, cultural supernatant; 2, dialyzed supernatant; 3, DEAE-Toyopearl active fraction

(a)

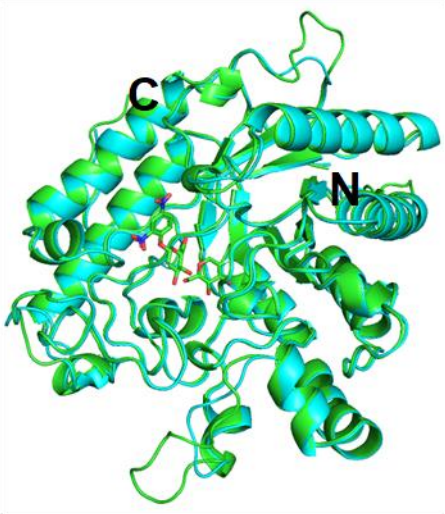

(b)

```
BGL_MK86          1:---MFAKLSRKALLTLSALAAVTGAIPVG--------VDEIHAPSVNYDADKIRGVNIGG 49
C_albicans_BGL    1:MQLSFILTSSVFILLLEFVKASVISNPFKPNGNLKFKRGGGHNVAWDYDNNVIRGVNLGG 60
                        *   *    * *    *     *              *     **   ***** **

BGL_MK86         50:WLVLEPWITPSIFD------EVGDAAVDEWTLTKVLGKEGARNRLLKHWESFISQADFDE 103
C_albicans_BGL   61:WFVLEPYMTPSLFEPFQNGNDQSGVPVDEYHWTQTLGKEAASRILQKHWSTWITEQDFKQ 120
                     * ****  *** *            ***   *  **** *   * ***   *   **

BGL_MK86        104:IAAAGLTHVRIPVGYWAVIPLIDEPYVNGQLDFLDQAIFWAQSAGLEVIVDLHGAPGSQN 163
C_albicans_BGL  121:ISNLGLNFVRIPIGYWAFQLLDNDPYVQGQVQYLEKALGWARKNNIRVWIDLHGAPGSQN 180
                     *   **  **** ****   *   *** **   * *  **      *  **********

BGL_MK86        164:GFDNSGRRGPIEWQQGDTVERTTAAIQALIDRYS--EYPNVVF--EALNEPSIPGGVDRG 219
C_albicans_BGL  181:GFDNSGLRDSYNFQNGDNTQVTLNVLNTIFKKYGGNEYSDVVIGIELLNEPLGP-VLNMD 239
                     ****** *     * **    *          *   **  **   * ****  *

BGL_MK86        220:LLSQYYGDFEQRVHKATPDAPLVLHDGFNPVDSWNGFLS----ENNVVIDNHHYEVFDNS 275
C_albicans_BGL  240:KLKQFFLDGYNSLRQTGSVTPVIIHDAFQVFGYWNNFLTVAEGQWNVVVDHHHYQVFSGG 299
                      * *   *           *   ** *     ** **       *** * *** **

BGL_MK86        276:LLTQDVNTHVSNVCAHSSGQLQKSDKWAIVGEWTGAMTDCAKYLNGKGVGARYDGTMSAD 335
C_albicans_BGL  300:ELSRNINDHISVACNWG-WDAKKESHWNVAGEWSAALTDCAKWLNGVNRGARYEGAYDNA 358
                     *    * * *  *        *   *   ***  * ***** ***   **** *

BGL_MK86        336:FSAGSCDGKSVGNVADLSDEDKVNTRRFIEGQLDAWEQKSGWVFWTWKTEGAPEWDMRQL 395
C_albicans_BGL  359:PYIGSC--QPMLDISQWSDEHKTDTRRYIEAQLDAFEYTGGWVFWSWKTENAPEWSFQTL 416
                       ***          *** *  *** ** **** *   ***** **** ****    *

BGL_MK86        396:LAEGVFPQPLDDRKFPGQCG--                                      415
C_albicans_BGL  417:TYNGLFPQPVTDRQFPNQCGFH                                     438
                     * ****  ** ** ***
```

Fig. 2-2. Comparison of structure and sequence of BGL_MK86 and BGL_Ca. (a) Superposition of the β-glucosidase structures from *A. chevalieri* MK86 (BGL_MK86: cyan, this study) and *Candida albicans* (BGL_Ca: green, PDB ID: 2PB1, complex with *p*-nitrophenyl-β-D-glucopyranoside and D-glucose). Structures were visualized using PyMOL version 2.5 and for comparison with BGL_Ca [identity with BGL_MK86, 43% (170/393 amino acids); GMQE value with BGL_MK86, 0.82]. **(b)** Sequence alignment of β-glucosidase from *A. chevalieri* MK86 (BGL_MK86) and *C. albicans* (*C. albicans*_BGL). Represent invariant GH family 5 residues including two catalytic glutamate resiudes are shown in yellow (80).

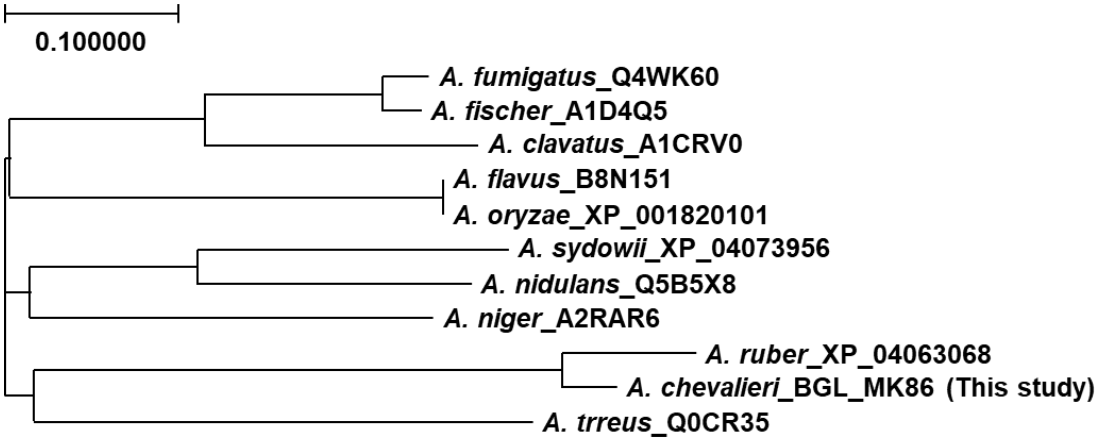

Fig. 2-3. Phylogenetic analysis of BGL_MK86 from *Aspergillus chevalieri* MK86 and β-glucosidases from *Aspergillus* spp. Multiple alignment of amino acid sequences was performed using GENETYX software ver. 14.0 (Genetyx Corp., Tokyo, Japan) and an unrooted phylogenetic tree was constructed using the neighbor-joining algorithm. Abbreviations: *A. chevalieri*_BGL_MK86, BglC from *A. chevalieri* MK86 (this study); *A. clavatus*_A1CRV0 [origin *A. clavatus* NRRL1, accession no. A1CRV0, identity (%) with BGL_MK86 56% (235/417 amino acids (a.a.))]; *A. fischer*_A1D4Q5 [*A. fischer* NRRL181, A1D4Q5, 56% (238/418 a.a.)]; *A. flavus*_B8N151 [*A. flavus* NRRL3357, B8N151, 60% (235/388 a.a.)]; *A. fumigatus*_Q4WK60 [*A. fumigatus* Af293, Q4WK60, 56% (236/418 a.a.)]; *A. nidulans*_Q5B5X8 [*A. nidulans* FGSC A4, Q5B5X8, 59% (226/378 a.a.)]; *A. niger*_A2RAR6 [*A. niger* CBS513.88, A2RAR6, 56% (236/416 a.a.)]; *A. oryzae*_XP_001820101 [*A. oryzae* RIB40, XP_001820101, 60% (235/388 a.a.)]; *A. ruber*_XP_04063068 [*A. ruber* CBS135.680, XP_04063068, 89% (373/416 a.a.)]; *A. sydowii*_XP_04073956 [*A. sydowii* CBS593.65, XP_04073956, 57% (240/416 a.a.)]; *A. trreus*_Q0CR35 [*A. terreus* NHI2624, Q0CR35, 56% (237/419 a.a.)]

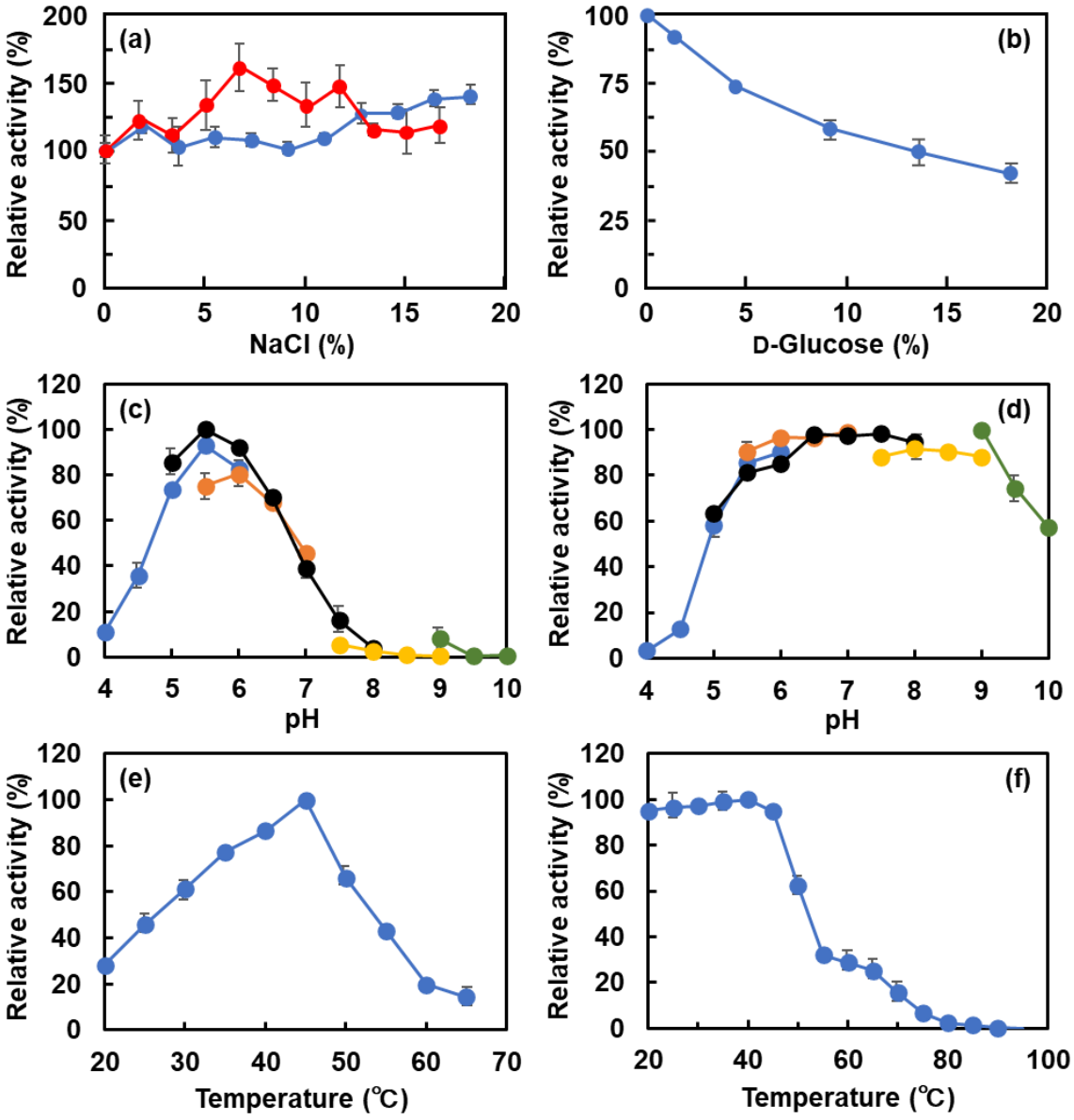

Fig. 2-4. Factors affecting enzymatic activity and stability of rBGL_MK86. **(a)** The effect of NaCl on hydrolysis of *p*-nitrophenyl-β-D-glucopyranoside (pNPBG) and laminarin from *Laminaria digitata* was determined at 40 °C for 30 min in a reaction mixture without and with NaCl. The relative activities were calculated based on the hydrolytic activities toward pNPBG (0.058 U/mg) and laminarin (1.2 U/mg) in the absence of NaCl. **(b)** The effect of D-glucose on hydrolysis of pNPBG was determined at 40 °C for 30 min in a reaction mixture without and with D-glucose. The relative

activities were calculated based on the hydrolytic activity toward pNPBG (0.058 U/mg). **(c)** Enzyme assays using pNPBG were carried out over pH range 4.0–10.0 at 40 °C for 30 min in the following 100 mM buffers: sodium acetate (pH 4.0–6.0, cyan), MES–NaOH (pH 5.5–7.0, orange), sodium potassium phosphate (pH 5.0–8.0, black), Tris–HCl (pH 7.5–9.0, yellow), and glycine–NaOH (pH 9.0–10.0, green). The relative activities were calculated based on the hydrolytic activity toward pNPBG at pH 5.5 (0.063 U/mg). **(d)** The purified enzyme was incubated at various pHs for 15 h, in the following 100 mM buffers: sodium acetate (pH 4.0–6.0, cyan), MES–NaOH (pH 5.5–7.0, orange), sodium potassium phosphate (pH 5.0–8.0, black), Tris–HCl (pH 7.5–9.0, yellow), and glycine–NaOH (pH 9.0–10.0, green); the residual activity toward pNPBG was measured at pH 6.0. The relative activities were calculated based on the hydrolytic activity toward pNPBG of enzyme preincubated at pH 6.5 (0.064 U/mg). **(e)** The effect of temperature on the activity of the purified enzyme was determined at 20–65 °C. The relative activities were calculated based on the hydrolytic activity toward pNPBG at 45 °C (0.067 U/mg). **(f)** The stability was evaluated by preincubating purified enzyme at 20–95 °C for 30 min; the residual activity toward pNPBG was then measured at pH 6.0. The relative activities were calculated based on the hydrolytic activity of enzyme preincubated at 40 °C (0.058 U/mg)

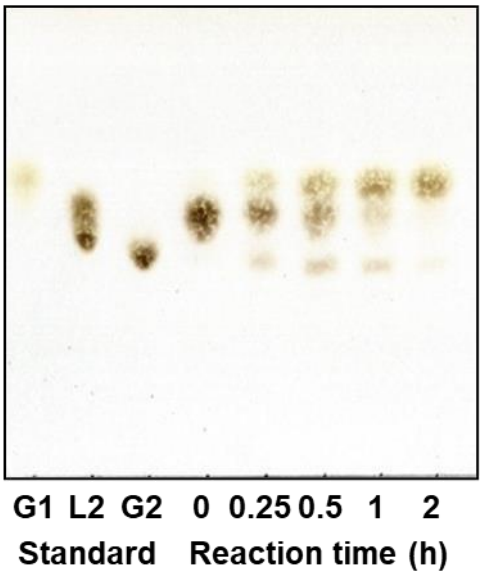

Fig. 2-5. Thin-layer chromatography (TLC) analysis of hydrolysis of laminaribiose by rBGL_MK86. Products were analyzed by TLC (Silica Gel 60 F254) with *n*-butanol-acetic acid–water (2:1:1, v/v/v) as the solvent. Plates were visualized by exposure to 10% sulfuric acid in ethanol. Lanes: G1, D-glucose; L2, laminaribiose; G2, gentiobiose; 0, 0.25, 0.5, 1, and 2, reaction time of incubation of laminaribiose with rBGL_MK86 (in h).

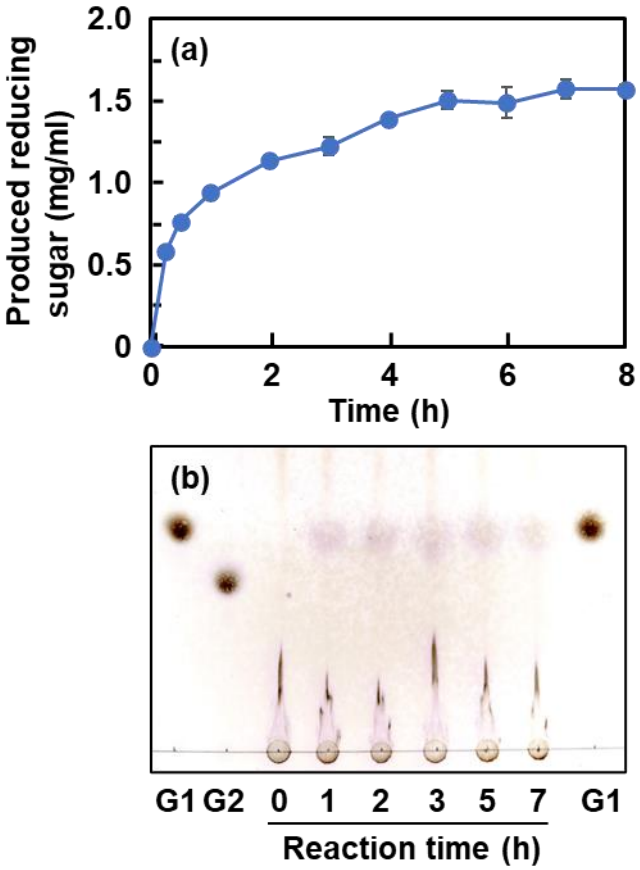

Fig. 2-6 Time course of crude laminarin hydrolysis by rBGL_MK86. The reactions were performed in 50 mM citrate buffer (pH 6.0) at 40 °C with the crude laminarin solution s (Table 2-4) and the purified rBGL_MK86 (0.4 U/ml). Total sugar content measured by the phenol–sulfuric acid method was 4.16 ± 0.28 mg/ml (as D-glucose equivalent) in the initial reaction mixture. **(a)** Produced reducing sugars (as D-glucose equivalent) were measured using the 3,5-dinitrosalicylic acid method. **(b)** The products formed in the reaction mixture were analyzed by TLC, as described in the legend of Fig. 2-5.

Table 2-1. Summary of purification of β-glucosidases including BGL_MK86 from *A. chevalieri* MK86

Purification step	Total activity (U)		Total protein (mg)		Specific activity (U/mg)		Recovery (%)	
Dialysis	23.6		151		0.156		100	
	BGL1	BGL2	BGL1	BGL2	BGL1	BGL2	BGL1	BGL2
DEAE-Toyopearl	13.1	0.40	15.6	6.24	0.840	0.064	55.5	1.7
Gel filtration	3.7	0.13	0.82	0.60	4.51	0.22	16	0.55
Butyl-Toyopearl	1.00	0.035	0.14	0.11	7.34	0.32	4.2	0.15

BGL_MK86 mentioned in the main text is BGL2 purified from the crude enzyme preparations from the solid-state fermented culture. BGL1 and BGL2 were separated by DEAE-Toyopearl chromatography (see Fig. 2-1).

Table 2-2. Substrate specificity of rBGL_MK86

Substrate	Enzyme activity (U/mg)
pNPBG	0.058±0.002
pNPAG	< 0.003
pNPBX	0.016±0.005
pNPAX	< 0.003
Soluble starch	< 0.003
CMC Na	0.14±0.025
Laminarin from *L. digitata*	1.2±0.13
Laminarin from *E. bicyclis*	0.11±0.014

Abbreviations: pNPAG, *p*-nitrophenyl-α-D-glucopyranoside; pNPBG, *p*-nitrophenyl-β-D-glucopyranoside; pNPAX, *p*-nitrophenyl-α-D-xylopyranoside; pNPBX, *p*-nitrophenyl-β-D-xylopyranoside; CMC Na, sodium carboxymethyl cellulose

Table 2-3. Kinetic parameter of rBGL_MK86

Concentration of NaCl [%(w/v)]	K_m (mM)	V_{max} (U/mg)	k_{cat} (s^{-1})	k_{cat}/K_m ($mM^{-1} \cdot s^{-1}$)
0	4.63±0.10	3.34±0.17	2.42±0.13	0.52±0.018
9.1	3.77±0.26	4.03±0.12	2.98±0.09	0.79±0.029
18.2	2.41±0.18	4.31±0.15	3.18±0.12	1.32±0.066

The activity toward *p*-nitrophenyl-β-D-glucopyranoside (0.8–10 mM) was measured for 10 min at 45°C with and without NaCl.

Table 2-4. Hydrolysis of crude and purified laminarin from *E. bicyclis* by rBGL_MK86

Prepared laminarin solution	Enzyme activity (U/mL)
1: Crude laminarin + water	0.12 ± 0.013^{A}
2: Crude laminarin + 50 mM sodium citrate buffer (pH 6.0)	0.126 ± 0.004^{A}
3: Partially purified laminarin + 50 mM sodium citrate buffer (pH 6.0)	0.342 ± 0.031
4: Commercially obtained laminarin + 50 mM sodium citrate buffer (pH 6.0)	0.131 ± 0.016^{A}

Enzyme activity sharing a superscript capital letter were not significantly different at the 5% level.

Table 2-5. Summary of purification of recombinant BGL_MK86 from *A. chevalieri* MK86

Purification step	Total activity (U)	Total protein (mg)	Specific activity (U/mg)	Recovery (%)
Cultural supernatant	4.0	1,200	0.003	100
Dialysis	1.7	92	0.018	42.5
DEAE-Toyopearl	1.3	4.4	0.30	32.5

Table 2-6. Effect of NaCl on hydrolysis for partially purified laminarin from *E. bicyclis* by rBGL_MK86

Concentration of NaCl [%(w/v)]	Enzyme activity (U/ml)	Relative activity (%)
0	0.332 ± 0.023^{A}	100
1.7	0.299 ± 0.043^{AB}	90
3.3	0.340 ± 0.051^{AC}	102
5.0	0.279 ± 0.031^{AD}	84
6.7	0.270 ± 0.012^{BCDE}	81
8.3	0.202 ± 0.028^{EF}	61
16.7	0.160 ± 0.009^{F}	48

Enzyme activity sharing a superscript capital letter were not significantly different at the 5% level.

Chapter 3

Effects of heterologous expression and N-glycosylation on the hyperthermostable endoglucanase of *Pyrococcus furiosus*

Introduction

Cellulase consists of endoglucanase, cellobiohydrolase, and β-glucosidase and plays a crucial role in the degradation of lignocellulosic biomass (95),(96). The mechanisms and functions of cellulase have been extensively investigated (95),(96), and endoglucanases (EC 3.2.1.4) have been shown to initiate the targeted breakdown of amorphous cellulose regions within lignocellulosic biomasses (95),(96). In collaboration with cellobiohydrolases and β-glucosidases, this initial breakdown facilitates the production of fermentable sugars (95),(96). Cellulases that are thermostable at elevated temperatures offer advantages in the saccharification process such as increased specific activity, greater stability, suppression of contaminant microbial growth, enhanced mass transfer due to reduced fluid viscosity, and augmented process flexibility (97). Furthermore, thermostable endoglucanases are resilient to extreme temperature and pH conditions (98) and can be applied immediately after biomass pretreatment using ionic liquids or within the context of one-pot *in situ* hydrolysis (99). Consequently, thermostable endoglucanases have been isolated and systematically engineered (100),(101). Similarly, endoglucanases from extremely thermophilic microorganisms, such as *Pyrococcus* spp. and *Sulfolobus* spp., have been characterized in detail (102)–(105); however, there is limited information regarding their functional modifications (106).

The hyperthermophilic archaeon *Pyrococcus furiosus* produces an endoglucanase

(EGPf, Gene ID: PF0854) belonging to glycoside hydrolase family 12 (GH12) (103). EGPf exhibits extraordinarily high optimum and denaturation temperatures (103). Therefore, studies have investigated the structure (107), substrate recognition mechanism (108), and cellulose hydrolysis ability of this endoglucanase in combination with other thermostable enzymes (109). Furthermore, heterologous expression has been conducted with *Escherichia coli* and the filamentous fungus *Talaromyces cellulolyticus* (110). However, apart from its thermostability, the features of recombinant EGPfs have not yet been characterized. Moreover, the effective heterologous expression and functional modification of *Pyrococcus* cellulases (111) that result from the strategies described above are unclear.

Protein engineering has successfully expressed microbial enzymes to enhance enzymatic activity, thermostability, and pH stability in *Pichia pastoris* (112)–(117) through post-translational modifications including the N-glycosylation observed in eukaryotes.

Protein N-glycosylation can occur through expression with the fungus *A. niger.* However, studies on the role of N-glycosylation in the enzymatic activity and stability of endoglucanases are limited (118), especially those relating to the industrially important thermostable endoglucanases. In this study, we tried to express the recombinant EGPf using *A. niger* for the purpose of enhancing the expression level and glycosylating EGPf. The heterologous expression of EGPf in *A. niger* was optimized through the use of multiple gene copies, and the properties of the recombinant EGPf were compared with those expressed in *E. coli.*

Materials and Methods

Strains and medium

The cloning procedures were conducted using *E. coli* DH5α (Takara Bio Inc., Shiga, Japan) as the host. *Aspergillus niger* NS48, which is a mutant strain of *A. niger* NBRC 4343 that has deficiencies in the nitrate reductase (*niaD*) and ATP sulfurylase (*sC*) (36),(119) genes, was used as the heterologous expression host for glycosylated EGPf (G_EGPf). *Escherichia coli* BL21 (DE3) served as the expression host for the unglycosylated EGPf (UG_EGPf). The *A. niger* transformants were cultivated in a modified DPY medium consisting of 4% (w/v) dextrin, 2% (w/v) polypeptone, 2% (w/v) yeast extract, 0.5% (w/v) KH_2PO_4, and 0.05% (w/v) $MgSO_4$-$7H_2O$.

Construction of expression vector

The expression vector pSENSU2512 for *A. niger* was constructed from the pUC118 vector (Fig. 3-1). The *enoA*12 promoter was used, which was based on the enolase gene promoter from *A. niger* and contained a 12-repeat cis-acting element (Region III) (120). The T2512 terminator from *A. oryzae*, which was developed in our laboratory (unpublished results), was used as the transcriptional terminator, and the selection marker was the *sC* gene from *A. niger*. The EGPf gene was synthesized using a *de novo* gene synthesis service (General Biosystems Inc., Durham, NC, USA). For secretory production in *A. niger*, the original signal sequence was replaced (110) by that of the Taka-amylase A gene from *A. oryzae* (TAA-signal). The codon usage of the TAA signal and EGPf genes were optimized for the most frequently used codons of *A. niger* (Table 3-1).

Heterologous expression of EGPf in A. niger and E. coli

The transformation of *A. niger* was conducted using previously reported procedures with slight modifications (40). The plasmids were linearized using the *Hpa*I restriction enzyme and introduced into *A. niger* NS48 through *sC*-based homologous recombination following a previously described method (40). Protoplasts were prepared from 1-day-old mycelial cultures using Yatalase-Plus- (Takara Bio Inc.) treatment for 3 h at 30°C. Transformants harboring the *sC* marker gene were selected on modified Czapek-Dox minimal agar medium without methionine (119), and G_EGPf-producing transformants were cultured in the modified DPY medium described above. The culture supernatant was collected by filtration and heat treated at 80°C for 30 min, the denatured proteins were removed by centrifugation, and the supernatant was dialyzed twice in 20 mM Tris-HCl buffer (pH 8.0) for 3 h. The protein concentration of the dialyzed solution was determined using a Pierce BCA Protein Assay Kit (Thermo Fisher Scientific, Waltham, MA, USA) with bovine serum albumin as the standard. The EGPf gene copy number of the chromosomal DNA was measured according to previously reported procedures (41).

The complete hydrolyzation of N-glycans in purified G_EGPf using commercially obtained endoglycosidases and the preparation of sufficient amounts of deglycosylated EGPf for characterization were challenging. Thus, UG_EGPf expression in the *E. coli* transformants was performed using a synthetic gene without the signal sequence described above, following previously reported procedures with slight modifications (108). The cultured cells were harvested by centrifugation, and cell extracts were obtained using the BugBuster Protein Extraction Reagent (Merck KGaA, Darmstadt, Germany). The extract was heat-treated at 80°C for 30 min and centrifuged to remove the denatured proteins. The supernatant was dialyzed twice in 20 mM Tris-HCl buffer (pH

8.0) for 3 h.

Enzyme and protein assay

The EGPf enzyme activity was measured using a modified version of a previously reported method (103). A mixture of 100 μL of 50 mM sodium phosphate buffer (pH 6.0) containing 0.5% (w/v) β-D-glucan from barley (barley β-glucan, Merck KGaA) and 5 μL of the appropriate concentration of enzyme solution was incubated at 80°C for 15 min. The reaction was terminated by adding 300 μL of 3,5-dinitrosalicylic acid reagent and incubating in boiling water for 5 min. After cooling to room temperature, the mixture was diluted with 1 mL of deionized water and absorbance was measured at 540 nm (121). One unit of enzyme activity was defined as the amount of enzyme required to produce reducing sugars equivalent to 1 μmol of D-glucose per minute under the assay conditions. Protein concentrations were determined using the Bio-Rad Protein Assay Dye Reagent Concentrate (Bio-Rad Laboratories, Inc., Hercules, CA, USA), with bovine serum albumin as the standard.

Purification and analysis of glycosylated and unglycosylated EGPf

The culture supernatant of EGPf-expressing *A. niger* was heat-treated at 80°C for 30 min. The pre-treated enzyme solution was dialyzed against 20 mM Tris-HCl buffer (pH 8.0) and applied to a HiTrap DEAE FF column (1 mL; Cytiva Sweden AB, Uppsala, Sweden) that was equilibrated with the same buffer. The highly active fractions were collected, precipitated with 80% saturated ammonium sulfate, and re-dissolved in 20 mM sodium acetate buffer (pH 5.0) containing 0.2 M arginine hydrochloride. The solution was then placed in a Superdex 75 Increase 10/300 GL column (Cytiva Sweden AB) that

was equilibrated with the same buffer. Highly active fractions were collected and dialyzed against 20 mM sodium acetate buffer (pH 5.0) to remove arginine hydrochloride.

Cell extracts of UG_EGPf-expressing *E. coli* were heat-treated, dialyzed, and purified using HiTrap DEAE FF anion column chromatography, as described above. Highly active fractions were collected and a final concentration of 0.75 M ammonium sulfate was added. This solution was placed in a HiTrap Butyl FF column (1 mL; Cytiva Sweden AB) that was equilibrated with 20 mM of Tris-HCl buffer (pH 8.0) containing 0.75 M ammonium sulfate. The active fraction was collected and further purified by gel filtration and arginine hydrochloride removal by dialysis, as described for the *A. niger*-expressed EGPf. The purity of each EGPf was determined by SDS-PAGE, followed by Coomassie Brilliant Blue (CBB) and periodic acid-Schiff (PAS) staining (65). G_EGPf was deglycosylated using Endo Hf (New England Biolabs, Ipswich, MA, USA) according to the manufacturer's instructions and analyzed using SDS-PAGE.

Determination of kinetic parameters

The reactions were performed under the conditions described above with barley β-glucan concentrations varying from 0.15 to 2.5 mg/mL. The K_m and V_{max} values were determined using non-linear regression analysis.

Effect of temperature on enzyme activity and stability

The half-life at 100°C was measured by adjusting the protein concentration of purified EGPf to 90 μg/mL. After treatment in a heat block at 100°C for 1 to 5 h for G_EGPf and 2 to 20 min for UG_EGPf, the residual activity was determined as described above. Deactivation rate constants were calculated from a plot of the natural logarithm of

the residual activity versus incubation time to estimate the half-life of each enzyme(122),(123). The optimal temperature was determined by varying the reaction temperature between 80°C and 120°C using the method described above. To prevent evaporation, an equivalent volume of liquid paraffin was layered on the reaction solution.

Effect of pH on enzyme stability

The purified G_EGPf (347.6 U/mg) and UG_EGPf (166.0 U/mg) samples were incubated at 37°C for 15 h in each of the following: 100 mM KCl-HCl buffer (pH 1.5–2.0), 100 mM glycine-HCl buffer (pH 2.5), 100 mM citrate buffer (pH 3.0–5.0), 100 mM sodium phosphate buffer (pH 6.0–8.0), 100 mM glycine-NaOH buffer (pH 9.0–10.0), and 100 mM Na_2HPO_4-NaOH buffer (pH 11.0–12.0). The level of residual activity in 50 mM sodium phosphate buffer, pH 6.0, containing 0.5% (w/v) barley β-glucan at 80°C was then determined. The relative activity was calculated based on these specific activities.

Effect of NaCl on enzyme activity

The enzyme activities of G_EGPf (361.5 U/mg) and UG_EGPf (188.9 U/mg) were determined in 50 mM sodium phosphate buffer (pH 6.0), containing 0.5% (w/v) barley β-glucan without and with NaCl. The relative activities were then calculated.

Effect of ionic liquid on enzyme activity

The ionic liquid tolerance was assessed by measuring specific activity in the presence of 0-50% (v/v) 1-butyl-3-methylimidazolium chloride ([Bmim]Cl) (Fujifilm Wako Pure Chemicals, Osaka, Japan).

Sequence analysis of EGPf

The N-glycosylation sites within the EGPf amino acid sequence (110) were predicted using the online tool NetNGlyc 1.0. EGPf, which contains eight Asn-X-Thr/Ser consensus sequences. Among these, five Asn residues (^{88}Asn, ^{98}Asn, ^{153}Asn, ^{276}Asn, and ^{307}Asn) were predicted to be N-glycosylated (Fig. 3-2). The 3D structure of EGPf (PDB no. 3WQ7) (124) that was visualized using PyMOL version 2.5 showed that the glycan was attached as a Man5GlcNAc2-type provisional structure using the online tool Glycoprotein Builder in GLYCAM.

Statistical analysis

All experimental data were obtained from a minimum of three parallel samples with similar or identical results. The error values represent the standard deviation (SD) of the mean of the three replicates. A Student's *t*-test was used to compare samples to detect statistical significance.

Results and Discussion

Heterologous expression and purification of EGPf in A. niger

Few studies have focused on the heterologous expression of extracellular enzymes from hyperthermophilic archaea using yeasts and molds, particularly in relation to comparisons to the *E. coli* expression system (110),(125). In this study, recombinant EGPf was successfully expressed as an active protein in *A. niger*. After the expressed recombinant EGPf was purified and subjected to SDS-PAGE analysis with CBB and PAS staining, the results revealed a glycosylated protein with a molecular mass of approximately 45-kDa (Fig. 3-3). A previous study with *T. cellulolyticus* showed that

although EGPf was expressed as a 28-kDa polypeptide, glycosylation was not observed (110). The yield of recombinant G_EGPf in *A. niger* transformants (3.67 mg/mL of culture) was significantly higher than that of recombinant EGPf in *T. cellulolyticus* transformants (0.63 mg/mL of culture) (110). A qPCR analysis revealed the insertion of five EGPf expression cassettes into the genomic DNA of *A. niger* transformants. Following the deglycosylation of purified G_EGPf by EndoHf, the molecular mass of the deglycosylated EGPf on SDS-PAGE was identical to that of the wild-type EGPf (28-kDa). The recombinant EGPf expressed in *T. cellulolyticus* exhibited thermostability similar to that of the wild-type EGPf; however, other enzyme properties were not evaluated in that study (110). To compare the role of N-glycosylation on the biochemical properties of EGPf, unglycosylated EGPf (UG_EGPf) was expressed in *E. coli* and purified according to previously described procedures (110), as a sufficient amount of deglycosylated EGPf could not be obtained using EndoHf. The specific activities of the purified enzymes were as follows: G_EGPf (360.0 U/mg) and UG_EGPf (173.5 U/mg) (Table 3-2 and 3-3).

Effect of glycosylation on kinetic characterization

EGPf exhibits a high specificity for barley β-glucan as it contains both β-1,3 and β-1,4 linkages, whereas carboxymethyl cellulose has only β-1,4 linkages (103). Despite this high specificity, no reports have been identified that describe the kinetic parameters of EGPf for barley β-glucan hydrolysis, unlike the status for *p*-nitrophenyl cellooligosaccharides (103). In this study, G_EGPf showed a twofold increase in specific activity for barley β-glucan compared to UG_EGPf, owing to enhanced substrate affinity and hydrolytic activity (Table 3-4). Both G_EGPf and UG_EGPf have been shown to have higher affinities for barley β-glucan than other GH family 12 endoglucanases in

Sulfolobus shibatae (K_m=1.772 mg/mL) (126), *Thielavia terrestris* (K_m=0.91 mg/mL) (127), *Aspergillus cervinus* (K_m=3.16 mg/mL) (127), and *Aspergillus terreus* (K_m=2.21 mg/mL) (128).

Effect of glycosylation on thermostability

G_EGPf and UG_EGPf were pre-incubated at 100°C in 20 mM sodium acetate buffer (pH 5.0). The half-life of UG_EGPf was estimated ($T_{1/2}$≈10 min) earlier than that of G_EGPf (Fig. 3-4). In contrast, G_EGPf maintained greater than 80% of its original activity even after 5 h of incubation (Fig. 3-4). The predicted half-life of glycosylated EGPf at 100°C was approximately 1,018 min according to previously reported calculations (122),(123). Endoglucanases with optimal activities within the range of 95–106°C were observed in *P. furiosus*, *P. horikoshii*, and *T. neapolitana* (39). Glycosylation has been confirmed to improve thermostability; therefore, the effect of glycosylation on the optimum temperature was investigated (Fig. 3-5). The specific activity of G_EGPf at 80°C was approximately twice that of UG_EGPf (Table 3-2 and 3-3). Furthermore, the difference at 120°C was greater than three times due to the thermostability of G_EGPf (Fig. 3-5). It was difficult to measure the enzyme activities at temperatures greater than 120℃ because the reaction solution was concentrated during the incubation. The preparation of glycosylated EGPf may be an effective method for long-term repeated enzymatic processes. In particular, complete saccharification of biomass can be achieved through a combination of hyperthermophilic exo-glucanases (129).

Effect of glycosylation on pH stability and salt tolerance

The glycosylation status of EGPf did not influence its pH stability or activity

under different pH and NaCl conditions. Both G_EGPf and UG_EGPf showed broad pH stability ranges; however, G_EGPf was more stable in acidic conditions (pH 1.5–2.0) than UG_EGPf (Fig. 3-6(A)). Enzymatic activity at 80°C was optimized at a pH of 6 for both enzymes (Fig. 3-7). Moreover, both endoglucanases exhibited moderate salt tolerances with a relative activity of approximately 60% in 2 M NaCl (Fig. 3-6(B)).

Ionic liquid tolerance of EGPf

Imidazolium-based ionic liquids (ILs) such as [Bmim]Cl are widely used to pretreat lignocellulosic materials to enhance their enzymatic hydrolysis (130),(131). ILs dissolve the crystalline structure of cellulose under mild conditions, thereby increasing its accessibility to enzymes (130). A higher enzymatic degradation efficiency has been reported with regenerated cellulose after IL treatment (130). However, ILs can inactivate hydrolytic enzymes in both neat and aqueous-IL media because of protein aggregation (99). Additionally, the cationic imidazolium moieties of ILs inside the carbohydrate-binding module could interact with the hydrophobic residues of the domain, thereby competing for the binding of substrates and directly blocking the hydrolysis pathway (99).

G_EGPf and UG_EGPf showed higher specific activities in the presence of 10-30% (v/v) [Bmim]Cl and maintenance of specific activities in 40% (v/v) [Bmim]Cl when compared to the activity in the absence of the IL (Fig. 3-6(C)). The IL tolerance profiles of both enzymes were similar and glycosylation of EGPf did not enhance its IL tolerance. However, G_EGPf showed twice the specific activity of UG_EGPf (Fig. 3-6(C)). A similar study showed that the *P. horikoshii* endoglucanase (PhEG) (family GH5) increased its activity with CMC in the presence of up to 35% (v/v) 1-ethyl-3-methylimidazolium acetate among eight tested ILs (132). Ionic liquid-stable halophilic

endoglucanases from *Stachybotrys microspora* retained their activity in the presence of 5% and 10% [Bmim]Cl (100% and 80%, respectively) (133).

Functional modification of EGPf by N-glycosylation

N-glycosylation can confer thermostability to cellulases when positioned within the aromatic amino acid and loop regions (134). Glycosylation significantly boosted the thermostability of EGPf, allowing it to retain over 80% of its activity after exposure to 100°C for 5 h with the optimal temperature being above 120°C (Fig. 3-4 and 3-5). Additionally, this process enhanced the catalytic activity when located within the active cleft (134). EGPf possesses eight potential N-glycosylation sites, which were determined through analysis of the Asn-X-Thr/Ser consensus sequence using the online tool NetNGly 1.0 (Fig. 3-2). Among these sites, the ^{88}Asn residue was positioned near the active cleft, whereas the other seven sites were located on the side opposite the active cleft (Fig. 3-2). Introducing N-glycosylation to this specific amino acid residue could potentially enhance the hydrolytic activity of EGPf given its proximity to the active center. N-glycosylation near the active site tunnel and/or cleft was observed to improve catalytic efficiency in *Penicillium veruculosum* cellobiohydrolase I (PvCel7A), with a glycosylation site at ^{45}Asn (135), and *Thielavia terrestris* β-1,4-endoglucanase (TtCel45A), with a glycosylation site at ^{65}Asn (118). In addition, N-glycosylation can enhance enzyme thermostability by forming hydrogen bonds with the protein surface, which protects against thermal denaturation; this has been demonstrated in the β-1,4-glucanases of *Aspergillus niger* (136) and *Ganoderma lucidum* (137). Moreover, glycosylated moieties may shield the hydrophobic areas of proteins from aqueous solvents, thereby improving protein solubility and reducing aggregate formation (134). Hyperthermophilic

endoglucanases from *Pyrococcus* spp. are highly stable and have cellulose hydrolyzing capability at temperatures above 90°C (138); therefore, these enzymes could be useful in industrial applications, such as detergents, food and feed, textile biopolishing agents, and biofuels. Further investigation of the kinetic parameter profiles, thermal and pH stabilities, and IL tolerances of G_EGPf and its partially deglycosylated mutants is required.

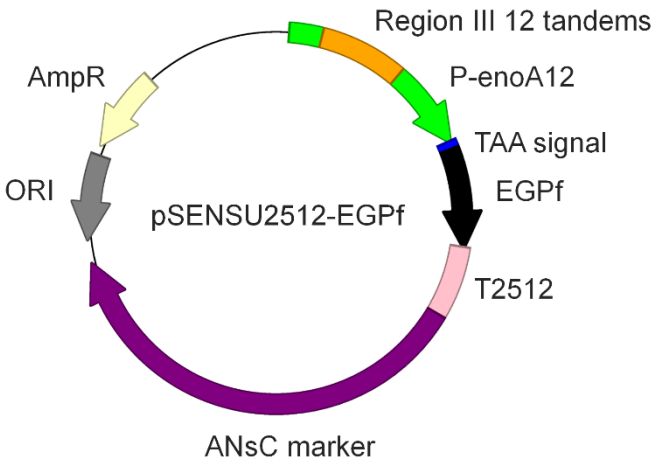

Fig. 3-1. pSENSU2512-EGPf plasmid map for transformation of *A. niger*. P-enoA12 indicates the promoter region, which is based on the *A. niger* enolase gene promoter containing the 12-repeat cis-element binding region (Region III 12 tandems). The signal sequence of the Taka-amylase A gene from *A. oryzae* (TAA signal) was added to the EGPf gene without the original signal sequence. T2512 indicates the transcriptional terminator and the ANsC marker signifies the *sC* gene from *A. niger* as the selection marker.

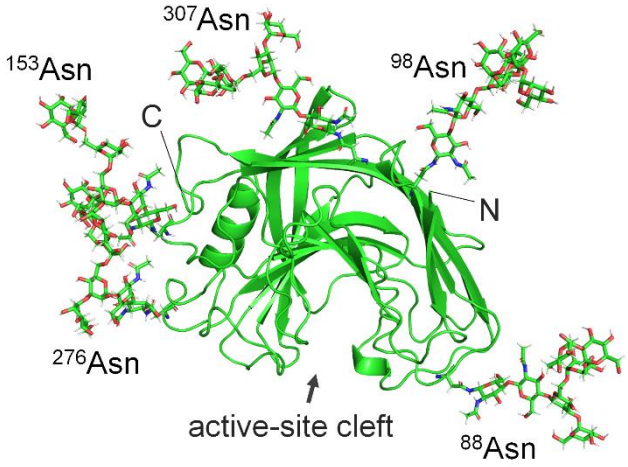

Fig. 3-2. The predicted glycosylation sites of EGPf. The EGPf structure was based on a previous report (124) and visualized using PyMOL version 2.5. The N-glycosylation sites were predicted using NetNglyc 1.0, and since the actual glycan structure is unknown, a Man5GlcNAc2-type glycan was added at each predicted glycosylation site as a provisional structure. The predicted glycosylation sites are indicated by the numbered asparagine residues (Asn). N and C signify the N- and C-terminal positions, respectively.

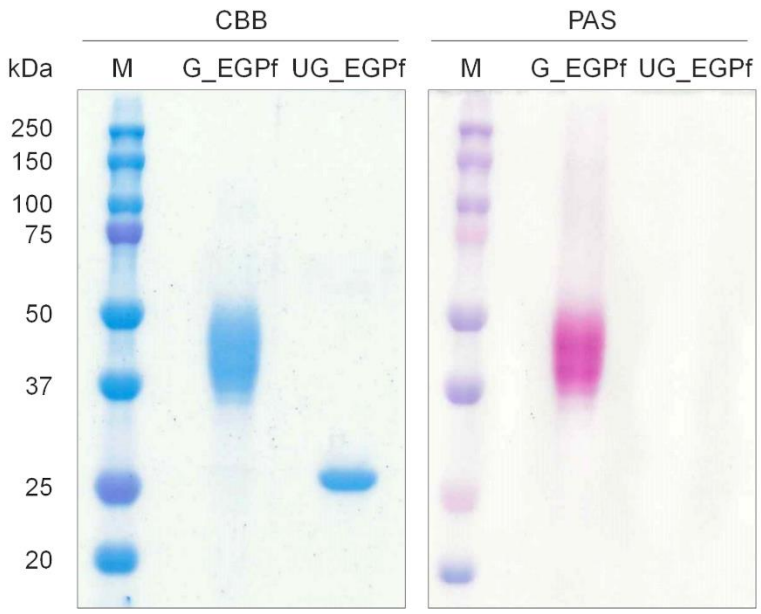

Fig. 3-3. SDS-PAGE analysis of heterologously expressed EGPfs. The purified glycosylated EGPf expressed in *A. niger* (G_EGPf) and unglycosylated EGPf expressed in *E. coli* (UG_EGPf) were subjected to SDS-PAGE. Results of Coomassie Brilliant Blue (CBB) and periodic acid-Schiff (PAS) staining are shown. Lane M indicates protein molecular mass markers. SDS-PAGE was conducted using a Mini-PROTEAN Tetra Cell gel electrophoresis system (Bio-Rad Laboratories, Inc., Hercules, CA, USA) according to the manufacturer's instructions. Purified G_EGPf and UG_EGPf samples were run at 20 mA for 1 h on a 10% (w/v) self-cast polyacrylamide gel.

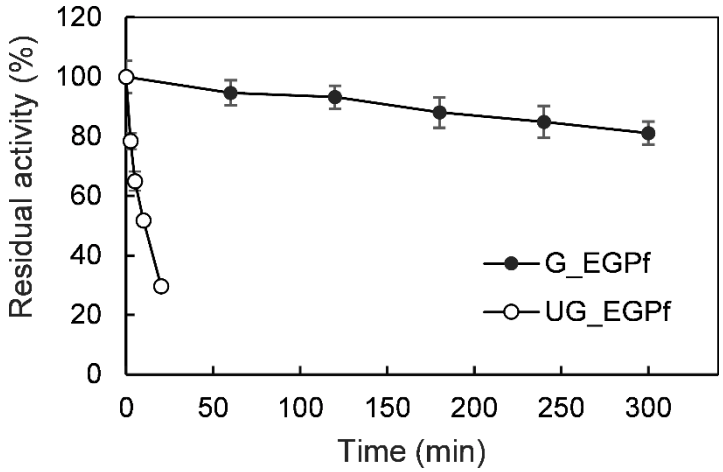

Fig. 3-4. Thermostability of glycosylated EGPf and unglycosylated EGPf. The protein concentrations of purified glycosylated EGPf (G_EGPf) and unglycosylated EGPf (UG_EGPf) were adjusted to 90 μg/mL. After pre-incubation at 100°C and sampling over time, the residual enzyme activities toward barley β-glucan were measured at 80°C. The specific activities of G_EGPf and UG_EGPf without preincubation measured 353.2 U/mg and 173.2 U/mg, respectively. The residual activity was then calculated based on these specific activities. The experiments were conducted in triplicate.

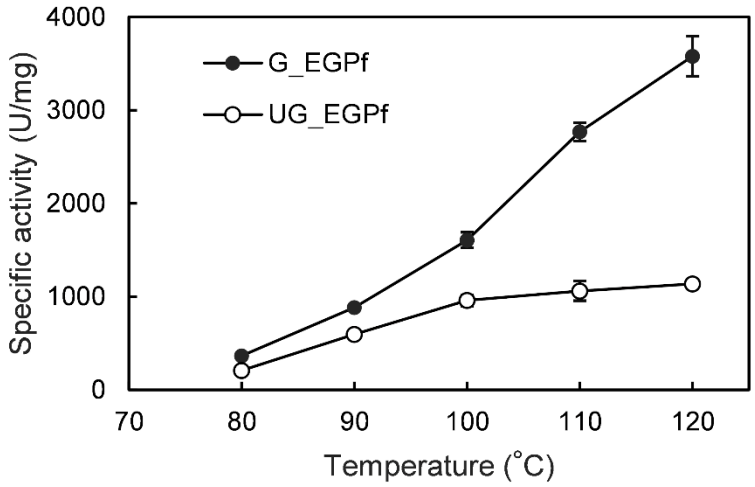

Fig. 3-5. Effect of temperature on enzyme activity. The hydrolytic activities toward barley β-glucan of purified glycosylated EGPf (G_EGPf, closed circle) and unglycosylated EGPf (UG_EGPf, open circle) were measured at temperatures ranging from 80 to 120 °C. The experiments were conducted in triplicate.

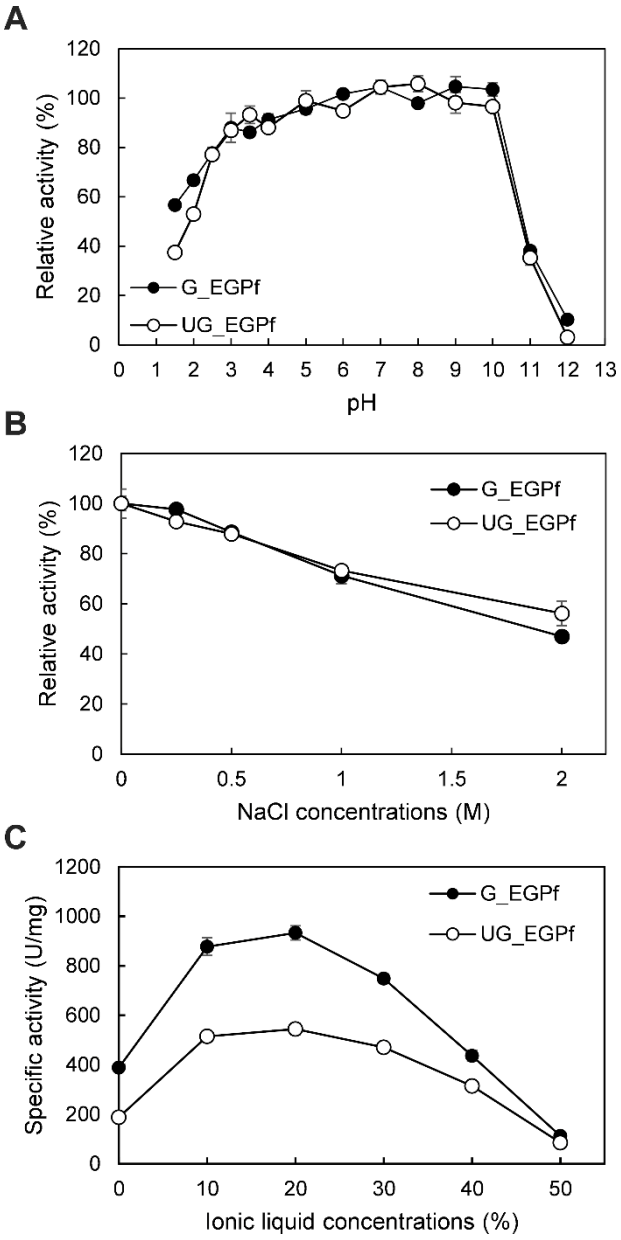

Fig. 3-6. Effect of various factors on endoglucanase stability and activity. (A) Effect of pH on stability. The purified glycosylated EGPf (G_EGPf, closed circle) and unglycosylated EGPf (UG_EGPf, open circle) were incubated at 37°C for 15 h in each of the following: 100 mM KCl-HCl buffer (pH 1.5–2.0), 100 mM glycine-HCl buffer (pH 2.5), 100 mM citrate buffer (pH 3.0–5.0), 100 mM sodium phosphate buffer (pH 6.0–8.0), 100 mM glycine-NaOH buffer (pH 9.0–10.0), and 100 mM Na_2HPO_4-NaOH buffer (pH 11.0–12.0). After incubation, the residual activity toward barley β-glucan was determined

in 50 mM sodium phosphate buffer, pH 6.0, containing 0.5% (w/v) barley β-glucan at 80°C. The specific activities of G_EGPf and UG_EGPf without incubation were 347.6 U/mg and 166.0 U/mg, respectively. The relative activity was calculated based on these specific activities. The experiments were conducted in triplicate. **(B)** Effect of NaCl concentration on endoglucanase activity. The enzyme activities of G_EGPf (closed circle) and UG_EGPf (open circle) were determined in 50 mM sodium phosphate buffer (pH 6.0), containing 0.5% (w/v) barley β-glucan without and with NaCl. The specific activities G_EGPf and UG_EGPf without NaCl were 361.5 U/mg and 188.9 U/mg, respectively. The relative activity was calculated based on these specific activities. The experiments were conducted in triplicate. **(C)** Effect of [Bmim]Cl concentration on endoglucanase activity. The enzyme activities of G_EGPf (closed circle) and UG_EGPf (open circle) were determined in 50 mM sodium phosphate buffer (pH 6.0), containing 0.5% (w/v) barley β-glucan without and with 1-butyl-3-methylimidazolium chloride ([Bmim]Cl). The experiments were conducted in triplicate.

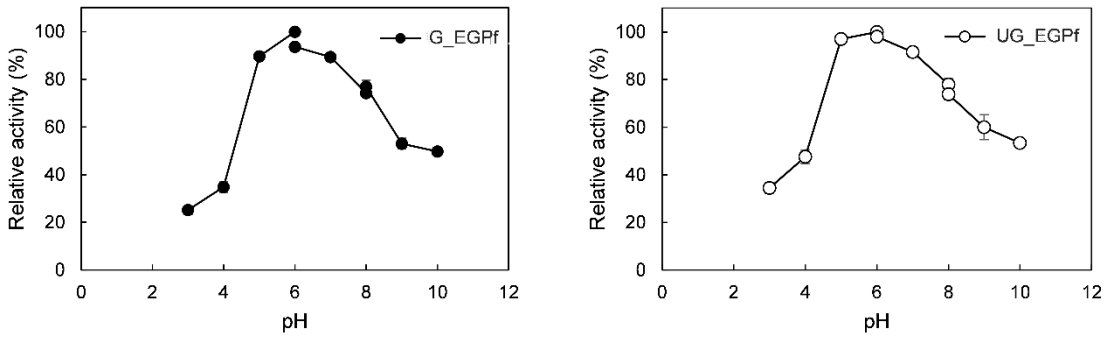

Fig. 3-7. Effect of pH on the activity of EGPf. Relative activities in the pH range of 3.0–10.0 at 80°C are shown. The pH was adjusted using a 50 mM citrate buffer (pH 3.0–6.0), sodium phosphate buffer (pH 6.0–8.0), or glycine-NaOH buffer (pH 8.0–10.0). The relative activities were calculated based on the specific activities in the 50 mM citrate buffer at pH 6.0 and 80°C. For G_EGPf and UG_EGPf, the specific activities were 365.5 U/mg and 169.9 U/mg, respectively.

Table 3-1. The codon-optimized sequence of TAA signal-EGPf gene

Sequence (5' to 3')
ATGATGGTCGCCTGGTGGTCCCTCTTCCTCTACGGTCTCCAGGTCGCCGCCC
CCGCCCTCGCCAAGGTCCTGAAGATCCGTTACCCTGACGATGGTGAGTGGCC
CGGCGCCCCCATCGACAAGGATGGCGATGGCAACCCTGAGTTCTACATCGAG
ATCAACCTGTGGAACATCCTTAACGCCACCGGCTTCGCTGAGATGACCTACAA
CCTTACCTCCGGTGTTCTCCACTACGTTCAGCAGCTGGACAACATCGTCCTCC
GCGATCGTAGCAACTGGGTCCACGGTTACCCTGAGATCTTCTACGGCAACAAG
CCTTGGAACGCCAACTACGCCACCGATGGCCCCATTCCCCTCCCTAGCAAGGT
CTCCAACCTCACCGACTTCTACCTCACTATCTCCTACAAGCTGGAGCCCAAGA
ACGGCCTGCCCATCAACTTCGCTATCGAGTCTTGGCTTACTCGTGAGGCTTG
GCGTACTACTGGCATCAACTCCGATGAGCAGGAGGTCATGATCTGGATCTACT
ACGATGGCCTGCAGCCCGCTGGCTCTAAGGTCAAGGAGATCGTCGTCCCCAT
CATCGTCAACGGTACCCCTGTCAACGCTACCTTCGAGGTCTGGAAGGCCAACA
TCGGTTGGGAGTACGTCGCCTTCCGCATCAAGACCCCCATCAAGGAGGGTAC
TGTTACCATCCCTTACGGCGCCTTCATCTCTGTTGCCGCCAACATCTCCTCCC
TGCCCAACTACACTGAGCTCTACCTTGAGGATGTCGAGATTGGTACCGAGTTC
GGTACTCCTTCTACCACTTCCGCTCACCTTGAGTGGTGGATCACCAACATCAC
TCTCACCCCTCTTGACCGCCCTCTGATCTCCTAA

Table 3-2. Summary of the purification of recombinant G_EGPf from *A. niger*

Fraction	Total activity (U)	Total protein (mg)	Specific activity (U/mg)	Recovery (%)
Cultural supernatant	440	7.7	57.1	100
Heat treatment	434	4.5	96.4	98.6
Dialysis	399	3.9	102.3	90.7
HiTrap DEAE FF	230	1.0	230.0	52.3
Superdex 75 Increase	90	0.25	360.0	20.5

Table 3-3. Summary of the purification of recombinant UG_EGPf from *E. coli*

Fraction	Total activity (U)	Total protein (mg)	Specific activity (U/mg)	Recovery (%)
Cell extract	485	72.1	6.7	100
Heat treatment	476	22.7	21.0	98.1
Dialysis	428	14.8	28.9	88.2
HiTrap DEAE FF	375	7.3	51.4	77.3
HiTrap Butyl FF	202	1.6	126.3	41.6
Superdex 75 Increase	59	0.34	173.5	12.2

Table 3-4. Kinetic parameters of glycosylated and unglycosylated EGPfs toward barley β-D-glucan

Enzyme	K_m (mg/ml)	k_{cat} (s^{-1})	k_{cat}/K_m (ml/s/mg)
G_EGPf	0.22±0.012	206.8±3.7	941.9±53.2
UG_EGPf	0.30±0.023	126.7±3.5	416.7±33.2

Abbreviations: G_EGPf, glycosylated EGPf expressed in *A. niger*; UG_EGPf, unglycosylated EGPf expressed in *E. coli*.

Concluding Discussion

In this study, we heterologously expressed, characterized, and functionally modified enzymes derived from extremophiles using koji molds such as *Aspergillus oryzae* and *Aspergillus niger* as a host. In Chapter 1, we focused on improving the salt tolerance of γ-glutamyl transpeptidase from *A. oryzae* (AOggtA) by creating a chimeric enzyme ASAOggtA with salt-tolerant GGT from *A. sydowii* (ASggtA), and found that the N-terminal sequence of ASggtA was important for salt tolerance. In Cahpter2, we heterologously expressed β-1,3-glucosidase (BGL_MK86) from *Aspergillus chevalieri*, a halophilic filamentous fungus. This enzyme was produced in solid culture using katsuobushi, but as a result of heterologous expression with *A. oryzae*, it was successfully produced in the culture supernatant. Characterization of the heterologous expression of BGL_MK86 indicated that this enzyme is highly salt tolerant and has the ability to hydrolyze crude laminarin in the presence of NaCl, indicating its potential for use in the saccharification of marine biomass.

It has been reported that the enzymes produced by xerophilic fungi isolated from katsuobushi, such as *A. sydowii* and *A. chevalieri*, are not only resistant to xerophilic conditions, but also have salt tolerance (29). Several filamentous fungi have been reported to be involved in the fermentation of katsuobushi (8),(39), and the enzymes produced by these filamentous fungi are also expected to have important properties such as tolerance to xerophilic conditions and salt tolerance. In this study, we were able to characterize these enzymes from xerophilic fungi by heterologously expressing in *Aspergillus oryzae*. By selecting *Aspergillus* spp. as a host for heterologous expression of these proteins derived from xerophilic filamentous fungi, the high expression efficiency of the proteins derived from the same genus, as well as their

high productivity, will enable consistent efforts toward their future industrial utilization. The enzyme from filamentous fungi isolated from katsuobushi is considered to be a useful source for isolating enzymes that have both high safety from food sources and unique properties such as salt tolerance. Heterologous expression and characterization of these enzymes derived from xerophilic fungi using *Aspergillus* spp. as hosts will be useful in the future to search for unknown useful enzymes.

In Chapter 3, endoglucanase from the hyperthermophilic archaeon *Pyrococcus furiosus* (EGPf) was heterologously expressed in *A. niger* as a host. EGPf was shown to be secreted as a glycoprotein when heterologously expressed in *A. niger*, and glycosylation enhanced enzyme activity and thermostability. For heterologous expression of archaeal enzymes, *E. coli* expression systems have generally been used, and few studies have been conducted on heterologous expression in eukaryotes, especially on the effects of glycosylation on archaeal enzymes (103),(110),(125). However, it has been reported that some archaea such as *P. furiosus* can add N-glycans to proteins (139), thus it is important to evaluate the effect of glycosylation on archaeal enzymes by heterologous expression in a host that can add N-glycans, as in this study. Many archaeal enzymes are known to be industrially important enzymes that are adapted to harsh conditions such as thermostability, salt tolerance, and acid tolerance (1)–(3) The importance of the integrated process from the heterologous expression of these enzymes from extremophiles using koji mold as a host to the evaluation of the effects of post-translational modifications including glycosylation and the subsequent construction of overexpression system was demonstrated.

Acknowledgements

神戸大学大学院農学研究科生命機能科学専攻 微生物資源化学研究室の竹中慎治教授には指導教官として本研究に取り組む機会と研究遂行における多大なるご支援を頂きました。特に雑誌投稿論文の執筆に際しては、私の未熟な論文に対し、精緻なアドバイスとお時間を割いていただきましたことに、心より感謝を申し上げます。同研究室の木村行宏准教授には本論文審査の副査としてだけでなく、日ごろから数多くのご指導を賜りました。また、報告会等でのご指摘は、私に新しい視点をもたらし、研究において大いに発展させる契機となりました。同専攻の宇野知秀教授には、本論文の副査として数多くのご助言を頂戴し、深く感謝いたします。

本研究の遂行にあたっては、産業技術総合研究所の石川一彦先生に大変親切かつ熱心なご支援を賜りました。超耐熱性エンドグルカナーゼの情報と耐熱性酵素の評価方法に関してのご指導は、研究の質を飛躍的に向上させました。雑誌投稿論文の執筆においても、先生の温かいご支援に心から感謝しております。

微生物資源化学研究室のメンバーには、日々の研究において助けられることが多くありました。特に西川有咲様、斉藤大輔様には、耐塩性γ-グルタミルトランスフェラーゼと耐塩性β-グルコシダーゼの特性解析において、尽力いただきました。彼らの協力なくしては、研究の成功はあり得ませんでした。心より感謝いたします。

大関株式会社 総合研究所の皆様には、日々の業務と研究において温かいサポートを賜りました。特に幸田明生所長、坪井宏和次長、坊垣隆之様には、博士課程への入学を快くお許しいただき、深く感謝しております。

本研究の遂行にあたっては、公私にわたり多くの方々にお世話になりました。お一人お一人のお名前を挙げることはできませんが、それぞれのお立場から頂戴したお力添えに心より感謝いたします。

References

1. **Mesbah, N. M.:** Industrial biotechnology based on enzymes from extreme environments, Front Bioeng Biotechnol, **10**, 1–16 (2022).

2. **Ortiz-Cortés, L. Y., Ventura-Canseco, L. M. C. and Abud-Archila, M.:** Evaluation of temperature, pH and nutrient conditions in bacterial growth and extracellular hydrolytic activities of two Alicyclobacillus spp. strains, Arch Microbiol, **203**, (2021).

3. **Solat, N. and Shafiei, M.:** A novel pH and thermo-tolerant halophilic alpha-amylase from moderate halophile Nesterenkonia sp. strain F: gene analysis, molecular cloning, heterologous expression and biochemical characterization, Arch Microbiol, **203**, (2021).

4. **Chettri, D., Verma, A. K., Sarkar, L. and Verma, A. K.:** Role of extremophiles and their extremozymes in biorefinery process of lignocellulose degradation, Extremophiles, **25**, 203–219 (2021).

5. **Zhu, D., Qaria, M. A., Zhu, B., Sun, J. and Yang, B.:** Extremophiles and extremozymes in lignin bioprocessing, Renew. Sustain. Energy Rev., **157**, 112069 (2022).

6. **Li, C., Zhou, J., Du, G., Chen, J., Takahashi, S. and Liu, S.:** Developing Aspergillus niger as a cell factory for food enzyme production, Biotechnol. Adv.,

44, 107630 (2020).

7. **Jin, F. J., Hu, S., Wang, B. T. and Jin, L.:** Advances in Genetic Engineering Technology and Its Application in the Industrial Fungus Aspergillus oryzae, Front. Microbiol., **12**, 1–14 (2021).

8. **Takenaka, S., Nakabayashi, R., Ogawa, C., Kimura, Y., Yokota, S. and Doi, M.:** Characterization of surface Aspergillus community involved in traditional fermentation and ripening of katsuobushi, Int. J. Food Microbiol., **327**, 108654 (2020).

9. **Esawy, M. A., Awad, G. E. A. and Wahab, W. A. A.:** Immobilization of halophilic Aspergillus awamori EM66 exochitinase on grafted k-carrageenan-alginate beads, 3 Biotech, **6**, (2016).

10. **Jiménez-Gómez, I., Valdés-Muñoz, G. and Moreno-Perlin, T.:** Haloadaptative responses of Aspergillus sydowii to extreme water deprivation: Morphology, compatible solutes, and oxidative stress at NaCl saturation, J Fungi, **6**, (2020).

11. **Saini, M., Kashyap, A., Bindal, S., Saini, K. and Gupta, R.:** Bacterial Gamma-Glutamyl Transpeptidase, an Emerging Biocatalyst: Insights Into Structure–Function Relationship and Its Biotechnological Applications, Front. Microbiol., **12**, 1–30 (2021).

12. **Yang, J., Bai, W., Zeng, X. and Cui, C.:** Gamma glutamyl peptides: The food source, enzymatic synthesis, kokumi-active and the potential functional properties – A review, Trends Food Sci. Technol., **91**, 339–346 (2019).

13. **Murty, N. A. R., Tiwary, E., Sharma, R., Nair, N. and Gupta, R.:** γ-Glutamyl transpeptidase from Bacillus pumilus KS 12: Decoupling autoprocessing from catalysis and molecular characterization of N-terminal region, Enzyme Microb. Technol., **50**, 159–164 (2012).

14. **Chi, M. C., Lo, H. F., Lin, M. G., Chen, Y. Y., Wang, T. F. and Lin, L. L.:** Mutational analysis of a highly conserved PLSSMXP sequence in the small subunit of bacillus licheniformis γ-glutamyltranspeptidase, Biomolecules, **9**, 1–18 (2019).

15. **Bindal, S., Dagar, V. K., Saini, M., Khasa, Y. P. and Gupta, R.:** High level extracellular production of recombinant γ-glutamyl transpeptidase from Bacillus licheniformis in Escherichia coli fed-batch culture, Enzyme Microb. Technol., **116**, 23–32 (2018).

16. **Sharma, E., Lal, M. K., Gulati, A. and Gulati, A.:** Heterologous expression, on-column refolding and characterization of gamma-glutamyl transpeptidase gene from Bacillus altitudinis IHB B1644: A microbial bioresource from

Western Himalayas, Process Biochem., **116**, 126–135 (2022).

17. **Bindal, S., Sharma, S., Singh, T. P. and Gupta, R.:** Evolving transpeptidase and hydrolytic variants of γ-glutamyl transpeptidase from Bacillus licheniformis by targeted mutations of conserved residue Arg109 and their biotechnological relevance, J. Biotechnol., **249**, 82–90 (2017).

18. **Calvio, C., Romagnuolo, F., Vulcano, F., Speranza, G. and Morelli, C. F.:** Evidences on the role of the lid loop of γ-glutamyltransferases (GGT) in substrate selection, Enzyme Microb. Technol., **114**, 55–62 (2018).

19. **Cho, H. Bin, Ahn, J. H., Yang, H. G., Lee, J., Park, W. J. and Kim, Y. W.:** Effects of pH and NaCl on hydrolysis and transpeptidation activities of a salt-tolerant γ-glutamyltranspeptidase from Bacillus amyloliquefaciens S0904, Food Sci. Biotechnol., **30**, 853–860 (2021).

20. **Minami, H., Suzuki, H. and Kumagai, H.:** Salt-tolerant γ-glutamyltranspeptidase from Bacillus subtilis 168 with glutaminase activity, Enzyme Microb. Technol., **32**, 431–438 (2003).

21. **Barzkar, N., Sohail, M., Tamadoni Jahromi, S., Nahavandi, R. and Khodadadi, M.:** Marine microbial L-glutaminase: from pharmaceutical to food industry, Appl. Microbiol. Biotechnol., **105**, 4453–4466 (2021).

22. **Ito, K. and Matsuyama, A.:** Koji molds for japanese soy sauce brewing: Characteristics and key enzymes, J. Fungi, **7**, (2021).

23. **Graziano, G. and Merlino, A.:** Molecular bases of protein halotolerance, Biochim. Biophys. Acta - Proteins Proteomics, **1844**, 850–858 (2014).

24. **Nandakumar, R., Yoshimune, K., Wakayama, M. and Moriguchi, M.:** Microbial glutaminase: Biochemistry, molecular approaches and applications in the food industry, J. Mol. Catal. B Enzym., **23**, 87–100 (2003).

25. **Wada, K., Irie, M., Suzuki, H. and Fukuyama, K.:** Crystal structure of the halotolerant γ-glutamyltranspeptidase from Bacillus subtilis in complex with glutamate reveals a unique architecture of the solvent-exposed catalytic pocket, FEBS J., **277**, 1000–1009 (2010).

26. **Pica, A., Russo Krauss, I., Castellano, I., La Cara, F., Graziano, G., Sica, F. and Merlino, A.:** Effect of NaCl on the conformational stability of the thermophilic γ-glutamyltranspeptidase from Geobacillus thermodenitrificans: Implication for globular protein halotolerance, Biochim. Biophys. Acta - Proteins Proteomics, **1834**, 149–157 (2013).

27. **Li, Z., Zhu, R., Liu, Y., Li, J., Gao, H. and Hu, N.:** γ-Glutamyltranspeptidase from Bacillus amyloliquefaciens: transpeptidation activity enhancement and L-

theanine production, Enzyme Microb. Technol., **140**, 109644 (2020).

28. **KATO, T., MAEDA, K., KASUYA, H. and MATSUDA, T.:** Complete Growth Inhibition of Bacillus subtilis by Nisin-Producing Lactococci in Fermented Soybeans, Biosci. Biotechnol. Biochem., **63**, 642–647 (1999).

29. **Nishikawa, A., Senba, H., Kimura, Y., Yokota, S., Doi, M. and Takenaka, S.:** Isolation and characterization of a salt-tolerant γ-glutamyl transpeptidase from xerophilic Aspergillus sydowii, 3 Biotech, **12**, 1–17 (2022).

30. **Mokashe, N., Chaudhari, B., Patil, U. and Patil, P.:** Operative utility of salt-stable proteases of halophilic and halotolerant bacteria in the biotechnology sector, Int J Biol Macromol, **117**, 493–522 (2018).

31. **Gao, X., Yin, Y. and Zhou, C.:** Purification, characterisation and salt-tolerance molecular mechanisms of aspartyl aminopeptidase from Aspergillus oryzae 3.042, Food Chem, **240**, 377–385 (2018).

32. **Gao, X., Yin, Y., Yan, J., Zhang, J., Ma, H. and Zhou, C.:** Separation, biochemical characterization and salt-tolerant mechanisms of alkaline protease from Aspergillus oryzae, J. Sci. Food Agric., **99**, 3359–3366 (2019).

33. **Esclapez, J., Pire, C., Bautista, V., Martínez-Espinosa, R. M., Ferrer, J. and Bonete, M. J.:** Analysis of acidic surface of Haloferax mediterranei glucose

dehydrogenase by site-directed mutagenesis, FEBS Lett., **581**, 837–842 (2007).

34. **Warden, A. C., Williams, M., Peat, T. S., Seabrook, S. A., Newman, J., Dojchinov, G. and Haritos, V. S.:** Rational engineering of a mesohalophilic carbonic anhydrase to an extreme halotolerant biocatalyst, Nat. Commun., **6**, 1–10 (2015).

35. **Li, Z., Li, X., Liu, T., Chen, S., Liu, H., Wang, H., Li, K., Song, Y., Luo, X., Zhao, J. and Zhang, T.:** The critical roles of exposed surface residues for the thermostability and halotolerance of a novel GH11 xylanase from the metagenomic library of a saline-alkaline soil, Int. J. Biol. Macromol., **133**, 316–323 (2019).

36. **Unkles, S. E., Campbell, E. I., de Ruiter-Jacobs, Y. M. J. T., Broekhuijsen, M., Macro, J. A., Carrez, D., Contreras, R., van den Hondel, C. A. M. J. J. and Kinghorn, J. R.:** The development of a homologous transformation system for Aspergillus oryzae based on the nitrate assimilation pathway: A convenient and general selection system for filamentous fungal transformation, MGG Mol. Gen. Genet., **218**, 99–104 (1989).

37. **Yamada, O., Lee, B. R., Gomi, K. and Iimura, Y.:** Cloning and functional analysis of the Aspergillus oryzae conidiation regulator gene brlA by its

disruption and misscheduled expression, J. Biosci. Bioeng., **87**, 424–429 (1999).

38. **Iimura, Y., Gomi, K. and Uzu, H.:** Complementation of the Methionine-auxotrophic Mutation, **51**, 323–328 (1987).

39. **Takenaka, S., Ogawa, C., Uemura, M., Umeki, T., Kimura, Y., Yokota, S. and Doi, M.:** Identification and characterization of extracellular enzymes secreted by Aspergillus spp. involved in lipolysis and lipid-antioxidation during katsuobushi fermentation and ripening, Int J Food Microbiol, **353**, 109299 (2021).

40. **Gomi, K., Iimura, Y. and Hara, S.:** Integrative Transformation of Aspergillus oryzae with a Plasmid Containing the Aspergillus nidulans argB Gene, Agric. Biol. Chem., **51**, 2549–2555 (1987).

41. **Wakai, S., Nakashima, N., Ogino, C., Tsutsumi, H., Hata, Y. and Kondo, A.:** Modified expression of multi-cellulases in a filamentous fungus Aspergillus oryzae, Bioresour. Technol., **276**, 146–153 (2019).

42. **Kobayashi, M., Sasaki, Y. and Kobayashi, S.:** Purification of Amylases and Other Enzymes by a Forced-affinity Chromatography Method, Biosci. Biotechnol. Biochem., **61**, 813–816 (1997).

43. **Sekizaki, H., Murakami, M., Itoh, K., Toyota, E. and Tanizawa, K.:** Chum

salmon trypsin-catalyzed peptide synthesis with inverse substrates as acyl donor components at low temperature, J. Mol. Catal. - B Enzym., **11**, 23–28 (2000).

44. **Klausen, M. S., Jespersen, M. C., Nielsen, H., Jensen, K. K., Jurtz, V. I., Sønderby, C. K., Sommer, M. O. A., Winther, O., Nielsen, M., Petersen, B. and Marcatili, P.:** NetSurfP-2.0: Improved prediction of protein structural features by integrated deep learning, Proteins Struct. Funct. Bioinforma., **87**, 520–527 (2019).

45. **Pickel, B., Pfannstiel, J., Steudle, A., Lehmann, A., Gerken, U., Pleiss, J. and Schaller, A.:** A model of dirigent proteins derived from structural and functional similarities with allene oxide cyclase and lipocalins, FEBS J., **279**, 1980–1993 (2012).

46. **Bindal, S. and Gupta, R.:** Thermo- and salt-tolerant chitosan cross-linked γ-glutamyl transpeptidase from Bacillus licheniformis ER15, Int. J. Biol. Macromol., **91**, 544–553 (2016).

47. **Shuai, Y., Zhang, T., Mu, W. and Jiang, B.:** Purification and Characterization of γ-Glutamyltranspeptidase from Bacillus subtilis SK11.004, J. Agric. Food Chem., **59**, 6233–6238 (2011).

48. **Gao, X., Liu, E., Yin, Y., Yang, L., Huang, Q., Chen, S. and Ho, C. T.:**

Enhancing activities of salt-tolerant proteases secreted by Aspergillus oryzae using atmospheric and room-temperature plasma mutagenesis, J Agric Food Chem, **68**, 2757–2764 (2020).

49. **Srimathi, S., Jayaraman, G., Feller, G., Danielsson, B. and Narayanan, P. R.:** Intrinsic halotolerance of the psychrophilic α-amylase from Pseudoalteromonas haloplanktis, Extremophiles, **11**, 505–515 (2007).

50. **Zhang, W., Xu, H., Wu, Y., Zeng, J., Guo, Z., Wang, L., Shen, C., Qiao, D. and Cao, Y.:** A new cold-adapted, alkali-stable and highly salt-tolerant esterase from Bacillus licheniformis, Int. J. Biol. Macromol., **111**, 1183–1193 (2018).

51. **Fitter, J. and Haber-Pohlmeier, S.:** Structural stability and unfolding properties of thermostable bacterial α-amylases: A comparative study of homologous enzymes, Biochemistry, **43**, 9589–9599 (2004).

52. **Scapini, T., Dalastra, C., Camargo, A. F., Kubeneck, S., Modkovski, T. A., Júnior, S. L. A. and Treichel, H.:** Seawater-based biorefineries: A strategy to reduce the water footprint in the conversion of lignocellulosic biomass, Bioresour. Technol., **344**, (2022).

53. **Wang, D., Zheng, Z. Y., Feng, J., Zhan, X. B., Zhang, L. M., Wu, J. R., Lin, C. C. and Zhu, L.:** Influence of sodium chloride on thermal denaturation of a

high-salt-tolerant neutral protease from Aspergillus oryzae, Food Sci. Biotechnol., **22**, 1–7 (2013).

54. **Luh, B. S.:** Industrial production of soy sauce, J. Ind. Microbiol., **14**, 467–471 (1995).

55. **Shan, P., Ho, C.-T., Zhang, L., Gao, X., Lin, H., Xu, T., Wang, B., Fu, J., He, R. and Zhang, Y.:** Degradation Mechanism of Soybean Protein B(3) Subunit Catalyzed by Prolyl Endopeptidase from Aspergillus niger during Soy Sauce Fermentation., J. Agric. Food Chem., **70**, 5869–5878 (2022).

56. **Morelli, C. F., Calvio, C., Biagiotti, M. and Speranza, G.:** PH-Dependent hydrolase, glutaminase, transpeptidase and autotranspeptidase activities of Bacillus subtilis γ-glutamyltransferase, FEBS J., **281**, 232–245 (2014).

57. **Rocha, R. A. R., Ribeiro, M. N., Silva, G. A., Rocha, L. C. R., Pinheiro, A. C. M., Nunes, C. A. and Carneiro, J. de D. S.:** Temporal profile of flavor enhancers MAG, MSG, GMP, and IMP, and their ability to enhance salty taste, in different reductions of sodium chloride, J. Food Sci., **85**, 1565–1575 (2020).

58. **Castellano, I., Di Salle, A., Merlino, A., Rossi, M. and La Cara, F.:** Gene cloning and protein expression of γ-glutamyltranspeptidases from Thermus thermophilus and Deinococcus radiodurans: Comparison of molecular and

structural properties with mesophilic counterparts, Extremophiles, **15**, 259–270 (2011).

59. **Rajput, R., Verma, V. V., Chaudhary, V. and Gupta, R.:** A hydrolytic γ-glutamyl transpeptidase from thermo-acidophilic archaeon Picrophilus torridus: Binding pocket mutagenesis and transpeptidation, Extremophiles, **17**, 29–41 (2013).

60. **Zheng, F., Vermaas, J. V., Zheng, J., Wang, Y., Tu, T., Wang, X., Xie, X., Yao, B., Beckham, G. T. and Luo, H.:** Activity and thermostability of GH5 endoglucanase chimeras from mesophilic and thermophilic parents, Appl. Environ. Microbiol., **85**, (2018).

61. **Masakari, Y., Hara, C., Araki, Y., Gomi, K. and Ito, K.:** Improvement in the thermal stability of Mucor prainii-derived FAD-dependent glucose dehydrogenase via protein chimerization, Enzyme Microb. Technol., **132**, 109387 (2020).

62. **Wang, X., Ma, R., Xie, X., Liu, W., Tu, T., Zheng, F., You, S., Ge, J., Xie, H., Yao, B. and Luo, H.:** Thermostability improvement of a Talaromyces leycettanus xylanase by rational protein engineering, Sci. Rep., **7**, 1–9 (2017).

63. **Wang, Q. and Xia, T.:** Importance of C-terminal region for thermostability of

GH11 xylanase from Streptomyces lividans, Appl. Biochem. Biotechnol., **144**, 273–282 (2008).

64. **Matsumoto, K., Takase, K., Yamamoto, Y., Doi, Y. and Taguchi, S.:** Chimeric enzyme composed of polyhydroxyalkanoate (PHA) synthases from ralstonia eutropha and aeromonas caviae enhances production of PHAs in recombinant escherichia coli, Biomacromolecules, **10**, 682–685 (2009).

65. **Zacharius, R. M., Zell, T. E., Morrison, J. H. and Woodlock, J. J.:** Glycoprotein staining following electrophoresis on acrylamide gels, Anal. Biochem., **30**, 148–152 (1969).

66. **Roth, J. C. G., Hoeltz, M. and Benitez, L. B.:** Current approaches and trends in the production of microbial cellulases using residual lignocellulosic biomass: a bibliometric analysis of the last 10 years, Arch Microbiol, **202**, (2020).

67. **Djelid, H., Flahaut, S. and Wauven, C. V:** Production of a halotolerant endo-1,4-β-glucanase by a newly isolated Bacillus velezensis H1 on olive mill wastes without pretreatment: purification and characterization of the enzyme, Arch Microbiol, **204**, (2022).

68. **Kim, E. J., Fathoni, A. and Jeong, G. T.:** Microbacterium oxydans, a novel alginate- and laminarin-degrading bacterium for the reutilization of brown-

seaweed waste, J Env. Manag., **13**, (2013).

69. **Wang, D. D., Kim, Y. J. and Hoang, V. A.:** Paenibacillus puernese sp. nov., a β-glucosidase-producing bacterium isolated from Pu'er tea, Arch Microbiol, **198**, (2015).

70. **Schwentke, J., Sabel, A. and Petri, A.:** The yeast Wickerhamomyces anomalus AS1 secretes a multifunctional exo-β-1,3-glucanase with implications for winemaking, Yeast, **31**, (2014).

71. **Tian, Y. F., Chen, Y. X. and Tong, X.:** Flavor differences of soybean and defatted soybean fermented soy sauce and its correlation with the enzyme profiles of the kojis, J Sci Food Agric, **103**, (2022).

72. **Musa, H., Kasim, F. H. and Gunny, A. A. N.:** Salt-adapted moulds and yeasts: potentials in industrial and environmental biotechnology, Proc Biochem, **69**, (2018).

73. **Qiu, W., Li, J. and Wei, Y.:** Genome sequencing of Aspergillus glaucus 'CCHA' provides insights into salt-stress adaptation, Peer J, **8**, (2020).

74. **Chung, D., Yu, W. J. and Lim, J. Y.:** Characterization of the proteolytic activity of a halophilic Aspergillus reticulatus strain SK1-1 isolated from a solar saltern, Microorganisms, **10**, (2022).

75. **Senba, H., Nishikawa, A., Kimura, Y., Tanaka, S., Matsumoto, J. ichi, Doi, M. and Takenaka, S.:** Improvement in salt-tolerance of Aspergillus oryzae γ-glutamyl transpeptidase via protein chimerization with Aspergillus sydowii homolog, Enzyme Microb. Technol., **167**, 110240 (2023).

76. **Riou, C., Salmon, J. M. and Vallier, M. J.:** Purification, characterization, and substrate specificity of a novel highly glucose-tolerant β-glucosidase from Aspergillus oryzae, Appl Env. Microbiol, **64**, (1998).

77. **Wang, C. M., Shyu, C. L. and Ho, S. P.:** Characterization of a novel thermophilic, cellulose-degrading bacterium Paenibacillus sp. strain B39, Lett Appl Microbiol, **47**, (2008).

78. **Miller, G. L.:** Use dinitrosalycylic acid reagent of determination of reducing sugar, Anal Chem, **31**, (1959).

79. **Miyanishi, N., Inaba, Y. and Okuma, H.:** Amperometric determination of laminarin using immobilized β-1,3-glucanase, Biosens Bioelectron, **19**, (2004).

80. **Cutfield, S. M., Davies, G. and Murshudov, G.:** The structure of the exo-β-(1,3)-glucanase from Candida albicans in native and bound forms: relationship between a pocket and groove in family 5 glycosyl hydrolases, J Mol Biol, **294**, (1999).

81. **Zada, N. S., Belduz, A. O. and Güler, H. I.:** Cloning, expression, biochemical characterization, and molecular docking studies of a novel glucose tolerant β-glucosidase from Saccharomonospora sp. NB11, Enzym. Microb Technol, **148**, (2021).

82. **Marvig, C. L., Kristiansen, R. M. and Madsen:** Identification and characterisation of organisms associated with chocolate pralines and sugar syrups used for their production, Int J Food Microbiol, **185**, (2014).

83. **Oritiz-Lemus, J. F., Campoy, S. and Martín, J. F.:** Biological control of mites by xerophile Eurotium species isolated from the surface of dry cured ham and dry beef cecina, J Appl Microbiol, **130**, (2021).

84. **Zhao, C., Guo, L. and Wang, L.:** Improving the yield of (+)-terrein from the salt-tolerant Aspergillus terreus PT06-2, World J Microbiol Biotechnol, **32**, (2016).

85. **Yin, Y. R., Sang, P. and Xiao, M.:** Expression and characterization of a cold-adapted, salt- and glucose-tolerant GH1 β-glucosidase obtained from Thermobifida halotolerans and its use in sugarcane bagasse hydrolysis, Biomass Convers Biorefin, **11**, (2021).

86. **Sun, J., Wang, W. and Yao, C.:** Overexpression and characterization of a novel

cold-adapted and salt-tolerant GH1 β-glucosidase from the marine bacterium Alteromonas sp. L82, J Microbiol, **56**, (2018).

87. **Wu, J., Geng, A. and Xie, R.:** Characterization of cold adapted and ethanol tolerant β-glucosidase from Bacillus cellulosilyticus and its application for directed hydrolysis of cellobiose to ethanol, Int J Biol Mcromol, **109**, (2018).

88. **Lee, J. M., Kim, Y. R. and Kim, J. K.:** Characterization of salt-tolerant β-glucosidase with increased thermostability under high salinity conditions from Bacillus sp. SJ-10 isolated from jeotgal, a traditional Korean fermented seafood, Bioprocess Biosyst Eng, **38**, (2015).

89. **Salgado, J. C. S., Meleiro, L. P. and Carli, S.:** Glucose tolerant and glucose stimulated β-glucosidases–A review, Bioresour Technol, **267**, (2018).

90. **Guo, Y., Yan, Q. and Yang, Y.:** Expression and characterization of a novel β-glucosidase, with transglycosylation and exo-β-1,3-glucanase activities, from Rhizomucor miehei, Food Chem, **175**, (2015).

91. **Jiang, C., Song, J. and Cong, S.:** Expression and characterization of a novel antifungal exo-β-1,3-glucanase from Chaetomium cupreum, Appl Biochem Biotechnol, **182**, (2016).

92. **Kim, D. H., Kim, D. H. and Lee, S. H.:** A novel β-glucosidase from

Saccharophagus degradans 2–40T for the efficient hydrolysis of laminarin from brown macroalgae, Biotechnol Biofuels, **11**, (2018).

93. **Cai, L. N., Xu, S. N. and Lu, T.:** Directed expression of halophilic and acidophilic β-glucosidases by introducing homologous constitutive expression cassettes in marine Aspergillus niger, J Biotechnol, **292**, (2019).

94. **Sun, N., Liu, X. and Zhang, B.:** Characterization of a novel recombinant halophilic β-glucosidase of Trichoderma harzianum derived from Hainan mangrove, BMC Microbiol, **22**, (2022).

95. **Blumer-Schuette, S. E., Kataeva, I., Westpheling, J., Adams, M. W. and Kelly, R. M.:** Extremely thermophilic microorganisms for biomass conversion: status and prospects, Curr. Opin. Biotechnol., **19**, 210–217 (2008).

96. **Patel, A. K., Singhania, R. R., Sim, S. J. and Pandey, A.:** Thermostable cellulases: Current status and perspectives, Bioresour. Technol., **279**, 385–392 (2019).

97. **Dadwal, A., Sharma, S. and Satyanarayana, T.:** Thermostable cellulose saccharifying microbial enzymes: Characteristics, recent advances and biotechnological applications, Int. J. Biol. Macromol., **188**, 226–244 (2021).

98. **Elleuche, S., Schäfers, C., Blank, S., Schröder, C. and Antranikian, G.:**

Exploration of extremophiles for high temperature biotechnological processes, Curr. Opin. Microbiol., **25**, 113–119 (2015).

99. **Xu, J., Xiong, P. and He, B.:** Advances in improving the performance of cellulase in ionic liquids for lignocellulose biorefinery, Bioresour. Technol., **200**, 961–970 (2016).

100. **Hebal, H., Boucherba, N., Binay, B. and Turunen, O.:** Activity and stability of hyperthermostable cellulases and xylanases in ionic liquids, Biocatal. Biotransformation, **39**, 242–259 (2021).

101. **Ajeje, S. B., Hu, Y., Song, G., Peter, S. B., Afful, R. G., Sun, F., Asadollahi, M. A., Amiri, H., Abdulkhani, A. and Sun, H.:** Thermostable Cellulases / Xylanases From Thermophilic and Hyperthermophilic Microorganisms: Current Perspective, Front. Bioeng. Biotechnol., **9**, 1–19 (2021).

102. **Egorova, K. and Antranikian, G.:** Industrial relevance of thermophilic Archaea, Curr. Opin. Microbiol., **8**, 649–655 (2005).

103. **Bauer, M. W., Driskill, L. E., Callen, W., Snead, M. A., Mathur, E. J. and Kelly, R. M.:** An endoglucanase, eg1A, from the hyperthermophilic archaeon Pyrococcus furiosus hydrolyzes β-1,4 bonds in mixed-linkage (1→3),(1→4)- β-D- glucans and cellulose, J. Bacteriol., **181**, 284–290 (1999).

104. **Ando, S., Ishida, H., Kosugi, Y. and Ishikawa, K.:** Hyperthermostable endoglucanase from Pyrococcus horikoshii, Appl. Environ. Microbiol., **68**, 430–433 (2002).

105. **Huang, Y., Krauss, G., Cottaz, S., Driguez, H. and Lipps, G.:** A highly acid-stable and thermostable endo-β-glucanase from the thermoacidophilic archaeon Sulfolobus solfataricus, Biochem. J., **385**, 581–588 (2005).

106. **Zhang, J., Shi, H., Xu, L., Zhu, X. and Li, X.:** Site-directed mutagenesis of a hyperthermophilic endoglucanase Cel12B from thermotoga maritima based on rational design, PLoS One, **10**, 1–14 (2015).

107. **Kim, H. W., Kataoka, M. and Ishikawa, K.:** Atomic resolution of the crystal structure of the hyperthermophilic family 12 endocellulase and stabilizing role of the DxDxDG calcium-binding motif in Pyrococcus furiosus, FEBS Lett., **586**, 1009–1013 (2012).

108. **Kataoka, M., Kim, H. W. and Ishikawa, K.:** Recognition mechanism of endocellulase for β-glucan containing β(1 → 3),(1 → 4) mixed-linkages, Carbohydr. Res., **522**, 108682 (2022).

109. **Driskill, L. E., Bauer, M. W. and Kelly, R. M.:** Synergistic interactions among β-laminarinase, β-1,4-glucanase, and β-glucosidase from the hyperthermophilic

archaeon Pyrococcus furiosus during hydrolysis of β-1,4-, β-1,3-, and mixed-linked polysaccharides, Biotechnol. Bioeng., **66**, 51–60 (1999).

110. **Kishishita, S., Fujii, T. and Ishikawa, K.:** Heterologous expression of hyperthermophilic cellulases of archaea Pyrococcus sp. by fungus Talaromyces cellulolyticus, J. Ind. Microbiol. Biotechnol., **42**, 137–141 (2015).

111. **Kang, H. J., Uegaki, K., Fukada, H. and Ishikawa, K.:** Improvement of the enzymatic activity of the hyperthermophilic cellulase from Pyrococcus horikoshii, Extremophiles, **11**, 251–256 (2007).

112. **Koseki, T., Ishida, N., Hirota, R., Shiono, Y. and Makabe, K.:** Mutational analysis of the effects of N-glycosylation sites on the activity and thermal stability of rutinosidase from Aspergillus oryzae, Enzyme Microb. Technol., **161**, 110112 (2022).

113. **Ge, F., Zhu, L., Aang, A., Song, P., Li, W., Tao, Y. and Du, G.:** Recent advances in enhanced enzyme activity, thermostability and secretion by N-glycosylation regulation in yeast, Biotechnol. Lett., **40**, 847–854 (2018).

114. **Chang, X., Xu, B., Bai, Y., Luo, H., Ma, R., Shi, P. and Yao, B.:** Role of N-linked glycosylation in the enzymatic properties of a thermophilic GH 10 xylanase from Aspergillus fumigatus expressed in Pichia pastoris, PLoS One, **12**,

1–13 (2017).

115. **Zhu, J., Liu, H., Zhang, J., Wang, P., Liu, S., Liu, G. and Wu, L.:** Effects of Asn-33 glycosylation on the thermostability of Thermomyces lanuginosus lipase, J. Appl. Microbiol., **117**, 151–159 (2014).

116. **Zou, S., Xie, L., Liu, Y., Kaleem, I., Zhang, G. and Li, C.:** N-linked glycosylation influences on the catalytic and biochemical properties of Penicillium purpurogenum β-d-glucuronidase, J. Biotechnol., **157**, 399–404 (2012).

117. **Vite-Vallejo, O., Palomares, L. A., Dantán-González, E., Ayala-Castro, H. G., Martínez-Anaya, C., Valderrama, B. and Folch-Mallol, J.:** The role of N-glycosylation on the enzymatic activity of a Pycnoporus sanguineus laccase, Enzyme Microb. Technol., **45**, 233–239 (2009).

118. **Han, C., Wang, Q., Sun, Y., Yang, R., Liu, M., Wang, S., Liu, Y., Zhou, L. and Li, D.:** Improvement of the catalytic activity and thermostability of a hyperthermostable endoglucanase by optimizing N-glycosylation sites, Biotechnol. Biofuels, **13**, 1–11 (2020).

119. **Yamada, O., Byung, Rho, L. and Gomi, K.:** Transformation System for Aspergillus oryzae with Double Auxotrophic Mutations, niaD and sC, Biosci.

Biotechnol. Biochem., **61**, 1367–1369 (1997).

120. **Minetoki, T., Kumagai, C., Gomi, K., Kitamoto, K. and Takahashi, K.:** Improvement of promoter activity by the introduction of multiple copies of the conserved region III sequence, involved in the efficient expression of Aspergillus oryzae amylase-encoding genes, Appl. Microbiol. Biotechnol., **50**, 459–467 (1998).

121. **Miller, G. L.:** Use of Dinitrosalicylic Acid Reagent for Determination of Reducing Sugar, Anal. Chem., **31**, 426–428 (1959).

122. **Lee, J. M., Moon, S. Y., Kim, Y.-R., Kim, K. W., Lee, B.-J. and Kong, I.-S.:** Improvement of thermostability and halostability of β-1,3-1,4-glucanase by substituting hydrophobic residue for Lys 48, Int. J. Biol. Macromol., **94**, 594–602 (2017).

123. **Kupski, L., Pagnussatt, F. A., Buffon, J. G. and Furlong, E. B.:** Endoglucanase and total cellulase from newly isolated Rhizopus oryzae and Trichoderma reesei: Production, characterization, and thermal stability, Appl. Biochem. Biotechnol., **172**, 458–468 (2014).

124. **Kataoka, M. and Ishikawa, K.:** A new crystal form of a hyperthermophilic endocellulase, Acta Crystallogr. Sect. FStructural Biol. Commun., **70**, 878–883

(2014).

125. **Piper, P. W., Emson, C., Jones, C. E., Cowan, D. A., Fleming, T. M. and Littlechild, J. A.:** Complementation of a pgk deletion mutation in Saccharomyces cerevisiae with expression of the phosphoglycerate-kinase gene from the hyperthermophilic Archaeon Sulfolobus solfataricus, Curr. Genet., **29**, 594–596 (1996).

126. **Boyce, A. and Walsh, G.:** Expression and characterisation of a thermophilic endo-1,4-β-glucanase from Sulfolobus shibatae of potential industrial application, Mol. Biol. Rep., **45**, 2201–2211 (2018).

127. **Rykov, S. V., Selimzyanova, A. I., Nikolaeva, A. Y., Lazarenko, V. A., Tsurin, N. V., Akentyev, P. I., Zverlov, V. V., Liebl, W., Schwarz, W. H. and Berezina, O. V.:** Unusual substrate specificity in GH family 12: structure–function analysis of glucanases Bgh12A and Xgh12B from Aspergillus cervinus, and Egh12 from Thielavia terrestris, Appl. Microbiol. Biotechnol., **106**, 1493–1509 (2022).

128. **Segato, F., Dias, B., Berto, G. L., de Oliveira, D. M., De Souza, F. H. M., Citadini, A. P., Murakami, M. T., Damásio, A. R. L., Squina, F. M. and Polikarpov, I.:** Cloning, heterologous expression and biochemical

characterization of a non-specific endoglucanase family 12 from Aspergillus terreus NIH2624, Biochim. Biophys. Acta - Proteins Proteomics, **1865**, 395–403 (2017).

129. **Kim, H. W. and Ishikawa, K.:** Complete Saccharification of Cellulose at High Temperature Using Endocellulase and β-Glucosidase from Pyrococcus sp, J. Microbiol. Biotechnol., **20**, 889–892 (2010).

130. **Elgharbawy, A. A., Alam, M. Z., Moniruzzaman, M. and Goto, M.:** Ionic liquid pretreatment as emerging approaches for enhanced enzymatic hydrolysis of lignocellulosic biomass, Biochem. Eng. J., **109**, 252–267 (2016).

131. **Dotsenko, A. S., Rozhkova, A. M., Zorov, I. N. and Sinitsyn, A. P.:** Protein surface engineering of endoglucanase Penicillium verruculosum for improvement in thermostability and stability in the presence of 1-butyl-3-methylimidazolium chloride ionic liquid, Bioresour. Technol., **296**, 122370 (2020).

132. **Hebal, H., Hämäläinen, J., Makkonen, L., King, A. W. T., Kilpeläinen, I., Bankar, S., Boucherba, N. and Turunen, O.:** Enhanced activity of hyperthermostable Pyrococcus horikoshii endoglucanase in superbase ionic liquids, Biotechnol. Lett., **44**, 961–974 (2022).

133. **Ben Hmad, I., Boudabbous, M., Belghith, H. and Gargouri, A.:** A novel ionic

liquid-stable halophilic endoglucanase from Stachybotrys microspora, Process Biochem., **54**, 59–66 (2017).

134. **Dong, C. Di, Patel, A. K., Madhavan, A., Chen, C. W. and Singhania, R. R.:** Significance of glycans in cellulolytic enzymes for lignocellulosic biorefinery – A review, Bioresour. Technol., **379**, 128992 (2023).

135. **Dotsenko, A. S., Gusakov, A. V., Volkov, P. V., Rozhkova, A. M. and Sinitsyn, A. P.:** N-linked glycosylation of recombinant cellobiohydrolase I (Cel7A) from Penicillium verruculosum and its effect on the enzyme activity, Biotechnol. Bioeng., **113**, 283–291 (2016).

136. **Yan, J., Liu, W., Li, Y., Lai, H. L., Zheng, Y., Huang, J. W., Chen, C. C., Chen, Y., Jin, J., Li, H. and Guo, R. T.:** Functional and structural analysis of Pichia pastoris-expressed Aspergillus Niger 1,4-β-endoglucanase, Biochem. Biophys. Res. Commun., **475**, 8–12 (2016).

137. **Liu, G., Li, Q., Shang, N., Huang, J. W., Ko, T. P., Liu, W., Zheng, Y., Han, X., Chen, Y., Chen, C. C., *and others*:** Functional and structural analyses of a 1,4-β-endoglucanase from Ganoderma lucidum, Enzyme Microb. Technol., **86**, 67–74 (2016).

138. **Akram, F., Haq, I. ul, Imran, W. and Mukhtar, H.:** Insight perspectives of

thermostable endoglucanases for bioethanol production: A review, Renew. Energy, **122**, 225–238 (2018).

139. **Fujinami, D., Matsumoto, M., Noguchi, T., Sonomoto, K. and Kohda, D.:** Structural elucidation of an asparagine-linked oligosaccharide from the hyperthermophilic archaeon, Pyrococcus furiosus, Carbohydr. Res., **387**, 30–36 (2014).